

## A2.4.4 Description of algorithms

Version: 2022-01-12, V1.0, Stanislav Mašláň, Marko Berginc

***Note: Consider this document as a permanent draft! Further changes are very likely as the algorithms are being further developed. However, the validation reports should reflect current state of the algorithms in the TWM tool unless noted otherwise.***

This document describes detailed internal function of algorithms developed in TracePQM activity A2.3.2 and their uncertainty calculation developed in A2.3.5. The algorithm files are located in the TWM project [4] in folder “octprog/QWTB” They are all integrated in the copy of QWTB toolbox [5]. This document won’t describe principle of the QWTB toolbox as it is documented on the project web page [5]. The method how the algorithms are called by the TWM toolbox, i.e. what input quantities they receive and what may be returned as a result is defined in the document [3].

In general, the goal of QWTB is to make a wrapper function (next it will be called just “wrapper”) that translates the algorithm specific inputs and outputs to a unified format of input and output quantities. This is job of the so called algorithm wrappers: PSFE, SP-WFFT, etc., which are already present in the QWTB toolbox. These wrappers also may or may not contain some uncertainty calculation method or methods. However, non of these wrappers apply any HW component corrections defined by the TWM documents [3], [2]. Therefore, there is a second layer of wrappers (these will be called “TWM wrappers” in the text), which starts with “TWM-” prefix, e.g.: TWM-PSFE, TWM-PWRTDI, etc. The TWM wrappers contain all signal corrections defined by TWM. TWM wrappers perform the necessary TWM correction, they call either a QWTB wrapper (e.g. PSFE) or calculate the result by themselves and combines and returns the corrected results. Note some of the wrappers may call several other wrappers to achieve the desired result. This approach reduces duplication of code in the QWTB toolbox. One of these repeatedly called wrappers is “SP-WFFT” algorithm which is used for spectrum analysis.

## Acknowledgment

Presented document was developed in scope of the EMPIR project TracePQM (15RPT04) [1]. The project received funding from the EMPIR programme co-financed by the Participating States and from the European Union’s Horizon 2020 research and innovation programme.



## References

- [1] EURAMET. Trace PQM - EMPIR project: Traceability Routes for Electrical Power Quality Measurement. <http://tracepqm.cmi.cz>. April 2022, [online].
- [2] Stanislav Mašláň. Activity A2.3.1 - Correction Files Reference Manual. <https://github.com/smaslan/TWM/tree/master/doc/A231CorrectionFilesReferenceManual.docx>.
- [3] Stanislav Mašláň. Activity A2.3.2 - Algorithms Exchange Format. <https://github.com/smaslan/TWM/tree/master/doc/A232AlgorithmExchangeFormat.docx>.
- [4] Stanislav Mašláň. TWM tool. <https://github.com/smaslan/TWM>.
- [5] Martin Šíra. QWTB toolbox. <https://qwtb.github.io/qwtb/>.

# Contents

<b>1</b>	<b>TWM-PSFE - Phase Sensitive Frequency Estimator</b>	<b>4</b>
1.1	TWM wrapper parameters . . . . .	4
1.2	PSFE algorithm description . . . . .	6
1.3	TWM wrapper description . . . . .	6
1.4	PSFE description . . . . .	6
1.5	Uncertainty estimator . . . . .	7
1.6	Validation . . . . .	10
<b>2</b>	<b>TWM-MODTDPS - Modulation analyzer in Time Domain, by quadrature Phase Shifting</b>	<b>12</b>
2.1	TWM wrapper parameters . . . . .	12
2.2	MODTDPS algorithm description . . . . .	14
2.3	Uncertainty estimator . . . . .	17
2.4	Validation . . . . .	19
<b>3</b>	<b>TWM-FPNLSF - Four Parameter Non Linear Sine Fit</b>	<b>22</b>
3.1	TWM wrapper parameters . . . . .	22
3.2	Algorithm description . . . . .	24
3.3	Uncertainty estimator . . . . .	25
3.4	Validation . . . . .	27
<b>4</b>	<b>TWM-HCRMS - Half Cycle RMS algorithm</b>	<b>30</b>
4.1	TWM wrapper parameters . . . . .	30
4.2	Algorithm description . . . . .	32
4.3	Uncertainty calculation . . . . .	34
4.4	Validation . . . . .	35
<b>5</b>	<b>TWM-InDiSwell - Interruption, Dip, Swell event detector</b>	<b>37</b>
5.1	TWM wrapper parameters . . . . .	37
5.2	Algorithm description . . . . .	39
5.3	Uncertainty calculation . . . . .	40
5.4	Validation . . . . .	40
<b>6</b>	<b>TWM-THDWFFT - THD from Windowed FFT</b>	<b>42</b>
6.1	TWM wrapper parameters . . . . .	42
6.2	Algorithm description and uncertainty evaluation . . . . .	44
6.3	Validation . . . . .	48
<b>7</b>	<b>TWM-PWRTDI - Power by Time Domain Integration</b>	<b>53</b>
7.1	TWM wrapper parameters . . . . .	53
7.2	Algorithm description . . . . .	57
7.2.1	Windowed RMS function “proc_wrms()” . . . . .	58
7.3	Uncertainty calculator and estimator . . . . .	60
7.3.1	Monte Carlo uncertainty calculator . . . . .	61
7.3.2	Fast uncertainty estimator . . . . .	62
7.4	Validation . . . . .	65
<b>8</b>	<b>TWM-WRMS - RMS value by Windowed Time Domain Integration</b>	<b>70</b>
8.1	TWM wrapper parameters . . . . .	70
8.2	Algorithm description . . . . .	72
8.3	Uncertainty calculator and estimator . . . . .	73
8.4	Validation . . . . .	73

<b>9</b>	<b>TWM-WFFT - Windowed FFT spectrum analysis</b>	<b>75</b>
9.1	TWM wrapper parameters . . . . .	75
9.2	Algorithm description . . . . .	77
9.3	Uncertainty calculator and estimator . . . . .	78
9.4	Validation . . . . .	78
<b>10</b>	<b>TWM-Flicker - Flicker algorithm</b>	<b>81</b>
10.1	TWM wrapper parameters . . . . .	81
10.2	Algorithm description . . . . .	82
10.2.1	QWTB algorithm wrapper “flicker_sim” . . . . .	83
10.3	Uncertainty estimator . . . . .	84
10.4	Validation . . . . .	84
<b>11</b>	<b>TWM-MFSF - Multi-Frequency Sine Fit</b>	<b>86</b>
11.1	TWM wrapper parameters . . . . .	86
11.2	Algorithm description . . . . .	88
11.2.1	QWTB algorithm MFSF . . . . .	89
11.2.2	Uncertainty calculation . . . . .	90
11.3	Validation . . . . .	93
<b>12</b>	<b>TWM-PWRFFT - Power by FFT</b>	<b>96</b>
12.1	TWM wrapper parameters . . . . .	96
12.2	Algorithm description . . . . .	100
12.2.1	Uncertainty calculation . . . . .	101
12.2.2	Validation . . . . .	101
<b>13</b>	<b>TWM-LowZ - Low Impedance Measurement Algorithm</b>	<b>104</b>
13.1	TWM wrapper parameters . . . . .	104
13.2	Algorithm description . . . . .	107
13.2.1	Uncertainty calculation . . . . .	110
13.2.2	Validation . . . . .	110

# 1 TWM-PSFE - Phase Sensitive Frequency Estimator

TWM-PSFE is a TWM wrapper for the Phase Sensitive Frequency Estimator algorithm (PSFE) [1]. PSFE is an algorithm for estimating the frequency, amplitude, and phase of the fundamental component in harmonically distorted waveforms. The algorithm minimizes the phase difference between the sine model and the sampled waveform by effectively minimizing the influence of the harmonic components. It uses a three-parameter sine-fitting algorithm for all phase calculations. The resulting estimates show up to two orders of magnitude smaller sensitivity to harmonic distortions than the results of the four-parameter sine fitting algorithm.

The TWM wrapper TWM-PSFE is designed for single-ended transducers. It will estimate only frequency in the differential input transducer mode. The algorithm is equipped by a fast uncertainty estimator for the frequency quantity only.

## 1.1 TWM wrapper parameters

The TWM wrapper accepts inputs and corrections (see [4] for details) specified in the table 1. List of output quantities is shown in the table 2. The TWM wrapper also accepts “calcset” options shown in the table 3.

Table 1: List of input quantities to the TWM-PSFE wrapper.

Name	Default	Unc.	Description
comp_timestamp	0	N/A	Enable compensation of phase shift by timestamp value: $\phi' = \phi - 2 \cdot \pi \cdot f_{est} \cdot time\_stamp$ .
y	N/A	No	Input sample data vector and complementary low-side input data vector <i>y_lo</i> for differential mode only.
y_lo	N/A	No	
Ts	N/A	No	Sampling period or sampling rate or sample time vector. Note the wrapper always calculates in equidistant mode, so <i>t</i> is used just to calculate <i>Ts</i> .
fs	N/A	No	
t	N/A	No	
lsb	N/A	No	
adc_nrng	1000	No	Either absolute ADC resolution <i>lsb</i> or nominal range value <i>adc_nrng</i> (e.g.: 5 V for 10 Vpp range) and <i>adc_bits</i> bit resolution of ADC.
adc_bits	40	No	
lo_lsb	N/A	No	
lo_adc_nrng	1000	No	
lo_adc_bits	40	No	
adc_offset	0	Yes	Digitizer input offset voltage.
lo_adc_offset	0	Yes	
adc_gain	1	Yes	Digitizer gain correction 2D table (multiplier).
adc_gain_f	□	No	
adc_gain_a	□	No	
lo_adc_gain	1	Yes	
lo_adc_gain_f	□	No	
lo_adc_gain_a	□	No	
adc_phi	0	Yes	Digitizer phase correction 2D table (additive).
adc_phi_f	□	No	
adc_phi_a	□	No	
lo_adc_phi	0	Yes	
lo_adc_phi_f	□	No	
lo_adc_phi_a	□	No	
adc_freq	0	Yes	Digitizer timebase error correction: $f_{tb}' = f_{tb} \cdot (1 + adc\_freq.v)$ The effect on the estimated frequency is opposite: $f_{est}' = f_{est} / (1 + adc\_freq.v)$
adc_jitter	0	No	Digitizer sampling period jitter [s].
adc_aper	0	No	ADC aperture value [s].

Table 1: List of input quantities to the TWM-PSFE wrapper.

Name	Default	Unc.	Description
adc_aper_corr lo_adc_aper	0 0	No	ADC aperture error correction enable: $A' = A \cdot \pi \cdot \text{adc\_aper} \cdot f\_est / \sin(\pi \cdot \text{adc\_aper} \cdot f\_est)$ $\phi_i' = \phi_i + \pi \cdot \text{adc\_aper} \cdot f\_est$
time_stamp	0	Yes	Relative timestamp of the first sample $y$ .
adc_sfdr adc_sfdr_f adc_sfdr_a lo_adc_sfdr lo_adc_sfdr_f lo_adc_sfdr_a	180 [] [] 180 [] []	No No No No No No	Digitizer SFDR 2D table.
adc_Yin_Cp adc_Yin_Gp adc_Yin_f lo_adc_Yin_Cp lo_adc_Yin_Gp lo_adc_Yin_f	1e-15 1e-15 [] 1e-15 1e-15 []	Yes Yes No Yes Yes No	Digitizer input admittance 1D table.
tr_type	“”	No	Transducer type string (“rvd” or “shunt”).
tr_gain tr_gain_f tr_gain_a	1 [] []	Yes No No	Transducer gain correction 2D table (multiplicative).
tr_phi tr_phi_f tr_phi_a	0 [] []	Yes No No	Transducer phase correction 2D table (additive).
tr_sfdr tr_sfdr_f tr_sfdr_a	180 [] []	No No No	Transducer SFDR 2D table.
tr_Zlo_Rp tr_Zlo_Cp tr_Zlo_f	1e3 1e-15 []	Yes Yes No	RVD transducer low-side impedance 1D table. Note this is related to loading correction and it has effect only for RVD transducer and will work only if <i>adc_Yin</i> is defined as well.
tr_Zbuf_Rs tr_Zbuf_Ls tr_Zbuf_f	0 0 []	Yes Yes No	Loading corrections: Transducer output buffer output series impedance 1D table. Leave unassigned to disable buffer from the correction topology.
tr_Zca_Rs tr_Zca_Ls tr_Zca_f	1e-9 1e-12 []	Yes Yes No	Loading corrections: Transducer high side terminal series impedance 1D table.
tr_Zcal_Rs tr_Zcal_Ls tr_Zcal_f	1e-9 1e-12 []	Yes Yes No	Loading corrections: Transducer low side terminal series impedance 1D table.
tr_Yca_Cp tr_Yca_D tr_Yca_f	1e-15 1e-12 []	Yes Yes No	Loading corrections: Transducer output terminals shunting impedance.
tr_Zcam tr_Zcam_f	1e-12 []	Yes No	Loading corrections: Transducer output terminals mutual inductance 1D table.
Zcb_Rs Zcb_Ls Zcb_f	1e-9 1e-12 []	Yes Yes No	Loading corrections: Cable series impedance 1D table.
Ycb_Rs Ycb_Ls Ycb_f	1e-15 1e-12 []	Yes Yes No	Loading corrections: Cable series impedance 1D table.

Table 2: List of output quantities of the TWM-PSFE wrapper. The uncertainty marked \* is just a contribution of corrections, but PSFE contribution is not included and not validated.

Name	Uncertainty	Description
f	Yes	Estimated frequency [Hz].
A	Yes*	Estimated amplitude.
ph	Yes*	Estimated phase angle [rad].

Table 3: List of “calcset” options supported by the TWM-PSFE wrapper.

Name	Description
calcset.unc	Uncertainty calculation mode. Supported: “none” or “guf”.
calcset.loc	Level of confidence [-].
calcset.verbose	Verbose level.

## 1.2 PSFE algorithm description

The algorithm implementation to the TWM structure consists of two levels: (i) wrapper “PSFE” and its uncertainty estimator; (ii) TWM wrapper “TWM-PSFE”. The overall structure is shown in fig. 1.

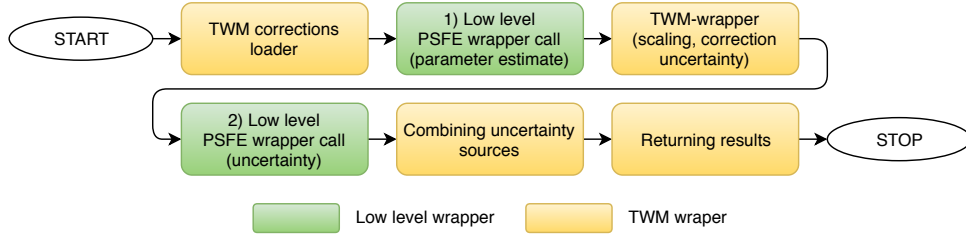


Figure 1: Overview of the TWM-PSFE algorithm wrapper.

## 1.3 TWM wrapper description

Block diagram of the internal structure of the TWM-PSFE wrapper is shown in fig. 2. The TWM wrapper partially supports differential transducer input (see [3] for definition). However, in the differential mode it only calculates frequency. The other parameters are ignored. Two differential inputs are directly subtracted ( $y - y_{lo}$ ) in the differential mode. This is not usable for amplitude or phase estimation, but it is sufficient for frequency estimation. The DC offset correction is applied directly to the time domain signal  $y$ . Next, the PSFE is called first time to obtain estimates of the unscaled waveform. The uncertainty is disabled, because not all required inputs to the uncertainty estimator are available at this point. In single-ended mode follow corrections of the estimated signal parameters along with the calculation of the correction uncertainties. When uncertainty calculation is enabled, the additional inputs, such as SFDR and LSB are calculated and PSFE is called again, but this time with uncertainty estimation enabled. The returned estimates are ignored, but the returned uncertainties are combined with the corrections contributions and returned along the estimates  $A$ ,  $\phi$  and  $f$ .

## 1.4 PSFE description

The “Phase-Sensitive Frequency Estimation” algorithm (PSFE) is used to estimate the parameters of non coherently sampled harmonically distorted sinewave signal. The main input parameter is the sampled record  $y(n \cdot T_s)$  having the length  $N$  and sampling period  $T_s$ . Optionally, the initial frequency estimation could be defined. The outputs of the algorithm are: (i) frequency, (ii) amplitude, and (iii) initial phase of the fundamental signal and (iv) offset of the sampled signal.

The concept of the PSFE algorithm is shown in fig. 3. First, the approximate frequency of the record is estimated using peak amplitude DFT bin frequency or using interpolated DFT frequency estimate. In the following, the record having  $N$  samples is divided in two equally length subrecords W1 and W2. The

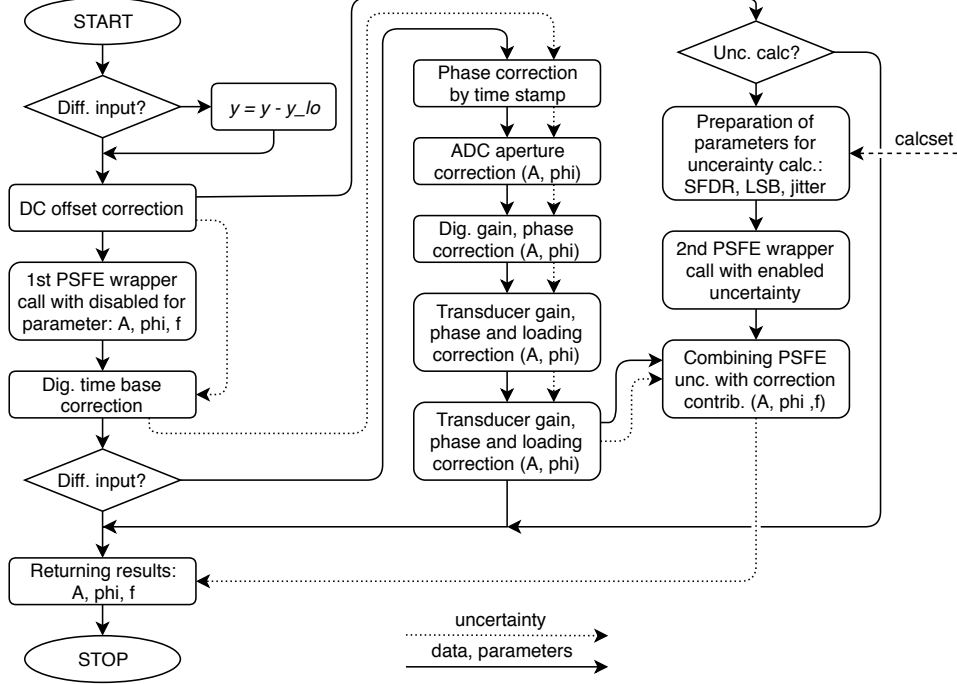


Figure 2: Detailed internal structure of the TWM-PSFE algorithm wrapper.

W1 starts at the beginning of the record while the W2 starts after  $d$  number of samples within the record where  $N/4 \leq d \leq N/2$ . The phases of W1 and W2 subrecords are estimated using three-parameters sine fitting algorithm (3PSF) and the estimated phases are then subtracted to obtain estimated sampled signal phase difference. When the subrecord distance  $d$  is selected to position two subrecords as close as possible to the integer number of signal periods, the 3PSF phase estimation error due to harmonics will almost completely cancel out in (the difference between the estimated phase and the fundamental signal phase  $\phi_1$  is a periodic function with frequency  $f$ , independent of the harmonic components in the sampled signal). Using equation 1 will thus provide a more accurate frequency estimate of the sampled signal and by repeating the procedure described above, the phase difference between the sine model and the sampled waveform will be minimised and the estimated frequency will converge toward the actual frequency of the sampled signal.

$$\hat{f} = \frac{\Delta \hat{\phi}_\epsilon}{2 \cdot \pi \cdot T_s \cdot d}. \quad (1)$$

The iterations  $j$  are completed when error according equation 2 is  $\epsilon < 2.4 \cdot 10^{-12}$  or when the number of iterations exceeds 20. However, the PSFE algorithm typically needs only a few iterations to converge to the final value. After obtaining the frequency, the amplitude and initial phase of the record are estimated using the 3PSF algorithm and complete sampled record  $y$ . The PSFE algorithm shows up to two orders of magnitude smaller sensitivity to harmonic distortions than the results of the four parameter sine fitting algorithm with only a slight increase in noise standard deviation and only a slight increase in computational requirements and estimation time, independent of the number of harmonic components.

$$\epsilon = \frac{|\Delta \hat{\phi}_{\epsilon,j-1} - \Delta \hat{\phi}_{\epsilon,j}|}{2 \cdot \pi \cdot N \cdot T_s \cdot d \cdot \hat{f}_{j-1}}. \quad (2)$$

## 1.5 Uncertainty estimator

Uncertainty estimator consists of two components: (i) Uncertainty of corrections, (ii) uncertainty of the PSFE algorithm itself. The algorithm uncertainty is evaluated in the PSFE wrapper, the corrections uncertainty and combining with the algorithm uncertainty is implemented in TWM-PSFE wrapper.

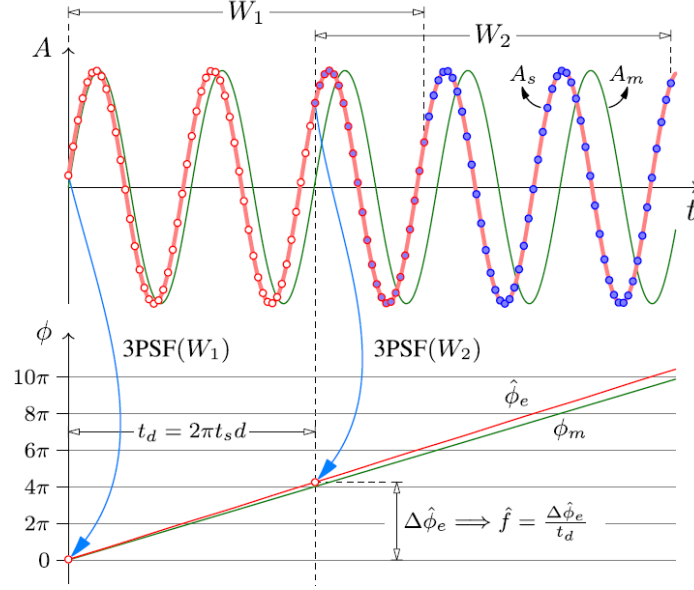


Figure 3: The principle of frequency estimation by measuring the phase difference between sampled data windows  $W_1$  and  $W_2$  [2].

Four uncertainty contributions for the PSFE algorithm were considered for the estimator (see Table 4): jitter, resolution, interharmonics and harmonics. Additionally, several other parameters related to the sampled signal or sampling (i.e. condition) are expected to affect the uncertainty, therefore enormous number of Monte Carlo simulations would be needed for accurate uncertainty analysis.

Table 4: A list of parameters that were varied during the Monte-Carlo simulations.

Uncertainty contribution	Variation range	Reference value
RMS jitter	1 ns - 10 ns	<b>1 ns</b> (0 ns)
resolution	10 pV - 100 mV	<b>10 μV</b> (0 V)
interharmonic's amplitude, $A_i$	0.1 mV - 0.2 V	<b>10 mV</b> (0 V)
harmonic's amplitude, $A_h$	1 mV - 0.5 mV	<b>50 mV</b> (0 V)
<b>Condition parameters</b>		
amplitude of the fundamental signal, $A_1$	0.1 V - 1000 V	1 V
frequency of the fundamental signal, $f_1$	10 Hz - 2 kHz	100 Hz
time stamp	0 s - 10 s	0.1 s
sampling frequency, $f_s$	500 Hz - 1 MHz	10 kHz
number of samples, $N$	500 Sa - 1 MSa	100 kSa
ADC gain at 1 MHz <sup>*1</sup>	1 - 1.5	1.5
ADC phase at 1 MHz <sup>*2</sup>	-0.5 rad - 0.5 rad	0.5 rad
ADC frequency	$1 \cdot 10^{-6}$ - $5 \cdot 10^{-3}$	$1 \cdot 10^{-3}$
transducer gain at 1 MHz <sup>*3</sup>	0.5 - 1.0	0.6
transducer phase at 1 MHz <sup>*4</sup>	-0.5 rad - 0.5 rad	-0.5 rad
ADC aperture correction	0 or 1	1
ADC aperture	10 μs - 40 μs	20 μs

\*1 1 at DC.

\*2 0 rad at DC.

\*3 1 at DC.

\*4 0 rad at DC.

Herein we used different and slightly simplified approach. We run 52 different Monte Carlo simulation sets. For each set only one uncertainty contribution was considered using the bold reference value given



in Table 4. The other three uncertainty contributions were neglected by using the reference values given in the brackets. Additionally, only one condition parameter has been varied at the time using the variation range as defined in Table 4 while we used the reference values for the other conditions parameters. We also verified the linearity of the uncertainty contribution by varying its value over a certain variation range while neglecting other uncertainty contributions (using the reference values in brackets) and keeping all condition parameters at reference values.

**Effect of jitter:** For each condition 5000 Monte-Carlo simulations were performed. We introduced a random jitter to each sample while keeping overall RMS jitter value at specified value. Additionally, the initial phase of the fundamental signal  $\phi_1$  was randomly varied between  $+\pi$  and  $-\pi$ . For each simulation a Gaussian distribution has been obtained. The uncertainty contribution of the frequency estimation  $u_{f,\text{jitter}}$  due to the jitter (Gaussian distribution,  $k = 1$ ) is defined by equation:

$$u_{f,\text{jitter}} = \left( \frac{1.341 \text{ Hz/s}}{2.981 + (0.622 \cdot N/\text{Sample})^{0.521}} \right) \cdot \frac{f_1}{1 \text{ Hz}} \cdot \text{jitter}, \quad (3)$$

where  $\text{jitter}$  is the value of sampling jitter.

**Effect of resolution:** For each condition 10000 Monte-Carlo simulations were performed. The value of each sample has been rounded according to the resolution setting. Additionally, the initial phase of the fundamental signal  $\phi_1$  was randomly varied between  $+\pi$  and  $-\pi$ . In this case a non-Gaussian distribution was obtained therefore the maximal error has been noted instead. The uncertainty contribution of the frequency estimation  $u_{f,\text{res}}$  due to the resolution (rectangular distribution) is defined by equation:

$$u_{f,\text{res}} = 0.23 \text{ mHz} \cdot \left( \frac{N}{100 \text{ kSa}} \right)^{-1.5} \cdot \left( \frac{f_s}{10 \text{ kHz}} \right)^{0.9} \cdot \frac{\text{res}}{A_1}, \quad (4)$$

where  $\text{res}$  is the absolute ADC resolution.

**Effect of interharmonics:** For each condition 5000 Monte-Carlo simulations were performed. In this case, one interharmonic with fixed amplitude  $A_i$  and with random frequency (between 1 Hz and  $f_1$ ) and with random initial phase (between  $+\pi$  and  $-\pi$ ) has been added to the fundamental signal. Additionally, the initial phase of the fundamental signal  $\phi_1$  was randomly varied between  $+\pi$  and  $-\pi$ . In this case a non Gaussian distribution was also obtained therefore the maximal error has been noted instead. The uncertainty contribution of the frequency estimation  $u_{f,\text{inter}}$  due to the presence of interharmonic (rectangular distribution) is defined by equation:

$$u_{f,\text{inter}} = 0.046 \text{ Hz} \cdot \frac{A_i}{A_1} \left( \frac{N}{100 \text{ kSa}} \right)^{-1} \cdot \frac{f_s}{10 \text{ kHz}}, \quad (5)$$

where  $A_i/A_1$  is the interharmonic to fundamental amplitude ratio.

**Effect of harmonics:** For each condition 5000 Monte-Carlo simulations were performed. In this case, one random harmonic component with fixed amplitude  $A_h$  and with random frequency (between  $2 \cdot f_1$  and  $n \cdot f_1 < 1 \text{ MHz}$ ) and random initial phase (between  $+\pi$  and  $-\pi$ ) has been added to the fundamental signal. Additionally, the initial phase of the fundamental signal  $\phi_1$  was randomly varied between  $+\pi$  and  $-\pi$  too. In this case a non Gaussian distribution was also obtained therefore the maximal error has been noted instead. The uncertainty contribution of the frequency estimation  $u_{f,\text{harm}}$  due to the presence of harmonic component (rectangular distribution) is defined by following equation (equation is valid only for  $N \geq 3000$ ):

$$u_{f,\text{harm}} = 40 \text{ mHz} \cdot \frac{A_h}{A_1}, \quad (6)$$

where  $A_h/A_1$  is the harmonic to fundamental amplitude ratio.

All uncertainty contributions are combined and recalculated for Gaussian distribution,  $k = 2$ :

$$u_f = 2 \cdot \sqrt{u_{f,\text{jitter}}^2 + \frac{u_{f,\text{res}}^2}{3} + \frac{u_{f,\text{inter}}^2}{3} + \frac{u_{f,\text{harm}}^2}{3}}, \quad (7)$$

## 1.6 Validation

The algorithm TWM-PSFE has many input quantities and some of them are matrices. That is too many possible degrees of freedom. Thus, varying the quantities in some systematic way would be very complicated if the validation should cover full range of used signals and corrections. Therefore, an alternative approach was used.

QWTB test function “alg\_test.m” was created, which performs the validation using randomly generated test setups. It randomizes the signal parameters, correction quantities and uncertainties and algorithm configurations in ranges expected to occur during the real measurements. The test is run many times to cover full operating range of the algorithm. Following operations are performed for each random test setup:

1. Generate reference signal with known frequency  $f$ .
2. Distort the signal by inverse corrections, i.e. simulate the transducers, and digitizer (e.g. gain errors, phase errors, DC offsets, quantisation errors, ...).
3. Run the algorithm TWM-PSFE on the signals with enabled uncertainty evaluation to obtain frequency estimates and their uncertainties.
4. Compare reference and estimated frequency and decide if the errors of the algorithm for particular frequency is smaller than the assigned uncertainties.
5. Repeat the test  $N$  times from step 1 with different setup parameters, with randomised corrections by their uncertainties, and with randomised noise, SFDR and jitter.
6. Check that at least 95 % of results passed (for default 95 % level of confidence). The evaluation is made for each calculated frequency separately.

Total number of Monte-Carlo simulations was 100000. The parameters of the input signal and the digitizer and transducer settings were randomly varied. The sampling frequency was between 500 Hz and 500 kHz and the number of samples between 500 Sa and 200 kSa. The frequency of fundamental signal was between 10 Hz and one tenth of the Nyquist frequency, but never above 5 kHz. The frequency of the harmonics and interharmonics were always above the frequency of the fundamental signal but below the Nyquist frequency. The number of harmonics that were added to the fundamental signal was generally 10, but the number was sometimes reduced if the Nyquist limit is to be exceeded. The number of interharmonics was 1. The amplitude of the fundamental signal was between 0.1 V and 1000 V and the amplitude of the harmonics and interharmonics between 0.00001 and 0.05 of the amplitude of the fundamental signal. The DC was between -10 V and +10 V. The phases of the fundamental signal as well as of the harmonics and interharmonics were individually and randomly varied between +3.14 rad and -3.14 rad. The ADC noise was between  $1e-11$  and  $1e-2$  of the amplitude of the fundamental signal while the jitter was between  $1e-9$  s and  $100e-9$  s. ADC aperture was between  $1e-5$  s and  $4e-5$  s, ADC gain between 1 and 1.5, ADC phase between +1.57 rad and -1.57 rad, frequency correction of the digitizer timebase between  $5e-8$  and  $5e-3$ , ADC offset between 0.00001 V and 0.005 V (random value for low-and high-side channel) and number of bits between 22 and 24. Relative time-stamp of the first sample was varied between 0 s and 10 s. The transducer gain was between 0.5 and 20 and the transducer phase was between +1.57 rad and -1.57 rad. The resistive voltage divider low-side impedance value (i.e. resistance and capacitance) were between  $100\ \Omega$  and  $500\ \Omega$  and 0.1 pF and 10 pF, respectively (only resistive voltage divider was used in the simulations). The randomisation of corrections was also enabled which means that not only the uncertainty of the algorithm but also the contributions of the correction uncertainties were included in the Monte-Carlo simulations. The success rate of the TWM-PSFE algorithm uncertainty estimator for the frequency estimation was 99.38 %.

## References

- [1] Rado Lapuh. Estimating the fundamental component of harmonically distorted signals from noncoherently sampled data. *IEEE Transactions on Instrumentation and Measurement*, 64(6):1419–1424, June 2015.

- [2] Rado Lapuh. *Sampling with 3458A*. Left Right d.o.o., Sep 2018.
- [3] Stanislav Mašláň. Activity A2.3.1 - Correction Files Reference Manual. <https://github.com/smaslan/TWM/tree/master/doc/A231CorrectionFilesReferenceManual.docx>.
- [4] Stanislav Mašláň. Activity A2.3.2 - Algorithms Exchange Format. <https://github.com/smaslan/TWM/tree/master/doc/A232AlgorithmExchangeFormat.docx>.

## 2 TWM-MODTDPS - Modulation analyzer in Time Domain, by quadrature Phase Shifting

TWM-MODTDPS is algorithm for calculation of the amplitude modulation parameters of non-coherently sampled signal in time domain. It was designed for basic estimation of the modulation parameters of a sinusoidal carrier modulated by sine wave or rectangular wave with duty cycle 50 %.

The algorithm operates in time domain and it is based on the so called “analytical signal”. It is capable to estimate the parameters up to modulating-to-carrier frequency ratio 33 %. The record must contain at least 3 periods of the modulating signal and it also requires at least 10 samples per period of carrier.

It is capable to use the differential transducer connection, however the uncertainty is not calculated for the differential mode. The algorithm is equipped by an uncertainty estimator, which covers most of the operating range. The estimator parameter space contains a few gaps where the algorithm may fail, which will be always indicated as an error message. These gaps problems may be prevented by changing the sampling parameters, e.g. by changing the samples count or a sampling rate.

### 2.1 TWM wrapper parameters

The input quantities supported by the algorithm are shown in table 5. Algorithm returns output quantities shown in table 6. Calculation setup supported by the algorithm is shown in table 7.

Table 5: List of input quantities to the TWM-MODTDPS wrapper.  
Details on the correction quantities can be found in [3].

Name	Default	Unc.	Description
wave_shape	“sine”	N/A	User string parameter that defines if the algorithm calculates “sine”: sinusoidal modulation or “rect”: rectangular modulation wave shape.
comp_err	0	N/A	Enable self-compensation of the algorithm error (non-zero value or “on” string).
y	N/A	No	Input sample data vector and complementary low-side input data vector $y_{lo}$ for differential mode only.
y_lo	N/A	No	
Ts	N/A	No	Sampling period or sampling rate or sample time vector. Note the wrapper always calculates in equidistant mode, so $t$ is used just to calculate $Ts$ .
fs	N/A	No	
t	N/A	No	
lsb	N/A	No	Either absolute ADC resolution $lsb$ or nominal range value $adc\_nrng$ (e.g.: 5 V for 10 Vpp range) and $adc\_bits$ bit resolution of ADC.
adc_nrng	1000	No	
adc_bits	40	No	
lo_lsb	N/A	No	
lo_adc_nrng	1000	No	
lo_adc_bits	40	No	Digitizer gain correction 2D table (multiplier).
adc_gain	1	Yes	
adc_gain_f	□	No	
adc_gain_a	□	No	
lo_adc_gain	1	Yes	
lo_adc_gain_f	□	No	
lo_adc_gain_a	□	No	
adc_phi	0	Yes	Digitizer phase correction 2D table (additive).
adc_phi_f	□	No	
adc_phi_a	□	No	
lo_adc_phi	0	Yes	
lo_adc_phi_f	□	No	
lo_adc_phi_a	□	No	

Table 5: List of input quantities to the TWM-MODTDPS wrapper.  
Details on the correction quantities can be found in [3].

Name	Default	Unc.	Description
adc_freq	0	Yes	Digitizer timebase error correction: $f_{tb'} = f_{tb} \cdot (1 + adc\_freq.v)$ The effect on the estimated frequency is opposite: $f_{est'} = f_{est} / (1 + adc\_freq.v)$
adc_jitter	0	No	Digitizer sampling period jitter [s].
adc_aper	0	No	ADC aperture value [s].
adc_aper_corr	0	No	ADC aperture error correction enable: $A' = A \cdot \pi \cdot adc\_aper \cdot f_{est} / \sin(\pi \cdot adc\_aper \cdot f_{est})$ $\phi_i' = \phi_i + \pi \cdot adc\_aper \cdot f_{est}$
lo_adc_aper	0	No	
time_stamp	0	Yes	Relative timestamp of the first sample $y$ .
time_shift_lo	0	Yes	Low-side channel time shift [s].
adc_sfdr	180	No	Digitizer SFDR 2D table.
adc_sfdr_f	□	No	
adc_sfdr_a	□	No	
lo_adc_sfdr	180	No	
lo_adc_sfdr_f	□	No	
lo_adc_sfdr_a	□	No	
adc_Yin_Cp	1e-15	Yes	Digitizer input admittance 1D table.
adc_Yin_Gp	1e-15	Yes	
adc_Yin_f	□	No	
lo_adc_Yin_Cp	1e-15	Yes	
lo_adc_Yin_Gp	1e-15	Yes	
lo_adc_Yin_f	□	No	
tr_type	“”	No	Transducer type string (“rvd” or “shunt”).
tr_gain	1	Yes	Transducer gain correction 2D table (multiplicative).
tr_gain_f	□	No	
tr_gain_a	□	No	
tr_phi	0	Yes	Transducer phase correction 2D table (additive).
tr_phi_f	□	No	
tr_phi_a	□	No	
tr_sfdr	180	No	Transducer SFDR 2D table.
tr_sfdr_f	□	No	
tr_sfdr_a	□	No	
tr_Zlo_Rp	1e3	Yes	RVD transducer low-side impedance 1D table. Note this is related to loading correction and it has effect only for RVD transducer and will work only if <i>adc_Yin</i> is defined as well.
tr_Zlo_Cp	1e-15	Yes	
tr_Zlo_f	□	No	
tr_Zbuf_Rs	0	Yes	Loading corrections: Transducer output buffer output series impedance 1D table. Leave unassigned to disable buffer from the correction topology.
tr_Zbuf_Ls	0	Yes	
tr_Zbuf_f	□	No	
tr_Zca_Rs	1e-9	Yes	Loading corrections: Transducer high side terminal series impedance 1D table.
tr_Zca_Ls	1e-12	Yes	
tr_Zca_f	□	No	
tr_Zcal_Rs	1e-9	Yes	Loading corrections: Transducer low side terminal series impedance 1D table.
tr_Zcal_Ls	1e-12	Yes	
tr_Zcal_f	□	No	
tr_Yca_Cp	1e-15	Yes	Loading corrections: Transducer output terminals shunting impedance.
tr_Yca_D	1e-12	Yes	
tr_Yca_f	□	No	
tr_Zcam	1e-12	Yes	Loading corrections: Transducer output terminals mutual inductance 1D table.
tr_Zcam_f	□	No	

Table 5: List of input quantities to the TWM-MODTDPS wrapper.  
Details on the correction quantities can be found in [3].

Name	Default	Unc.	Description
Zcb_Rs	1e-9	Yes	Loading corrections: Cable series impedance 1D table.
Zcb_Ls	1e-12	Yes	
Zcb_f	$\emptyset$	No	
Ycb_Rs	1e-15	Yes	Loading corrections: Cable series impedance 1D table.
Ycb_Ls	1e-12	Yes	
Ycb_f	$\emptyset$	No	

Table 6: List of output quantities of the TWM-MODTDPS wrapper.

Name	Uncertainty	Description
f0	Yes	Frequency of the carrier [Hz].
A0	Yes	Amplitude of the carrier.
f_mod	Yes	Modulating frequency [Hz].
A_mod	Yes	Modulating amplitude.
mod	Yes	Modulating depth [%].
dVV	Yes	$\Delta V/V$ depth [%]. Alternative expression of <i>mod</i> , i.e.: $dVV = 2 \cdot mod$ .
cpm	Yes	Changes per minute. Alternative expression of <i>f_mod</i> , i.e.: $cpm = 120 \cdot f\_mod$ .
env	No	Modulation envelope.
env_t	No	Modulation envelope <i>env</i> time vector.

Table 7: List of “calcset” options supported by the TWM-MODTDPS wrapper.

Name	Description
calcset.unc	Uncertainty calculation mode. Supported: “none” or “guf” for uncertainty estimator.
calcset.loc	Level of confidence [-].
calcset.verbose	Verbose level.

## 2.2 MODTDPS algorithm description

The overview of the TWM wrapper structure is shown in the fig. 4. The algorithm supports differential transducer inputs. The TWM wrapper first estimates the carrier frequency  $f_0$  and mean amplitude of the modulated signal  $A_0$  by a PSFE algorithm. It uses these two values to obtain and apply gain and aperture error corrections for the high-side channel  $y$  (and for low-side channel  $y_{lo}$  in the differential mode).

In the differential transducer mode, the wrapper also applies high-to-low side time shift correction and phase correction to the low-side input  $y_{lo}$  by time shifting it according to the estimate  $f_0$ . This trivial phase synchronization of the high-low side phase obviously works only to one frequency  $f_0$  and it is dependent on its correct estimation, however it turned out to be sufficient for the purposes of this algorithm. Next, the wrapper calculates voltage difference  $y = y - y_{lo}$ , so the differential is reduced to single ended input  $y$ . The transducer gain correction in the differential mode uses additional voltage vectors  $Y(f_0), \phi(f_0)$  and  $Y_{lo}(f_0), \phi_{lo}(f_0)$  obtained from the two spectra calculated by another QWTB algorithm “SP-WFFT”. Although the vectors have absolute values distorted by the spectral leakage, their ratio stays fixed, so it is enough to make the transducer transfer and loading correction function work. At this point the signal is single ended and scaled.

The next step is the main algorithm for the estimation of modulation parameters “mod\_tdps()” which is shown in fig. 5. The algorithm internally calls the function “mod\_fit\_sin()” (see fig. 6), which does the parameter estimation itself.

The algorithm itself is based on the estimation of the carrier frequency  $f_0$  by means of PSFE algorithm [2]. Once the carrier  $f_0$  is known, the algorithm applies 90deg phase shift to the input signal  $y$  and builds

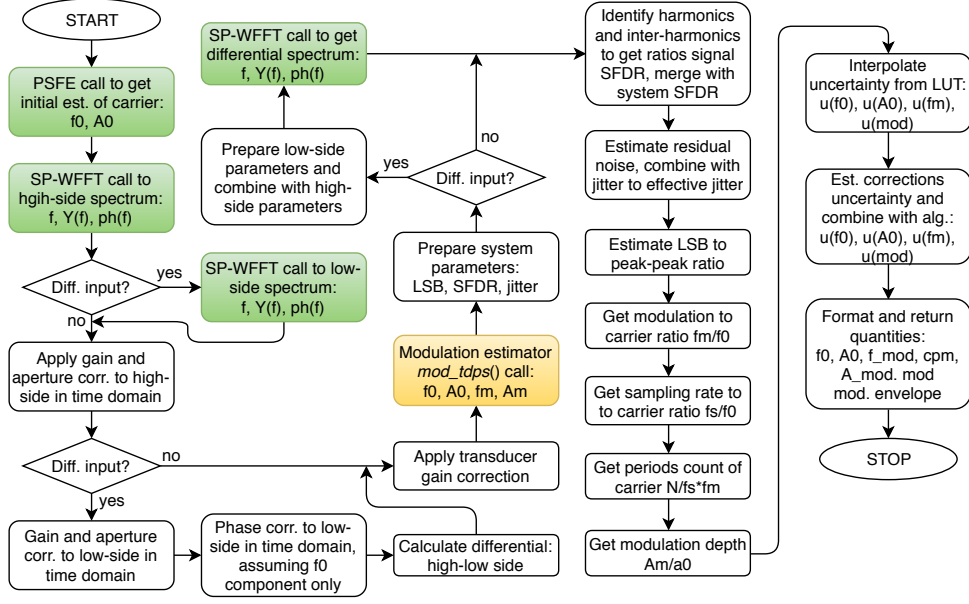


Figure 4: Overview of the TWM-MODTDPS algorithm wrapper. Green cells are calls to other QWTB wrappers. Gold blocks are calls of the local functions which are described in the text.

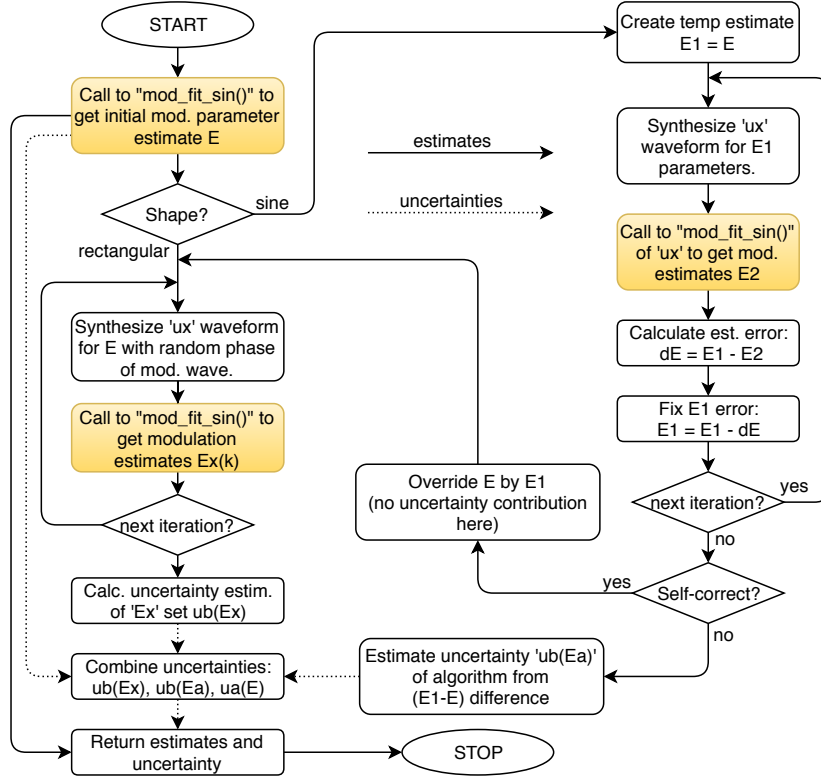


Figure 5: Overview of the “mod\_tdps()” function of the TWM-MODTDPS algorithm wrapper. Gold blocks are calls of local functions of the algorithm.

two virtual quadrature signals (analytical signals):

$$ya(t) = y(t) + j \cdot y\left(t + \frac{\pi}{2 \cdot f_0}\right), \quad (8)$$

$$yb(t) = y(t) - j \cdot y\left(t - \frac{\pi}{2 \cdot f_0}\right), \quad (9)$$

$$15 \quad (10)$$

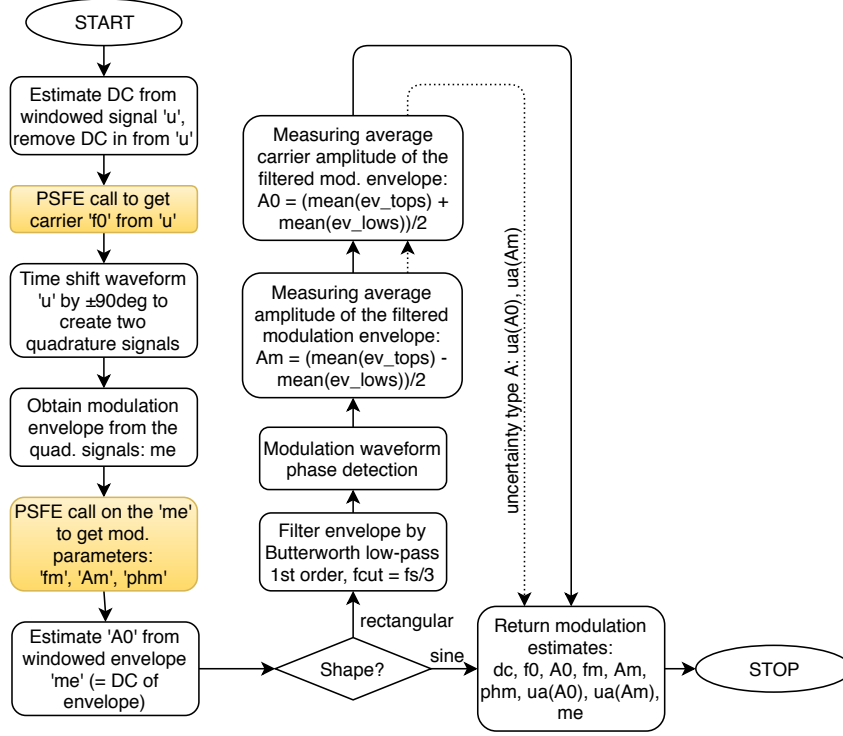


Figure 6: Overview of the “mod\_fit\_sin()” function of the TWM-MODTDPS algorithm wrapper. Gold blocks are calls of local functions of the algorithm.

The average of amplitudes of the signals  $ya(t)$  and  $yb(t)$  is roughly equal to the modulation envelope:

$$ev(t) = 0.5 \cdot (|ya(t)| + |yb(t)|) \quad (11)$$

The envelope  $ev(t)$  is used as an input to the next call of the PSFE algorithm which returns modulation amplitude  $Am$ , modulation frequency  $fm$  and modulation phase  $phm$ . The algorithm differs for the sinusoidal and rectangular wave shape from this point.

In the sinusoidal mode, the carrier amplitude  $A0$  is obtained as a DC value of the envelope  $ev(t)$  using a windowed average method with Blackman window:

$$A0 = \frac{\sum_{t=1}^N w(t) \cdot e(t)}{\sum_{t=1}^N w(t)}, \quad (12)$$

where the  $w(t)$  are coefficients of the Blackman window and  $N$  is samples count of the envelope. This trivial method obtains acceptable suppression of errors caused by the non-coherent window size if at least three modulating periods were recorded.

In the rectangular mode, the  $A0$  from PSFE cannot be used. Only the modulation frequency estimate  $fm$  and phase estimate  $phm$  are relevant. The envelope  $ev(t)$  is filtered by a low-pass 1st order Butterworth filter with cutoff frequency  $fs/6$ . This reduces the noise caused by the harmonic and inter-harmonic spurs present in the envelope  $ev(t)$  but does not distort the shape too much at high modulation frequencies. Next, the phase  $phm$  of the modulation wave is used to detect the tops and lows of the filtered envelope rectangular wave. It was experimentally decided to use 15 % to 30 % of the periods for detection of the tops and 75 % to 85 % for the lows. The modulation parameters are calculated according to formulas:

$$A0 = \frac{1}{2M} \sum_{m=1}^M [\text{tops} \{ev(t), m\} - \text{lows} \{ev(t), m\}], \quad (13)$$

$$Am = \frac{1}{2M} \sum_{m=1}^M [\text{tops} \{ev(t), m\} + \text{lows} \{ev(t), m\}], \quad (14)$$



where  $m$  is the period index and  $M$  is total count of modulation periods in the signal. The type A uncertainty estimate is calculated from the differences between the periods  $m$ .

In the sine wave mode, the algorithm also contains a self-correcting routine that is capable to reduce the inherent error of the algorithm itself (see diagram in fig. 5). The idea is following: First, the algorithm core function “mod\_fit\_sin()” is called on the real waveform data  $y$  to obtain the initial estimate  $E$  of the modulation parameters. Next, a new simulated waveform  $y_{\text{sim}}$  is synthesized so it has the modulation parameters  $E$ . The core function “mod\_fit\_sin()” is called again on the waveform  $y_{\text{sim}}$  to obtain estimates  $E2$ . Finally, an algorithm error  $dE = E2 - E$  is calculated. The whole operation is repeated three times in a loop which was sufficient to get stable error  $dE$ . The  $dE$  is either used as a correction to the initial  $E$  (when self-correction is enabled) or it is used to estimate algorithm error uncertainty contribution, when self-correction is disabled. This method significantly reduced the error of the algorithm even for high modulation frequencies. The performance was evaluated so the uncertainty calculation reflects sensitivity of this method to the imperfect input signal.

The “mod\_tdps()” function automatically calculates estimate of maximum error caused by the uncertain phase shift of the modulating waveform. It is calculated by repeating the estimator 10 times for different phase shifts and calculating maximum error. This is part of the total uncertainty budget.

## 2.3 Uncertainty estimator

The algorithm is too complex for evaluation of the uncertainty following the GUM guide. It is also relatively slow, so the Monte-Carlo uncertainty calculation for an interactive application would be too slow especially for waveforms longer than few thousand of samples. Therefore, a fast uncertainty estimator was developed. The estimator is based on the massive lookup tables (LUT) that contains precalculated uncertainties for various combinations of the parameters of the input signal.

First step for creation of the estimator was selection of the relevant signal parameters. The set was chosen so it is minimalist, because each parameter means one more dimension of the simulation and thus additional data in the LUT. Selection is follows:

1. **Modulating periods count:** The count of modulating signal periods in the recored waveform.
2. **Samples per period of carrier:** The ratio of sampling rate and carrier frequency  $fs/f0$ .
3. **Relative modulation frequency:** The ratio of the modulating frequency to carrier  $fm/f0$ .
4. **Total SFDR:** Combination of system SFDR (corrections) and signal SFDR (harmonics and interharmonics).
5. **Effective jitter:** Total effective sampling jitter in seconds. This also includes equivalent value of the residual RMS noise found in the signal. The jitter value is normalized to the carrier frequency.
6. **Bit resolution:** The bits count per used peak-to-peak ADC range. This is theoretically replaceable by rms noise, but it may easily lead to nonlinear behaviour for low resolutions. Therefore, this parameter was simulated separately.
7. **Modulation depth:** The ratio of the modulating amplitude to the carrier amplitude  $Am/A0$ .

The simulation ranges of the parameters were chosen according to table 8. The ranges were chosen to cover the typical operating range, however most of the dependencies are extrapolable in one direction.

Fro simplicity it was assumed all the parameters may be correlated, so all combinations of the seven parameters were generated ( $6 \times 5 \times 8 \times 4 \times 5 \times 6 \times 8 = 230400$  combinations). At least 1000 Monte-Carlo (MC) iteration cycles of following sequence of operations was performed for each combination:

1. Get one combination of simulation parameters  $E_{ref}$ .
2. Randomize  $E_{ref}$  parameters in a small range (few percent), so each MC iteration generates a bit different signal. This is to prevent unfortunate selection of a combination  $E_{ref}$  where the uncertainty is exceptionally low, e.g. due to the coherent sampling.
3. Generate other random parameters, such as DC offset, phase shift of the modulation signal, random spurs up to SFDR parameter value, etc.

Table 8: Simulation ranges and steps of the parameters for uncertainty estimator of MODTDPS algorithm.

Name	Description
Modulating periods count	Log. space: 3 to 30, 6 steps
Samples per period of carrier	Log. space: 10 to 100, 5 steps
Relative modulation frequency	Log. space: 0.01 to 0.33, 8 steps
Total SFDR	List: [120; 80; 60; 30] dB, 4 steps
Effective jitter	Log. space: $10^{-9}$ to $10^{-2}$ , 5 steps
Bit resolution	Log. space: 6 to 24 bits, 6 steps
Modulation depth	Log. space: 0.01 to 0.99, 8 steps

4. Synthesize modulated waveform of known parameters.
5. Distort the waveform by: spurs, jitter, quantisation, etc.
6. Perform estimation of the modulation parameters  $E_x$  by “mod.tdps()” algorithm. Note the uncertainties returned by the “mod.tdps()” itself are ignored, as they will be calculated on runtime during actual measurements.
7. Compare estimates  $E_x$  to generated parameters  $E_{ref}$ :  $\Delta E_x(k) = E_x - E_{ref}$ .

The set of algorithm errors  $\Delta E_x(k)$  from the MC iterations  $k$  for each combination of parameters is processed according to the GUM guide, supplement 1 [1]. The whole batch of combinations was processed on the supercomputer, so it took only three days per configuration (“sine”, “rect”, with or without self-corrections). The 1000 MC cycles was enough to obtain stable estimates. Output of the calculation is 7-dimensional matrix of uncertainties of modulation parameters:  $f_0$ ,  $f_m$ ,  $A_0$  and  $A_m$ . The 7D array was manually inspected along various axes (= along simulation parameters), however it was not possible to find a simple empiric formulas that would cover full range of any axis. There were always some non-linearity dependencies on the other axes. All tries resulted either in significant over or underestimation of uncertainty in some part of the parameter space.

Therefore, the whole 7D matrix was simply compressed to the log. space and 16bit integers (resolution better 0.005) and saved to a compressed MAT file as lookup table (LUT). The size of LUT is roughly 1.7 MBytes per configuration which is still acceptable and thus it was decided to not continue with further optimisations. The LUT contains definitions of the axes (parameters), their permissible ranges, interpolation modes (linear or logarithmic) and definition of the estimator action, when the parameter is out of range (error or limit at max/min known value). A multidimensional interpolator was developed which is capable to read the LUT and return interpolated values of the quantities stored in the LUT. The usable range of parameters is shown in the table 9. Note the interpolator permits to extrapolate outside the stated limits, which should prevent problems around the limits. The additional permissible range is set to up to  $\pm 5\%$  of given range.

Table 9: Permissible range of signal parameters for the uncertainty estimator. The values in parenthesis are permissible, but outside simulation range. The actions when the min or max value of axis is reached are: “error” - generate error; “const” - return value of uncertainty at min. or max. of simulated range.

Name	Range	On min	On max
Modulating periods count	3 to 30 (3 to $\infty$ )	error	const
Samples per period of carrier	10 to 100 (10 to $\infty$ )	error	const
Relative modulation frequency	0.01 to 0.33 (0 to 0.33)	const	error
Total SFDR	120 to 30 dB ( $\infty$ to 30 dB)	error	const
Effective jitter	$10^{-9}$ to $10^{-2}$ ( $10^{-\infty}$ to $10^{-2}$ )	const	error
Bit resolution	6 to 24 bits (6 to $\infty$ bits)	error	const
Modulation depth	0.01 to 0.99	error	error

The estimator itself in the TWM-MODTDPS wrapper is based on the estimated modulation parameters and spectrum analysis of the input signal  $y$ . It obtains the parameters of the LUT axes by following procedure:

1. Calculate the basic parameters from corrections and estimated modulation parameters: (i) Modulating periods count; (ii) Samples per period of carrier; (iii) Relative modulation frequency; (iv) Modulation depth; (v) Bit resolution.
2. Perform spectrum analysis to obtain: (i) Harmonics (except the ones belonging to modulation sidebands); (ii) Interharmonics; (iii) RMS noise estimate. These value are used to calculate signal SFDR estimate and noise, which is converted to equivalent jitter at the carrier frequency  $f_0$ .
3. Interpolate the LUT table for given configuration to get the algorithm uncertainty.
4. Calculate estimate of uncertainty of the corrections. This covers estimate of the error caused by the fact the signal scaling is made at a single frequency spot  $f_0$  instead of complicated frequency dependent correction.
5. Combine uncertainties: (i) Runtime calculated uncertainty from “mod.tdps()” itself; (ii) Uncertainty from the LUT table; (iii) Uncertainty of the corrections.

## 2.4 Validation

The algorithm TWM-MODTDPS has many input quantities (71 in differential transducer input mode) and some of them are matrices. That is too many possible degrees of freedom. Thus, varying the quantities in some systematic way would be very complicated if the validation should cover full range of used signals and corrections. Therefore, an alternative approach was used.

QWTB test function “alg.test.m” was created, which performs the validation using randomly generated test setups. It randomizes the signal parameters, correction quantities and uncertainties and algorithm configurations in ranges expected to occur during the real measurements. The test is run many times to cover full operating range of the algorithm. Following operations are performed for each random test setup:

1. Generate signal  $y$  with known modulation parameters  $M_{\text{ref}}$ .
2. Distort the signal  $y$  by inverse corrections, i.e. simulate the transducers, and digitizer (e.g. gain errors, quantisation, SFDR ...).
3. Run the algorithm TWM-MODTDPS with enabled uncertainty evaluation to obtain the harmonic levels  $M_x$  and their uncertainties  $u(M_x)$ .
4. Compare the reference and calculated harmonics and distortion and check if the deviations are lower than assigned uncertainties:

$$\text{pass}(i) = |(M_{\text{ref}} - M_x)| < u(M_x), \quad (15)$$

where  $i$  is test run index.

5. Repeat  $N$  times from step 1, with the same test setup parameters, but with randomised corrections by their uncertainties, and with randomised noise, SFDR and jitter.
6. Check that at least 95 % of  $\text{pass}(i)$  results passed (for 95 % level of confidence). The evaluation is made for each estimated modulation parameter separately. So it is possible to inspect which parameter fails.

The test runs count per test setup was set to  $N = 500$ , which is far from optimal infinite set, but due to the computational requirements it could not have been much higher.

The algorithm in the uncertainty estimation mode was tested in 6 different configurations with at least 5000 test setups per each. I.e. the algorithm was ran 15 million times in total (6x5000x500). The processing itself was performed on a supercomputer [4] and it took about 15 days at 300 parallel octave instances.

The randomization ranges of the signal are shown in table 10. The randomization ranges of the corrections are shown in table 11.

The test results were split into several groups given by the randomiser setup: (i) Wave shape; (ii) Randomisation of corrections by uncertainty enabled/disabled. When the randomisation of corrections is

disabled, the test runs cover only the algorithm itself and the contributions of the correction uncertainties are ignored.

The summary of the validation test results is shown in table 12. The success rate without corrections randomisation was close to 100 %. The success rate with corrections randomisation was a bit worse, because the success rate of the individual test runs within the test setup was just around 95 %. Therefore, the decision pass/fail is problematic. The obtained set of test results was manually investigated and no cases with far outliers were detected, e.g. the failed test setups contained occasional estimates offsets just around the uncertainty boundaries. Also no cases where all test runs failed were found.

Table 10: Validation range of the signal for TWM-MODTDPS algorithm.

<b>Parameter</b>	<b>Range</b>
Sampling rate	9 to 11 kHz (no need to randomize in wider range, as all other parameters are generated relative to this rate).
Samples count	3 to 100 kSamples.
Carrier frequency	Random, so it is higher than 50 Hz and there are at least 10 samples per period.
Carrier amplitude	Random from 10 to 100% of nominal input range.
Modulating frequency	Random, so there are always at least 3 modulating periods in the record and so the ratio to carrier frequency is up to 32% (24% for rectangular wave shape).
Modulating depth	Random, 2 to 98%.
DC offset	Random up to $\pm 2\%$ of carrier amplitude.
Phase angle	Random for carrier, modulating frequency and spur harmonics.
SFDR	-100 to -60 dBc, 10 harmonic spurs of carrier, each spur has random level up to SFDR, frequencies are randomised by $\pm 10\%$ of carrier frequency.
Digitizer RMS noise	1 to 50 $\mu\text{V}$ .
Sampling jitter	1 to 100 ns.

Table 11: Validation range of the correction for the TWM-MODTDPS algorithm.

Parameter	Range
Transducer type	Random 'shunt' or 'rvd'.
Nominal input range	5 to 70 V (5 to 70 A)
Aperture	1 ns to 100 $\mu$ s
Digitizer gain	Randomly generated frequency transfer simulating NI 5922 FIR-like gain ripple (possibly the worst imaginable shape) and some ac-dc dependence. The transfer matrix has up to 50 frequency spots. Nominal gain value is random from 0.95 to 1.05 with uncertainty 5 to 50 $\mu$ V/V. Maximum ac-dc value at $fs/2$ is up to $\pm 1\%$ with uncertainty up to 250 $\mu$ V/V. Gain ripple amplitude is random from 0.005 to 0.03 dB with up to 5 periods between 0 and $fs/2$ .
Digitizer SFDR	Value based on table 10.
Transducer SFDR	Value based on table 10. Note the "SFDR" from table 10 is randomly split between digitizer and transducer SFDR correction.
Digitizer DC offset	$\pm 2$ mV with uncertainty 0.1 mV.
Digitizer bit resolution	16 to 28 bits.
Digitizer nominal range	1 V
Transducer gain	Randomly generated frequency transfer. The transfer matrix has 30 to 50 frequency spots. Nominal gain value is random (see above) with relative uncertainty 50 $\mu$ V/V. Maximum ac-dc value at $fs/2$ is up to $\pm 2\%$ with uncertainty up to 250 $\mu$ V/V. Gain ripple amplitude is 0.005 dB with 4 to 10 periods between 0 and $fs/2$ .

Table 12: Validation results of the algorithm TWM-MODTDPS. The "passed test" shows percentage of passed tests under conditions defined in tables 10 and 11.

Wave shape	Self-corr.	Rand. corr.	Passed test [%]			
			$A_0$	$A_m$	$f_0$	$f_m$
sine	on	no	100.00	100.00	100.00	100.00
		yes	100.00	100.00	100.00	100.00
sine	off	no	100.00	100.00	100.00	99.98
		yes	100.00	100.00	100.00	100.00
rect	off	no	100.00	100.00	100.00	100.00
		yes	100.00	100.00	100.00	100.00

## References

- [1] JCGM. *Evaluation of measurement data - Supplement 1 to the "Guide to the expression of uncertainty in measurement" - Propagation of distributions using a Monte Carlo method*. Bureau International des Poids et Mesures.
- [2] Rado Lapuh. Estimating the fundamental component of harmonically distorted signals from noncoherently sampled data. *IEEE Transactions on Instrumentation and Measurement*, 64(6):1419–1424, June 2015.
- [3] Stanislav Mašláň. Activity A2.3.2 - Algorithms Exchange Format. <https://github.com/smaslan/TWM/tree/master/doc/A232AlgorithmExchangeFormat.docx>.
- [4] Miroslav Valtr. ČMI HPC System Online. [https://translate.google.cz/translate?sl=cs&tl=en&js=y&prev=\\_t&hl=cs&ie=UTF-8&u=http%3A%2F%2Fprutok.cmi.cz%2Fsc%2Fdoku.php%3Fid%3Dsystem&edit-text=](https://translate.google.cz/translate?sl=cs&tl=en&js=y&prev=_t&hl=cs&ie=UTF-8&u=http%3A%2F%2Fprutok.cmi.cz%2Fsc%2Fdoku.php%3Fid%3Dsystem&edit-text=), 2014.

### 3 TWM-FPNLSF - Four Parameter Non Linear Sine Fit

This algorithm fits a sine wave to the recorded data by means of non-linear least squares fitting method using 4 parameter (frequency, amplitude, phase and offset) model. Due to non-linear characteristic, convergence is not always achieved. When run in Matlab, function “lsqnonlin” in Optimization toolbox is used. When run in GNU Octave, function “leasqr” in GNU Octave Forge package optim is used. Therefore results can differ.

This algorithm, in general, is not suitable for distorted signals. It offers good results for signals with low harmonic content if at least 10 periods of signal are recorded with preferably at least 50 samples per period. The algorithm also requires initial estimate of the frequency accurate to  $\pm 500$  ppm.

The algorithm supports differential transducer connection. The integrated uncertainty estimator was developed only for the GNU Octave version. This should be still kept in mind when using the algorithm with Matlab despite the Matlab version seems to give always more accurate results than GNU Octave.

#### 3.1 TWM wrapper parameters

The input quantities supported by the algorithm are shown in the table 13. Algorithm returns output quantities shown in the table 14. Calculation setup supported by the algorithm is shown in table 15.

Table 13: List of input quantities to the TWM-FPNLSF wrapper.  
Details on the correction quantities can be found in [3].

Name	Default	Unc.	Description
f_est	N/A	N/A	Initial estimate of the sine frequency. The estimate should be accurate to at least 500 ppm.
comp_timestamp	0	N/A	Enable compensation of phase shift by time stamp value: $\phi' = \phi - 2 \cdot \pi \cdot f_{fit} \cdot time\_stamp$ .
y	N/A	No	Input sample data vector and complementary low-side input data vector <i>y_lo</i> for differential mode only.
y_lo	N/A	No	
Ts	N/A	No	Sampling period or sampling rate or sample time vector.
fs	N/A	No	Note the wrapper always calculates in equidistant mode, so <i>t</i> is used just to calculate <i>Ts</i> .
t	N/A	No	
lsb	N/A	No	Either absolute ADC resolution <i>lsb</i> or nominal range value
adc_nrng	1000	No	<i>adc_nrng</i> (e.g.: 5 V for 10 Vpp range) and <i>adc_bits</i> bit resolution of ADC.
adc_bits	40	No	
lo_lsb	N/A	No	
lo_adc_nrng	1000	No	
lo_adc_bits	40	No	
adc_offset	0	Yes	Digitizer input offset voltage.
lo_adc_offset	0	Yes	
adc_gain	1	Yes	Digitizer gain correction 2D table (multiplier).
adc_gain_f	□	No	
adc_gain_a	□	No	
lo_adc_gain	1	Yes	
lo_adc_gain_f	□	No	
lo_adc_gain_a	□	No	
adc_phi	0	Yes	Digitizer phase correction 2D table (additive).
adc_phi_f	□	No	
adc_phi_a	□	No	
lo_adc_phi	0	Yes	
lo_adc_phi_f	□	No	
lo_adc_phi_a	□	No	

Table 13: List of input quantities to the TWM-FPNLSF wrapper.  
Details on the correction quantities can be found in [3].

Name	Default	Unc.	Description
adc_freq	0	Yes	Digitizer timebase error correction: $f_{tb}' = f_{tb} \cdot (1 + adc\_freq.v)$ The effect on the estimated frequency is opposite: $f_{est}' = f_{est} / (1 + adc\_freq.v)$
adc_jitter	0	No	Digitizer sampling period jitter [s].
adc_aper	0	No	ADC aperture value [s].
adc_aper_corr	0	No	ADC aperture error correction enable: $A' = A \cdot pi \cdot adc\_aper \cdot f_{est} / \sin(pi \cdot adc\_aper \cdot f_{est})$ $phi' = phi + pi \cdot adc\_aper \cdot f_{est}$
lo_adc_aper	0		
time_stamp	0	Yes	Relative timestamp of the first sample $y$ .
time_shift_lo	0	Yes	Low-side channel time shift [s].
adc_sfdr	180	No	Digitizer SFDR 2D table.
adc_sfdr_f	□	No	
adc_sfdr_a	□	No	
lo_adc_sfdr	180	No	
lo_adc_sfdr_f	□	No	
lo_adc_sfdr_a	□	No	
adc_Yin_Cp	1e-15	Yes	Digitizer input admittance 1D table.
adc_Yin_Gp	1e-15	Yes	
adc_Yin_f	□	No	
lo_adc_Yin_Cp	1e-15	Yes	
lo_adc_Yin_Gp	1e-15	Yes	
lo_adc_Yin_f	□	No	
tr_type	“”	No	Transducer type string (“rvd” or “shunt”).
tr_gain	1	Yes	Transducer gain correction 2D table (multiplicative).
tr_gain_f	□	No	
tr_gain_a	□	No	
tr_phi	0	Yes	Transducer phase correction 2D table (additive).
tr_phi_f	□	No	
tr_phi_a	□	No	
tr_sfdr	180	No	Transducer SFDR 2D table.
tr_sfdr_f	□	No	
tr_sfdr_a	□	No	
tr_Zlo_Rp	1e3	Yes	RVD transducer low-side impedance 1D table. Note this is related to loading correction and it has effect only for RVD transducer and will work only if $adc\_Yin$ is defined as well.
tr_Zlo_Cp	1e-15	Yes	
tr_Zlo_f	□	No	
tr_Zbuf_Rs	0	Yes	Loading corrections: Transducer output buffer output series impedance 1D table. Leave unassigned to disable buffer from the correction topology.
tr_Zbuf_Ls	0	Yes	
tr_Zbuf_f	□	No	
tr_Zca_Rs	1e-9	Yes	Loading corrections: Transducer high side terminal series impedance 1D table.
tr_Zca_Ls	1e-12	Yes	
tr_Zca_f	□	No	
tr_Zcal_Rs	1e-9	Yes	Loading corrections: Transducer low side terminal series impedance 1D table.
tr_Zcal_Ls	1e-12	Yes	
tr_Zcal_f	□	No	
tr_Yca_Cp	1e-15	Yes	Loading corrections: Transducer output terminals shunting impedance.
tr_Yca_D	1e-12	Yes	
tr_Yca_f	□	No	
tr_Zcam	1e-12	Yes	Loading corrections: Transducer output terminals mutual inductance 1D table.
tr_Zcam_f	□	No	

Table 13: List of input quantities to the TWM-FPNLSF wrapper.  
Details on the correction quantities can be found in [3].

Name	Default	Unc.	Description
Zcb_Rs	1e-9	Yes	Loading corrections: Cable series impedance 1D table.
Zcb_Ls	1e-12	Yes	
Zcb_f	<input type="checkbox"/>	No	
Ycb_Rs	1e-15	Yes	Loading corrections: Cable series impedance 1D table.
Ycb_Ls	1e-12	Yes	
Ycb_f	<input type="checkbox"/>	No	

Table 14: List of output quantities of the TWM-FPNLSF wrapper.

Name	Uncertainty	Description
f	Yes	Frequency of the carrier [Hz].
A	Yes	Amplitude of the carrier.
phi	Yes	Phase of main signal component [rad].
ofs	Yes	DC offset of signal.

Table 15: List of “calcset” options supported by the TWM-FPNLSF wrapper.

Name	Description
calcset.unc	Uncertainty calculation mode. Supported: “none” or “guf” for uncertainty estimator.
calcset.loc	Level of confidence [-].
calcset.verbose	Verbose level.

### 3.2 Algorithm description

The wrapper TWM-FPNLSF overview is shown in fig. 7. It first calls the core function “FPNLSF\_loop()” on the unscaled high-side input signal  $y$  to get initial estimate of the signal frequency  $fx$ . This is necessary to get gain and phase correcting coefficients. Follows the signal scaling in the time domain, i.e. application of the digitizer DC offset, gain, phase and aperture corrections.

The wrapper also allows differential input sensor connection. In this case it compensates the high-low side phase error by time shifting the low-side signal  $y_{lo}$  according to the estimated frequency component  $fx$ . Such a phase correction of course works only for the single frequency component  $fx$ , but the results were acceptable as it is the main signal component. Next, it calculates differential signal  $y_d = y - y_{lo}$ . Only additional difference is the TWM defines relatively complex transducer loading corrections scheme (see [2]). This is ensured by the function “correction\_transducer\_loading()”. However, the function operates in frequency domain, whereas FPNLSF operates in time domain and the algorithm expects non-coherent sampling. Therefore, an additional step is done to obtain scaling transducer correction factor. The windowed FFT of the high and low-side signals  $y$  and  $y_{lo}$  is calculated by “SP-WFFT” algorithm. The voltage vectors are obtained from the FFTs are used as an inputs to the “correction\_transducer\_loading()”. Although the voltage vectors are distorted by the spectral leakage, their ratio stays unaffected, so the transducer scaling factor obtained from the “correction\_transducer\_loading()” is sufficiently accurate. At this point, the differential signals  $y$  and  $y_{lo}$  are reduced to single ended signal  $y_d$  which is correctly scaled. The “FPNLSF\_loop()” is called again on the differential signal  $y_d$ . Next calculation steps are identical for single ended and differential modes.

The FPNLSF algorithm itself and its uncertainty analysis was described in [4]. The basic principle is use of the non-linear least square minimising algorithm to fit the input signal  $y$  by a four parameter sine wave model:

$$y_m = o + A \cdot \sin(2\pi ft + \phi), \quad (16)$$



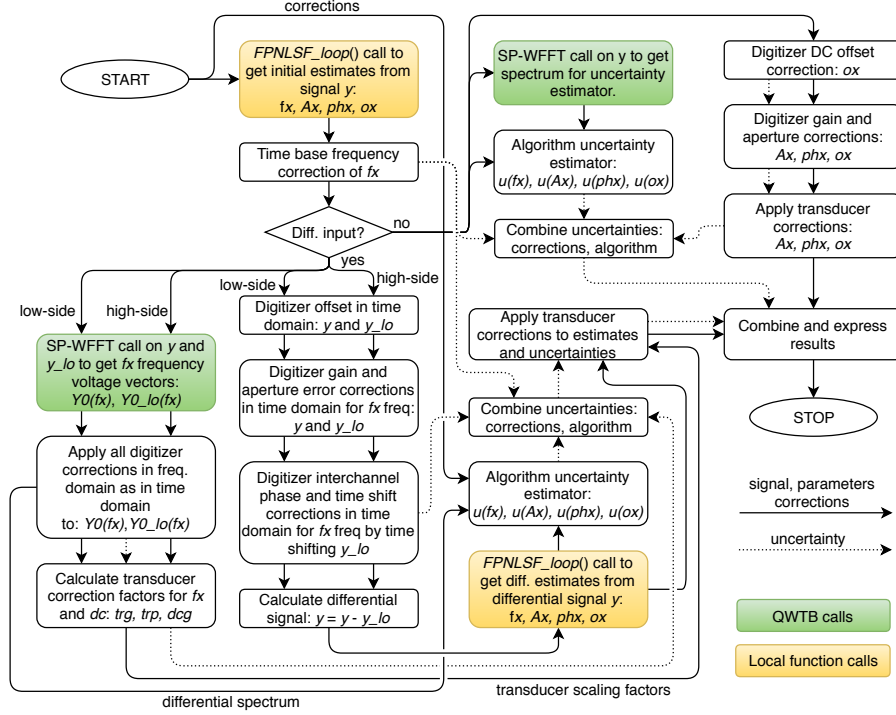


Figure 7: Overview of the TWM-FPNLSF algorithm wrapper.

where  $o$  is DC offset,  $A$  is amplitude,  $t$  is time vector,  $f$  is sine frequency and  $\phi$  is phase angle. This method is quite sensitive to harmonics and especially interharmonics and also requires good initial estimates for the minimising algorithm, however for clean signals it offers acceptable estimates of the fundamental component.

The core function of the TWM-FPNLSF wrapper is function “FPNLSF\_loop()”. Structure is shown in fig. 8. The function accompanies the FPNLSF algorithm itself by several supporting functions. First major problem to solve was its sensitivity to the precision of initial estimate of the parameters, especially frequency  $f_{est}$ . It was merely impossible to perform the Monte Carlo (MC) uncertainty calculation of the FPNLSF itself as the FPNLSF minimising process often ended in a local minima, which is not always detectable. So the histogram of the MC iterations contained many far outliers, which made the uncertainty unusable. Therefore, the permissible range of initial estimate  $f_{est}$  was set to  $\pm 500$  ppm from the actual signal frequency. The FPNLSF was placed in a retry loop that tries repeatedly run the FPNLSF with slightly randomised initial estimates until the fitted frequency  $f$  is within the  $\pm 500$  ppm range. The retry loop also contains limit for the total retries count and total timeout, so it won't get locked up. The loop was also accompanied by initial zero cross estimation, which tries to obtain at least approximate initial phase estimate.

### 3.3 Uncertainty estimator

The algorithm is too complex for GUF uncertainty calculation. It is also relatively slow, so the Monte-Carlo uncertainty calculation for an interactive application would be too slow especially for waveforms longer than few thousand samples. Therefore, a fast uncertainty estimator was developed. The estimator is based on the lookup tables (LUT) that contains precalculated uncertainties for various combinations of the input signal parameters.

First step for creation of the estimator was selection of the relevant signal parameters. The set was chosen so it is minimalist, because each parameter means one more dimension of the simulation and thus additional data in the LUT. Selection is follows:

1. **Periods count:** The count of signal periods in the recored waveform.
2. **Samples per period:** The ratio of sampling rate and fundamental frequency  $fs/f_0$ .

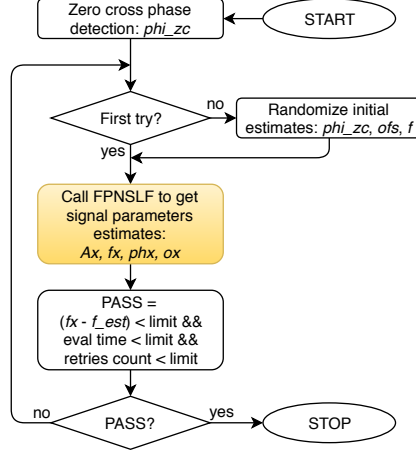


Figure 8: The structure of the “FPNLSF\_loop()” function of the TWM-FPNLSF algorithm wrapper.

3. **Total SFDR:** Combination of system SFDR (corrections) and signal SFDR (harmonics and interharmonics).
4. **Effective jitter:** Total effective sampling jitter in seconds. This also includes equivalent value of the residual RMS noise found in the signal. The jitter value is normalized to the carrier frequency.
5. **Bit resolution:** The bits count per used peak-to-peak ADC range. This is theoretically replaceable by the jitter (resp. noise), but it may easily lead to nonlinear behaviour for low resolutions. Therefore, this parameter was simulated separately.

The simulation ranges of the parameters were chosen according to table 16. The ranges were chosen to cover the typical operating range, however most of the dependencies is extrapolable in one direction.

Table 16: Simulation ranges and steps of the parameters for uncertainty estimator of “FPNLSF\_loop()” function.

Name	Description
Periods count	List: [10; 20; 50; 100], 4 steps
Samples per period	Log. space: 10 to 1000, 10 steps
Total SFDR	List: [180; 120; 80; 40; 30] dB, 4 steps
Effective jitter	Log. space: $10^{-9}$ to $10^{-2}$ , 9 steps
Bit resolution	Log. space: 4 to 24 bits, 8 steps

Fro simplicity it was assumed all the parameters may be correlated, so all combinations of the five parameters were generated ( $4 \times 10 \times 4 \times 9 \times 8 = 11520$  combinations). 1000 Monte-Carlo (MC) iteration cycles of following sequence of operations was performed for each combination:

1. Get one combination of simulation parameters  $E_{ref}$ .
2. Randomize  $E_{ref}$  parameters in a small range (few percent), so each MC iteration generates a bit different signal. This is to prevent unfortunate selection of a combination  $E_{ref}$  where the uncertainty is exceptionally low, e.g. due to the coherent sampling.
3. Generate other random parameters, such as DC offset, phase shift of the signal, random spurs up to SFDR parameter value, etc.
4. Synthesize modulated waveform of known parameters.
5. Distort the waveform by: spurs, jitter, quantisation, etc.
6. Perform estimation of the signal parameters  $E_x$  by “FPNLSF\_loop()” algorithm.

7. Compare estimates  $E_x$  to generated parameters  $E_{ref}$ :  $\Delta E_x(k) = E_x - E_{ref}$ .

The set of algorithm errors  $\Delta E_x(k)$  from the MC iterations  $k$  for each combination of parameters was processed according to the GUM guide, supplement 1 [1]. The whole batch of combinations was processed on the supercomputer, so it took only two days. The 1000 MC cycles was enough to obtain stable estimates. Output of the calculation was a 5-dimensional matrix of uncertainties of signal parameters estimates: frequency, amplitude, phase and DC offset. The 5D array was manually inspected along various axes (= along simulation parameters) to verify there are no extrema. As the array is relatively small it was decided to not look for empirical formulas to reduce the axes. Therefore, the whole 5D matrix was simply compressed to the log. space and 16bit integers (resolution better 0.005) and saved to a compressed MAT file as lookup table (LUT). The size of LUT is roughly 120 kBytes, which is still acceptable. The LUT contains definitions of the axes (parameters), their permissible ranges, interpolation modes (linear or logarithmic) and definition of the estimator action, when the parameter is out of range (error or limit at max/min value). A multidimensional interpolator was developed which is capable to read the LUT and return interpolated values (or errors) of the quantities stored in the LUT. The usable range of parameters is shown in the table 17. Note the interpolator permits to extrapolate outside the stated limits, which should prevent problems around limits. The additional permissible range is set to up to  $\pm 5\%$  of given axis range.

Table 17: Permissible range of signal parameters for the uncertainty estimator of “FPNLSF.loop()” function. The values in parenthesis are permissible, but outside simulation range. The actions when the min or max value is reached are: “error” - generate error; “const” - return value of uncertainty at min. or max. of simulated range.

Name	Range	On min	On max
Periods count	10 to 100 (10 to $\infty$ )	error	const
Samples per period	10 to 1000 (10 to $\infty$ )	error	const
Total SFDR	180 to 30 dB ( $\infty$ to 30 dB)	error	const
Effective jitter	$10^{-9}$ to $10^{-2}$ ( $10^{-\infty}$ to $10^{-2}$ )	const	error
Bit resolution	4 to 24 bits (4 to $\infty$ bits)	error	const

The estimator itself in the TWM-FPNLSF wrapper is based on the estimated parameters of the signal returned by the “FPNLSF.loop()” and spectrum analysis of the input signal  $y$ . It obtains the parameters of the LUT axes by following procedure:

1. Calculate the basic parameters from corrections and estimated parameters: (i) Periods count; (ii) Samples per period; (iii) Bit resolution.
2. Perform spectrum analysis of  $y$  (or  $y_d$  for differential mode) to obtain: (i) Harmonics; (ii) Interharmonics; (iii) RMS noise estimate. These value are used to calculate signal SFDR estimate and noise, which is converted to the equivalent jitter at the fitted frequency  $fx$ .
3. Interpolate the LUT table for given parameters to get the algorithm uncertainty.
4. Calculate estimate of uncertainty of the corrections.
5. Combine uncertainties: (i) Uncertainty from the LUT table; (ii) Uncertainty of the corrections.

Note the precalculated LUT was calculated on the GNU Octave system, which is using different minimising algorithm than Matlab. However, the long validation test was performed with generating many random signal parameters and no case where the calculated estimates were outside the uncertainty were found for Matlab. In fact, the Matlab version seems to give much better results than GNU Octave. However, this fact should be still kept in mind, as there may be some case, where Matlab performs worse.

### 3.4 Validation

The algorithm TWM-FPNLSF has many input quantities and some of them are matrices. That is too many possible degrees of freedom. Thus, varying the quantities in some systematic way would be

very complicated if the validation should cover full range of used signals and corrections. Therefore, an alternative approach was used.

QWTB test function “alg\_test.m” was created, which performs the validation using randomly generated test setups. It randomizes the signal parameters, correction quantities and uncertainties and algorithm configurations in ranges expected to occur during the real measurements. The test is run many times to cover full operating range of the algorithm. Following operations are performed for each random test setup:

1. Generate signal with known frequency, amplitude, phase and DC of the fundamental signal.
2. Distort the signal by inverse corrections, i.e. simulate the transducers, and digitizer (e.g. gain errors, quantisation, SFDR ...).
3. Run the algorithm TWM-FPNLSF with enabled uncertainty evaluation to obtain the estimated values and corresponding uncertainties of frequency, amplitude, phase and DC of the fundamental signal.
4. Compare the reference and calculated values and check if the deviations are lower than assigned uncertainties.
5. Repeat  $N$  times from step 1, with different test setup parameters, different corrections randomised by their uncertainties, and with randomised noise, SFDR and jitter.
6. Check that at least 95 % of results passed (for 95 % level of confidence).

The total number of Monte-Carlo simulations was 100000. The parameters of the input signal, the digitizer and transducer settings were randomly varied. The sampling frequency was between 5 kHz and 500 kHz and the number of samples between 1 kSa and 200 kSa. The frequency of fundamental signal was between 0.5 Hz and 45 kHz. The frequency of the harmonics and interharmonics were always above frequency of the fundamental signal but below the Nyquist frequency. The number of harmonics that were added to the fundamental signal was generally 10, but the number was sometimes reduced if the Nyquist limit is to be exceeded. The number of interharmonics was 1. The amplitude of the fundamental signal was between 0.1 V and 10 V and the amplitude of the harmonics and interharmonics between 0.000001 and 0.01 of the amplitude of the fundamental signal. The DC was between -0.1 and +0.1 of the amplitude of the fundamental signal. The phases of the fundamental signal as well as of the harmonics and interharmonics were individually and randomly varied between +3.14 rad and -3.14 rad. The ADC noise was between  $1e-11$  and  $1e-3$  of the amplitude of the fundamental signal while the jitter was between  $1e-9$  s and  $1e-6$  s. ADC aperture was between  $1e-6$  s and  $4e-5$  s, ADC gain between 1 and 1.5, ADC phase between +1.57 rad and -1.57 rad, frequency correction of the digitizer timebase between  $-5e-3$  and  $5e-3$ , ADC offset between 0.005 V and 0.005 V (random value for low- and high-side channel) and number of bits between 22 and 24. Relative time-stamp of the first sample was varied between -10 s and 10 s. The transducer gain was between 0.5 and 20 and the transducer phase was between +1.57 rad and -1.57 rad. The resistive voltage divider low-side impedance value (i.e. resistance and capacitance) were between 100  $\Omega$  and 500  $\Omega$  and 0.1 pF and 10 pF, respectively (only resistive voltage divider was used in the simulations). The randomisation of corrections was also enabled which means that not only the uncertainty of the algorithm but also the contributions of the correction uncertainties were included in the Monte-Carlo simulations. The success rate of the TWM-FPNLSF algorithm for the frequency estimation was 99.70 %, amplitude estimation 98.36 %, phase estimation 99.36 % and DC offset estimation 99.07 %.

## References

- [1] JCGM. *Evaluation of measurement data - Supplement 1 to the “Guide to the expression of uncertainty in measurement” - Propagation of distributions using a Monte Carlo method*. Bureau International des Poids et Mesures.
- [2] Stanislav Mašláň. Activity A2.3.1 - Correction Files Reference Manual. <https://github.com/smaslan/TWM/tree/master/doc/A231CorrectionFilesReferenceManual.docx>.

- [3] Stanislav Mašláň. Activity A2.3.2 - Algorithms Exchange Format. <https://github.com/smaslan/TWM/tree/master/doc/A232AlgorithmExchangeFormat.docx>.
- [4] M. Šíra and S. Mašláň. Uncertainty analysis of non-coherent sampling phase meter with four parameter sine wave fitting by means of monte carlo. In *29th Conference on Precision Electromagnetic Measurements (CPEM 2014)*, pages 334–335, Aug 2014.

## 4 TWM-HCRMS - Half Cycle RMS algorithm

Algorithm for calculation of the so called half cycle RMS values or sliding window RMS values of a single phase waveform. It calculates RMS value of signal in length of one period with window step defined by the method of calculation. That is, according to the IEC 61000-3-40: (i) Class A - half-cycle step; (ii) Class S - “sliding window” step (20 windows per period for this implementation). Examples of the calculated values for the modes A and S are shown in fig. 9.

The algorithm is designed so it can handle non-coherent sampling and also it is capable to compensate slow frequency drifts. It uses PSFE and resampling technique to ensure coherent sampling internally. The user can enter signal frequency manually if coherent sampling was ensured by the digitizer.

In general, the algorithm will work better with higher sampling rates. At least 100 samples should be recorded per period of the fundamental component (= sampling rate 5 kSa/s for 50 Hz networks). The higher is better, because the RMS algorithm will better suppress the harmonic and interharmonic content.

The algorithm is for single-ended input only and it is equipped with fast uncertainty estimator.

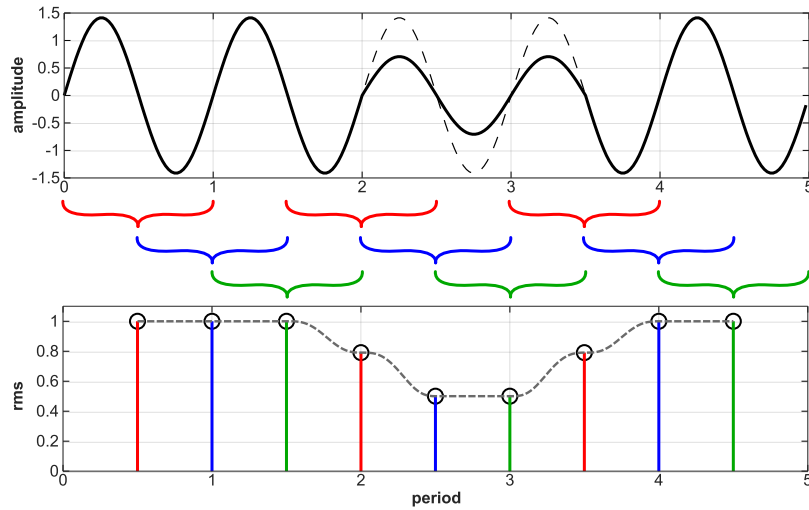


Figure 9: Example of Half Cycle RMS calculation for a “dip” event. The circles in RMS plot show values calculated according IEC 61000-3-40 “class A”, the dashed line shows result of sliding window mode for “class S”.

### 4.1 TWM wrapper parameters

The input quantities supported by the algorithm are shown in the table 18. Algorithm returns output quantities shown in the table 19. Calculation setup supported by the algorithm is shown in table 20.

Table 18: List of input quantities to the TWM-HCRMS wrapper.  
Details on the correction quantities can be found in [1].

Name	Default	Unc.	Description
mode	“A”	N/A	Mode of calculation: “A” for class A or “S” for class S.
nom_f	N/A	N/A	Optional user defined frequency of the fundamental frequency. The algorithm will identify the fundamental frequency by itself when it is not assigned.
y	N/A	No	Input sample data vector.
Ts	N/A	No	Sampling period or sampling rate or sample time vector.
fs	N/A	No	Note the wrapper always calculates in equidistant mode, so
t	N/A	No	$t$ is used just to calculate $Ts$ .

Table 18: List of input quantities to the TWM-HCRMS wrapper.  
Details on the correction quantities can be found in [1].

Name	Default	Unc.	Description
adc_lsb	N/A	No	Either absolute ADC resolution <i>lsb</i> or nominal range value <i>adc_nrng</i> (e.g.: 5 V for 10 Vpp range) and <i>adc_bits</i> bit resolution of ADC.
adc_nrng	1000	No	
adc_bits	40	No	
adc_offset	0	Yes	Digitizer input offset voltage.
adc_gain	1	Yes	Digitizer gain correction 2D table (multiplier).
adc_gain_f	$\square$	No	
adc_gain_a	$\square$	No	
adc_phi	0	Yes	Digitizer phase correction 2D table (additive).
adc_phi_f	$\square$	No	
adc_phi_a	$\square$	No	
adc_freq	0	Yes	Digitizer timebase error correction: $f_{tb'} = f_{tb} \cdot (1 + adc\_freq.v)$ The effect on the estimated frequency is opposite: $f_{est'} = f_{est} / (1 + adc\_freq.v)$
adc_jitter	0	No	Digitizer sampling period jitter [s].
adc_aper	0	No	ADC aperture value [s].
adc_aper_corr	0	No	ADC aperture error correction enable: $A' = A \cdot pi \cdot adc\_aper \cdot f_{est} / \sin(pi \cdot adc\_aper \cdot f_{est})$ $phi' = phi + pi \cdot adc\_aper \cdot f_{est}$
time_stamp	0	Yes	Relative timestamp of the first sample <i>y</i> .
adc_sfdr	180	No	Digitizer SFDR 2D table.
adc_sfdr_f	$\square$	No	
adc_sfdr_a	$\square$	No	
adc_Yin_Cp	1e-15	Yes	Digitizer input admittance 1D table.
adc_Yin_Gp	1e-15	Yes	
adc_Yin_f	$\square$	No	
tr_type	""	No	Transducer type string ("rvd" or "shunt").
tr_gain	1	Yes	Transducer gain correction 2D table (multiplicative).
tr_gain_f	$\square$	No	
tr_gain_a	$\square$	No	
tr_phi	0	Yes	Transducer phase correction 2D table (additive).
tr_phi_f	$\square$	No	
tr_phi_a	$\square$	No	
tr_sfdr	180	No	Transducer SFDR 2D table.
tr_sfdr_f	$\square$	No	
tr_sfdr_a	$\square$	No	
tr_Zlo_Rp	1e3	Yes	RVD transducer low-side impedance 1D table. Note this is related to loading correction and it has effect only for RVD transducer and will work only if <i>adc_Yin</i> is defined as well.
tr_Zlo_Cp	1e-15	Yes	
tr_Zlo_f	$\square$	No	
tr_Zbuf_Rs	0	Yes	Loading corrections: Transducer output buffer output series impedance 1D table. Leave unassigned to disable buffer from the correction topology.
tr_Zbuf_Ls	0	Yes	
tr_Zbuf_f	$\square$	No	
tr_Zca_Rs	1e-9	Yes	Loading corrections: Transducer high side terminal series impedance 1D table.
tr_Zca_Ls	1e-12	Yes	
tr_Zca_f	$\square$	No	
tr_Zcal_Rs	1e-9	Yes	Loading corrections: Transducer low side terminal series impedance 1D table.
tr_Zcal_Ls	1e-12	Yes	
tr_Zcal_f	$\square$	No	
tr_Yca_Cp	1e-15	Yes	Loading corrections: Transducer output terminals shunting impedance.
tr_Yca_D	1e-12	Yes	
tr_Yca_f	$\square$	No	

Table 18: List of input quantities to the TWM-HCRMS wrapper.  
Details on the correction quantities can be found in [1].

Name	Default	Unc.	Description
tr_Zcam	1e-12	Yes	Loading corrections: Transducer output terminals mutual inductance 1D table.
tr_Zcam_f	$\emptyset$	No	
Zcb_Rs	1e-9	Yes	Loading corrections: Cable series impedance 1D table.
Zcb_Ls	1e-12	Yes	
Zcb_f	$\emptyset$	No	
Ycb_Rs	1e-15	Yes	Loading corrections: Cable series impedance 1D table.
Ycb_Ls	1e-12	Yes	
Ycb_f	$\emptyset$	No	

Table 19: List of output quantities of the TWM-HCRMS wrapper.

Name	Uncertainty	Description
t	Yes	Time vector of the calculated samples [s].
env	Yes	Calculated half-cycle RMS values $env(t)$ .
f0	Yes	Average detected fundamental frequency.

Table 20: List of “calcset” options supported by the TWM-HCRMS wrapper.

Name	Description
calcset.unc	Uncertainty calculation mode. Supported: “none” or “guf” for uncertainty estimator.
calcset.loc	Level of confidence [-].
calcset.verbose	Verbose level.
calcset.dbg_plots	Non-zero value to enable plotting of debugging/signal analysis plots.

## 4.2 Algorithm description

The overview of the wrapper TWM-HCRMS structure is shown in the diagram in fig. 10. It starts with signal scaling and corrections. First step is digitizer timebase correction. Follows removal of the digitizer DC offset. Next, the signal  $y$  is split into DC and AC components. Next, the wrapper calls PSFE to estimate fundamental frequency  $f0_{est}$  of the signal  $y$  unless user defined  $f_{nom}$  in algorithm parameters. The frequency  $f0_{est}$  is used to obtain and apply the gain, phase, aperture error corrections and transducer corrections to DC and AC components separately. Note the AC corrections are applied in time domain and applies only for the  $f0_{est}$  frequency. No frequency dependent corrections were implemented as the required accuracy of the algorithm is not critical for the PQ events detection. The scaled DC and AC components are merged back to the single time domain signal  $y$ , which is ready for the processing.

The processing itself is performed by function “hcrms\_calc\_pq()” which is shown in the fig. 11. The first step of the algorithm is detection of the fundamental frequency and resampling to coherent sampling if user did not defined  $f_{nom}$  parameter. The algorithm uses PSFE algorithm called 200 times using a sliding window of size  $N/200$  with step  $N/200$ . So the development of the fundamental frequency  $f0(t)$  in time is found (see example in fig. 12, top-left). The time development  $f0(t)$  is filtered and the outliers caused by the PQ events are removed based on the simple heuristic algorithm. The removed portions usually happens on the edges of the “dip”-like events. The missing parts are replaced by the interpolation, so the frequency  $f0(t)$  is known in full range of the processing time  $t$ . The  $f0(t)$  is used to calculate resampling coefficients to achieve pseudo-coherent sampling in the full duration of the signal. The resampling by the dynamic frequency ratio is performed using ordinary spline interpolation, which seems to produce the least harmonic distortion of the resampled signal  $yx$ . The samples count per period



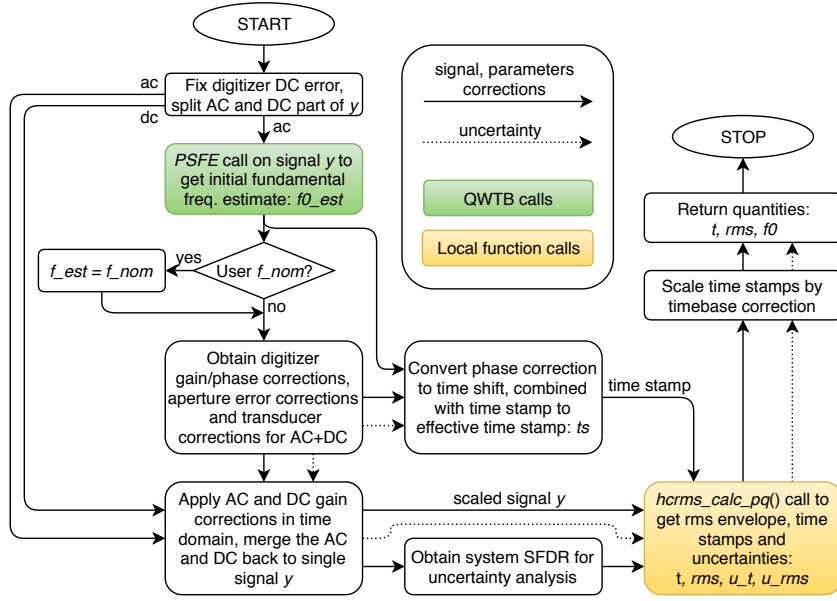


Figure 10: Overview of the TWM-HCRMS wrapper for evaluation of the RMS envelope in time.

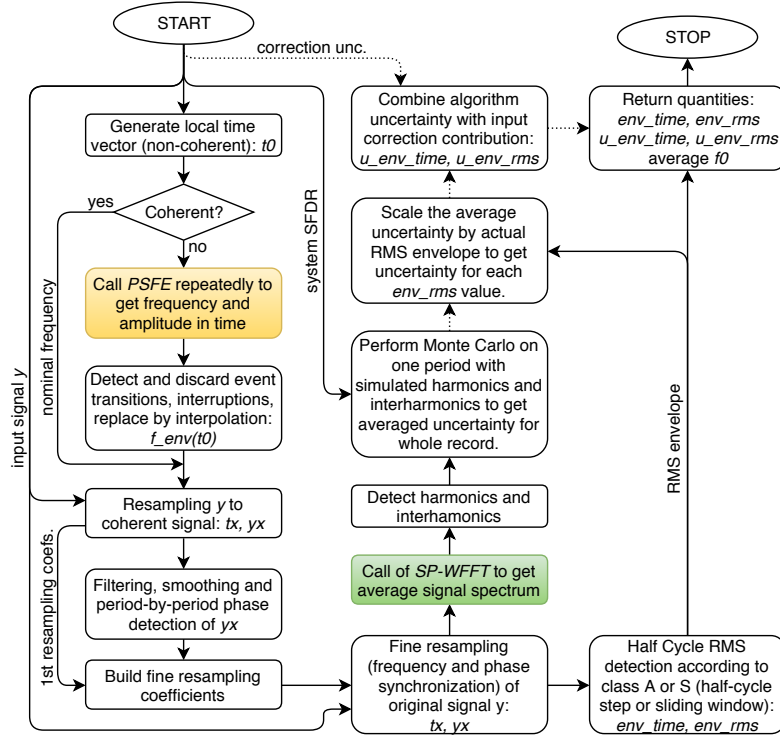


Figure 11: Detailed structure of the main half-cycle RMS calculator and uncertainty evaluator.

of the resampled signal is chosen to be divisible by factor 2 for class A (so each period can be split to half) or by 20 for class S (the algorithm calculates only 20 sliding windows per period).

The next step is period-by-period phase detection and synchronization of  $yx$ . This is almost useless when there are at least 100 samples per period, however the first resampling is not absolutely precise, so this additional step improves the coherent sampling of each period. The wrapper first filters the resampled  $yx$  by a very narrow passband filter to  $yxf$ , which removes the harmonics. Next, the  $yxf$  is split per periods and send to FFT, which calculates phase error of each period  $\phi_{i-p}(p)$  (see example in

fig. 12, top-right). Heuristic algorithm discards the parts of  $\phi_p(p)$  affected by the PQ events same as for the first resampling step and the missing parts are replaced by the interpolation and it also upsamples the phase value for each time sample to  $\phi_p(t)$ . The  $\phi_p(t)$  is finally used to fine tune the first resampling coefficients and the resampling is performed again on the original data  $y$  to get synchronised signal  $y_x$ . Example of the phase detection after the resampling is shown in fig. 12, bottom-left.

Follows the main RMS calculation algorithm which calculates RMS value with step 1/2-period (class A) or 1/20-period (class S) by ordinary non-windowed discrete RMS method:

$$rms(p) = \sqrt{\frac{1}{N1T} \cdot \sum_{k=1}^N yx(k + p \cdot N1T)^2}, \quad (17)$$

where  $k$  is sample index,  $p$  is window offset in periods and  $N1T$  is length of the period in samples.

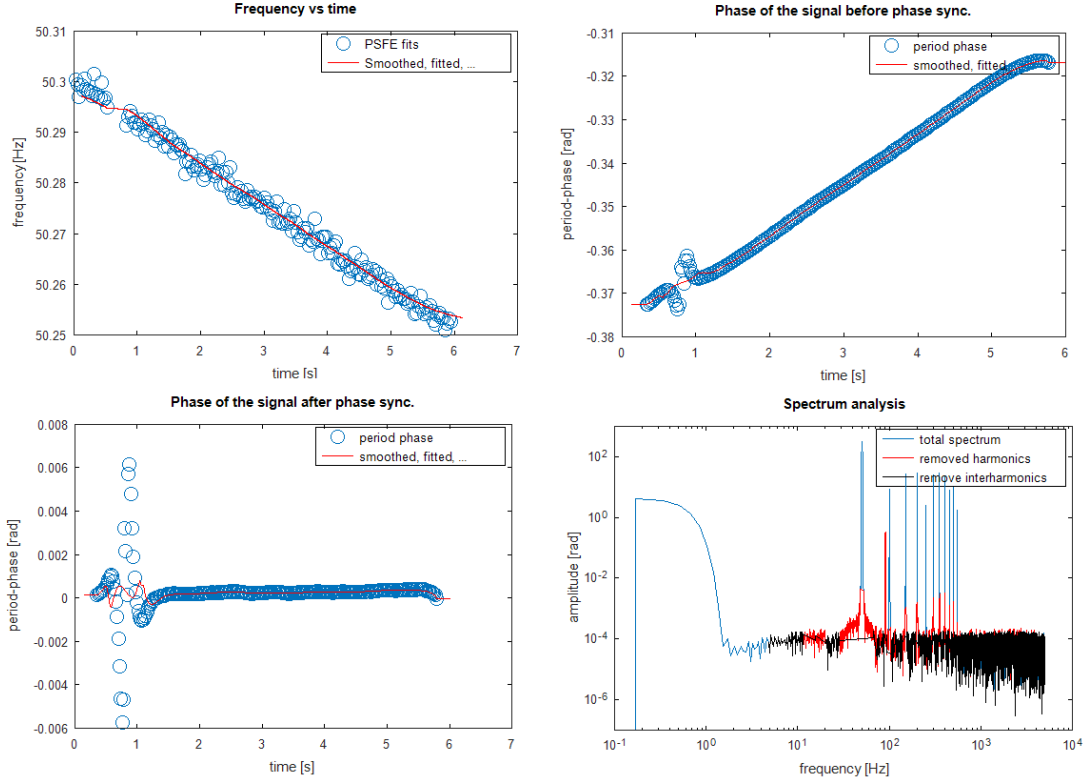


Figure 12: Debug plots showing the intermediated stages of TWM-HCRMS signal processing.

### 4.3 Uncertainty calculation

The algorithm is relatively straightforward and not excessively slow, so the calculation of uncertainty is performed on runtime when the “guf” option in “calcset” is selected. The core of the calculation is based on the spectrum analysis of the resampled signal  $y_x$ . The spectrum is used to identify dominant harmonic and interharmonic components (example is shown in fig. 12, bottom-right). Follows a small Monte Carlo loop which simulates the effect of harmonics and interharmonics on the RMS value of one period of the signal. It also simulates uncertain quality of the resampling, i.e. non-perfect coherency. The loop uses just 200 cycles and it is fast as it is performed on one period only.

The previous steps were performed on the conditions identified from the averaged spectrum of the whole record. Therefore, if the record contained PQ events, such as “dip” or “swell”, the estimated uncertainty will be inaccurate. So the calculated uncertainty is scaled proportionally for each period by the actual RMS level. This simple method based on average spectrum analysis showed good agreement with repeated calculation for each single period, so it was decided to use it as a solution of choice. The

only disadvantage is the uncertainty around event edges is larger than it may be, however RMS method does not allow exact localisation of the events, so tries to fix this often lead to the underestimation.

The final step is combining the uncertainty coming from the corrections with the uncertainty of the algorithm and assigning it to the particular RMS samples. Note the uncertainty estimator also assigns the uncertainty to the timestamps of each RMS value, however these are almost irrelevant as the technique for detecting the PQ events introduces uncertainty orders of magnitude higher.

#### 4.4 Validation

The algorithm TWM-HCRMS has many input quantities and some of them are matrices. That is too many possible degrees of freedom. Thus, varying the quantities in some systematic way would be very complicated if the validation should cover full range of used signals and corrections. Therefore, an alternative approach was used.

QWTB test function “alg\_test.m” was created, which performs the validation using randomly generated test setups. It randomizes the signal parameters, correction quantities and uncertainties and algorithm configurations in ranges expected to occur during the real measurements. The test is run many times to cover full operating range of the algorithm. The Following operations were performed:

1. Generate signal with known reference values.
2. Distort the reference signal by inverse corrections, i.e. simulate the transducers, and digitizer (e.g. gain errors, quantisation, SFDR ...).
3. Run the algorithm TWM-HCRMS with enabled uncertainty evaluation to obtain the estimated values and corresponding uncertainties of the meanRMS, maxRMS and minRMS (i.e. the output parameters of the algorithm).
4. Compare the reference and calculated values and check if the deviations are lower than assigned uncertainties.
5. Repeat  $N$  times from step 1, with different setup parameters, with different corrections randomised by their uncertainties, and with randomised noise, SFDR and jitter.
6. Check that at least 95 % of results passed (for 95 % level of confidence).

The total number of Monte-Carlo simulations was 50000. The parameters of the input signal, the digitizer and transducer settings were randomly varied. The sampling frequency was 10 kHz and the number of samples between 40 kSa and 100 kSa (i.e. simulation time was between 4 s and 10 s). The frequency of fundamental signal was between 20 Hz and 240 Hz and the drift of the frequency between -0.00005 Hz and 0.00005 Hz. The frequency of the harmonics and interharmonics were always above frequency of the fundamental signal but below the Nyquist frequency. The number of harmonics that were added to the fundamental signal was 10 and the number of interharmonics was 1. The nominal RMS of the signal was between 10 V and 1000 V, the spurious free dynamic range was between  $1e-3$  and  $1e-1$ . The DC value was between -5 V and +5 V. The phases of the fundamental signal as well as of the harmonics and interharmonics were individually and randomly varied between +3.14 rad and -3.14 rad. The ADC noise was between  $1e-11$  V and  $1e-4$  V, ADC aperture was between  $1e-6$  s and  $4e-5$  s, ADC gain between 1 and 1.5, ADC phase between +1.57 rad and -1.57 rad, frequency correction of the digitizer timebase between  $-5e-3$  and  $5e-3$ , ADC offset between -0.00001 V and 0.005 V (random value for low-and high-side channel). Relative time-stamp of the first sample was varied between -10 s and 10 s. The transducer gain was between 10 and 500 and the transducer phase was between +1.57 rad and -1.57 rad. The resistive voltage divider low-side impedance value (i.e. resistance and capacitance) were between 100  $\Omega$  and 500  $\Omega$  and 0.1 pF and 10 pF, respectively (only resistive voltage divider was used in the simulations). The randomisation of corrections was disabled which means that only the uncertainty of the algorithm without the contributions of the correction uncertainties were included in the Monte-Carlo simulations.

The success rate of the TWM-HCRMS algorithm was 100 % for the mean RMS estimation, 97.49 % for the max RMS estimation and 97.41 % for the min RMS estimation. The time of event was estimated by another algorithm.

## References

- [1] Stanislav Mašláň. Activity A2.3.2 - Algorithms Exchange Format. <https://github.com/smaslan/TWM/tree/master/doc/A232AlgorithmExchangeFormat.docx>.

## 5 TWM-InDiSwell - Interruption, Dip, Swell event detector

This algorithm detects power quality events “dip”, “swell” and “interruption” for a single phase systems according to the IEC 61000-3-40, “class A” (half-cycle step) or “class S” (sliding window). It returns relative event time, duration and its residual RMS value in percents relative to the entered nominal level *nom\_rms*. Note the result provided for the classes A and S should be identical as long as the event is synchronised with the nominal frequency. However that is rarely the case of real life situations, so the selection must be made depending on the prescription for the given PQ meter test or PQ event calibrator.

The algorithm internally uses RMS envelope detector TWM-HCRMS, so the accuracy of the detection depends on its properties. In general, the algorithm will work better with higher sampling rates. At least 100 samples should be recorded per period of the fundamental component (= sampling rate 5 kSa/s for 50 Hz networks). The higher is better, because the RMS algorithm will better suppress the harmonic and interharmonic content.

The algorithm is for single-ended input only and it is equipped with fast uncertainty estimator.

Example of the detected event as plotted by the algorithm is shown in the fig. 13.

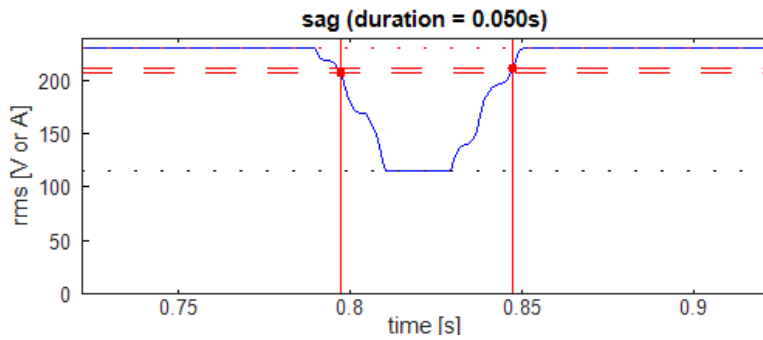


Figure 13: Example of the “dip” event evaluated according to the class S of IEC 61000-3-40.

### 5.1 TWM wrapper parameters

The input quantities supported by the algorithm are shown in the table 21. Algorithm returns output quantities shown in the table 22. Calculation setup supported by the algorithm is shown in table 23.

Table 21: List of input quantities to the TWM-InDiSwell wrapper.  
Details on the correction quantities can be found in [1].

Name	Default	Unc.	Description
mode	“A”	N/A	Mode of calculation: “A” for class A or “S” for class S.
nom_f	N/A	N/A	Optional user defined frequency of the fundamental frequency. The algorithm will identify the fundamental frequency by itself when it is not assigned.
nom_rms	230	N/A	Optional user defined nominal RMS value of the network. The event thresholds will be related to this value.
sag_thresh	90	N/A	Optional threshold value for “sag” (resp. “dip”) event evaluation. It is percent of nominal level <i>nom_rms</i> .
swell_thresh	110	N/A	Optional threshold value for “swell” event evaluation. It is percent of nominal level <i>nom_rms</i> .
int_thresh	10	N/A	Optional threshold value for “interruption” event evaluation. It is percent of nominal level <i>nom_rms</i> .
hyst	2	N/A	Detection hysteresis in percent of nominal level <i>nom_rms</i> .
plot	0	N/A	Enables plotting of the detected events. One plot per event type will be generated with detection levels, RSM envelope and markers of the event.
y	N/A	No	Input sample data vector.

Table 21: List of input quantities to the TWM-InDiSwell wrapper.  
Details on the correction quantities can be found in [1].

Name	Default	Unc.	Description
Ts	N/A	No	Sampling period or sampling rate or sample time vector.
fs	N/A	No	Note the wrapper always calculates in equidistant mode, so
t	N/A	No	$t$ is used just to calculate $Ts$ .
adc_lsb	N/A	No	Either absolute ADC resolution $lsb$ or nominal range value
adc_nrng	1000	No	$adc\_nrng$ (e.g.: 5 V for 10 Vpp range) and $adc\_bits$ bit res-
adc_bits	40	No	olution of ADC.
adc_offset	0	Yes	Digitizer input offset voltage.
adc_gain	1	Yes	Digitizer gain correction 2D table (multiplier).
adc_gain_f	$\square$	No	
adc_gain_a	$\square$	No	
adc_phi	0	Yes	Digitizer phase correction 2D table (additive).
adc_phi_f	$\square$	No	
adc_phi_a	$\square$	No	
adc_freq	0	Yes	Digitizer timebase error correction: $f_{tb'} = f_{tb} \cdot (1 + adc\_freq.v)$ The effect on the estimated frequency is opposite: $f_{est'} = f_{est} / (1 + adc\_freq.v)$
adc_jitter	0	No	Digitizer sampling period jitter [s].
adc_aper	0	No	ADC aperture value [s].
adc_aper_corr	0	No	ADC aperture error correction enable: $A' = A \cdot \pi \cdot adc\_aper \cdot f_{est} / \sin(\pi \cdot adc\_aper \cdot f_{est})$ $\phi_i' = \phi_i + \pi \cdot adc\_aper \cdot f_{est}$
time_stamp	0	Yes	Relative timestamp of the first sample $y$ .
adc_sfdr	180	No	Digitizer SFDR 2D table.
adc_sfdr_f	$\square$	No	
adc_sfdr_a	$\square$	No	
adc_Yin_Cp	1e-15	Yes	Digitizer input admittance 1D table.
adc_Yin_Gp	1e-15	Yes	
adc_Yin_f	$\square$	No	
tr_type	""	No	Transducer type string ("rvd" or "shunt").
tr_gain	1	Yes	Transducer gain correction 2D table (multiplicative).
tr_gain_f	$\square$	No	
tr_gain_a	$\square$	No	
tr_phi	0	Yes	Transducer phase correction 2D table (additive).
tr_phi_f	$\square$	No	
tr_phi_a	$\square$	No	
tr_sfdr	180	No	Transducer SFDR 2D table.
tr_sfdr_f	$\square$	No	
tr_sfdr_a	$\square$	No	
tr_Zlo_Rp	1e3	Yes	RVD transducer low-side impedance 1D table. Note this is
tr_Zlo_Cp	1e-15	Yes	related to loading correction and it has effect only for RVD
tr_Zlo_f	$\square$	No	transducer and will work only if $adc\_Yin$ is defined as well.
tr_Zbuf_Rs	0	Yes	Loading corrections: Transducer output buffer output se-
tr_Zbuf_Ls	0	Yes	ries impedance 1D table. Leave unassigned to disable buffer
tr_Zbuf_f	$\square$	No	from the correction topology.
tr_Zca_Rs	1e-9	Yes	Loading corrections: Transducer high side terminal series
tr_Zca_Ls	1e-12	Yes	impedance 1D table.
tr_Zca_f	$\square$	No	
tr_Zcal_Rs	1e-9	Yes	Loading corrections: Transducer low side terminal series
tr_Zcal_Ls	1e-12	Yes	impedance 1D table.
tr_Zcal_f	$\square$	No	

Table 21: List of input quantities to the TWM-InDiSwell wrapper.  
Details on the correction quantities can be found in [1].

Name	Default	Unc.	Description
tr_Yca_Cp tr_Yca_D tr_Yca_f	1e-15 1e-12 []	Yes Yes No	Loading corrections: Transducer output terminals shunting impedance.
tr_Zcam tr_Zcam_f	1e-12 []	Yes No	Loading corrections: Transducer output terminals mutual inductance 1D table.
Zcb_Rs Zcb_Ls Zcb_f	1e-9 1e-12 []	Yes Yes No	Loading corrections: Cable series impedance 1D table.
Ycb_Rs Ycb_Ls Ycb_f	1e-15 1e-12 []	Yes Yes No	Loading corrections: Cable series impedance 1D table.

Table 22: List of output quantities of the TWM-InDiSwell wrapper.

Name	Uncertainty	Description
t	Yes	Time vector of the calculated samples [s].
env	Yes	Calculated half-cycle RMS values $env(t)$ .
f0	No	Average detected fundamental frequency.
sag_start	Yes	Sag (dip) event start relative time stamp [s].
sag_dur	Yes	Sag (dip) event duration [s].
sag_res	Yes	Sag (dip) event residual RMS level [%].
swell_start	Yes	Swell event start relative time stamp [s].
swell_dur	Yes	Swell event duration [s].
swell_res	Yes	Swell event residual RMS level [%].
int_start	Yes	Interruption event start relative time stamp [s].
int_dur	Yes	Interruption event duration [s].
int_res	Yes	Interruption event residual RMS level [%].

Table 23: List of “calcset” options supported by the TWM-InDiSwell wrapper.

Name	Description
calcset.unc	Uncertainty calculation mode. Supported: “none” or “guf” for uncertainty estimator.
calcset.loc	Level of confidence [-].
calcset.verbose	Verbose level.
calcset.dbg_plots	Non-zero value to enable plotting of debugging/signal analysis plots of the TWM-HCRMS, which is used internally by the TWM-InDiSwell.

## 5.2 Algorithm description

The algorithm TWM-InDiSwell internally uses algorithm TWM-HCRMS to calculate RMS envelope of the signal. Therefore, all input signal conditioning of  $y$  is performed in the TWM-HCRMS. The TWM-HCRMS output RMS values and corresponding time stamps are used to detect events according to the preset thresholds. The detection method follows the IEC 61000-3-40 standard. The start of event is assigned to the first RMS sample whose value exceeds the threshold. End of event is assigned to the first sample whose RMS value returned below the  $(threshold - hysteresis)$ , which prevents multiple events detection around the threshold. Flowchart of the algorithm is shown in fig. 14.

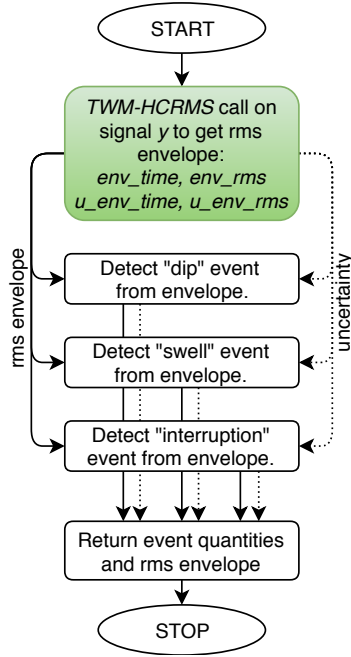


Figure 14: Flowchart of the algorithm wrapper TWM-InDiSwell. Note the green cells are calls to another QWTB/TWM wrappers.

### 5.3 Uncertainty calculation

The main component of uncertainty is the output of TWM-HCRMS. However, due to the principle of detection, especially for class A, the uncertainty of the event start can never be lower than half of the period, as that is the resolution of the RMS detector. The duration uncertainty cannot be lower than one full period, as the same resolution applies to the end of the event. The resolution in the class S mode is higher, however the uncertainty remains the same as that is the requirement of the IEC standard.

### 5.4 Validation

The validation of the TWM-InDiSwell algorithm has not been performed by the Monte-Carlo simulations since the algorithm is usually used with the TWM-HCRMS algorithm. It was instead tested on numerous typical cases such as shown in Fig. 15. The uncertainty is always one half-cycle as suggested by the standard, so the detected events were always within or exactly on the uncertainty limit as the time resolution is also one half-cycle.

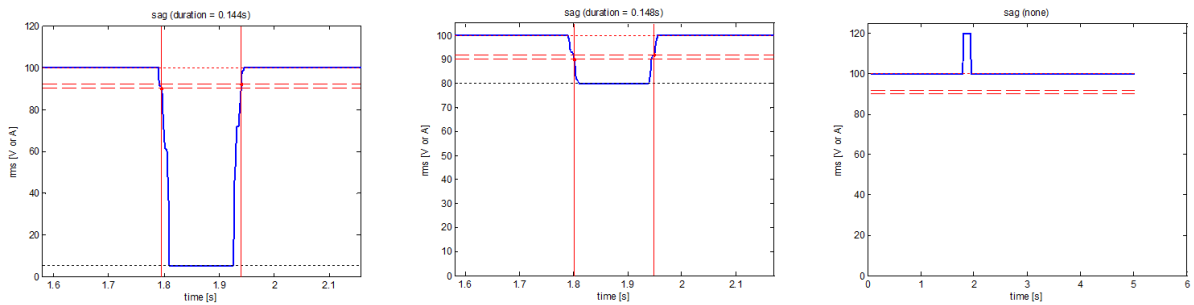


Figure 15: Validation test examples for the TWM-InDiSwell algorithm.



## References

- [1] Stanislav Mašláň. Activity A2.3.2 - Algorithms Exchange Format. <https://github.com/smaslan/TWM/tree/master/doc/A232AlgorithmExchangeFormat.docx>.

## 6 TWM-THDWFFT - THD from Windowed FFT

This algorithm is designed for calculation of the harmonics and Total Harmonic Distortion (THD) of the non-coherently sampled signal. It uses windowed FFT to detect the harmonic amplitudes, which limits the achievable accuracy of the harmonics detection due to the window scalloping effect. However, the algorithm was initially designed for THD calculation of the low-distortion signals, where the accuracy was not critical. The relative expanded uncertainty of the harmonics is at least 0.015 % (or 0.005 % after highly experimental correction method). On the other hand, the algorithm was designed to compensate the spectral leakage of the noise to the harmonics near noise level, so it offers decent accuracy for the very low distortions near self-THD of the digitizer itself.

The algorithm supports direct processing of a multiple records which are used to produce averaged spectrum before the main calculation. This possibility should be preferred instead of repeated call of the algorithm for each record as it reduces the noise. The algorithm supports only single-ended transducer connection.

The algorithm returns: (i) Full spectrum; (ii) Identified harmonics; (iii) THD coefficients according various definitions; (iv) RMS noise estimate; (v) THD+Noise estimate.

Example of the algorithm output is shown in fig. 16.

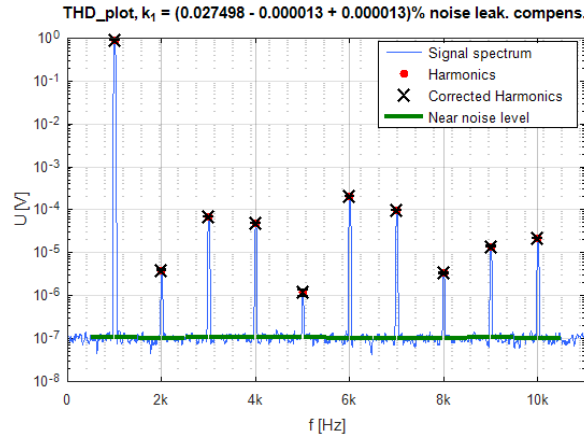


Figure 16: Example of the TWM-THDWFFT algorithm output.

### 6.1 TWM wrapper parameters

The input quantities supported by the algorithm are shown in table 24. Algorithm returns output quantities shown in table 25. Calculation setup supported by the algorithm is shown in table 26.

Table 24: List of input quantities to the TWM-THDWFFT wrapper. Details on the correction quantities can be found in [4].

Name	Default	Unc.	Description
f0	N/A	N/A	Optional user defined frequency of fundamental component. Do not assign to enable auto detection.
f0_mode	“PSFE”	N/A	Optional selection of the fundamental frequency auto detection mode.
scallop_fix	0	N/A	Non-zero value to enable experimental window scalloping error correction. It will try to use known scalloping error of the window at given frequency to correct the error, however it will work only for stable signals when the fundamental frequency detection is accurate.

Table 24: List of input quantities to the TWM-THDWFFT wrapper. Details on the correction quantities can be found in [4].

Name	Default	Unc.	Description
H	10	N/A	Optional limit of maximum harmonics count to analyse (including fundamental). Note the high values will significantly increase calculation time!
band	inf	N/A	Optional bandwidth limit which can reduce the harmonics count to analyse. This also affects the bandwidth of the noise calculation.
plot	0	N/A	Non-zero value, “on”, “true” or “enabled” string enables plotting of the detected harmonics.
y	N/A	No	Input matrix of the samples. One column per record (the algorithm can directly calculate average of multiple records).
Ts	N/A	No	Sampling period or sampling rate or sample time vector.
fs	N/A	No	Note the wrapper always calculates in equidistant mode, so
t	N/A	No	$t$ is used just to calculate $Ts$ .
adc_lsb	N/A	No	Either absolute ADC resolution $lsb$ or nominal range value
adc_nrng	1000	No	$adc\_nrng$ (e.g.: 5 V for 10 Vpp range) and $adc\_bits$ bit res-
adc_bits	40	No	olution of ADC.
adc_jitter	0	No	Digitizer sampling period jitter [s].
adc_aper_corr	0	No	ADC aperture error correction enable: $A' = A \cdot \pi \cdot adc\_aper \cdot f\_est / \sin(\pi \cdot adc\_aper \cdot f\_est)$ $\phi_i' = \phi_i + \pi \cdot adc\_aper \cdot f\_est$
adc_aper	0	No	ADC aperture value [s].
adc_gain	1	Yes	Digitizer gain correction 2D table (multiplier).
adc_gain_f	$\emptyset$	No	
adc_gain_a	$\emptyset$	No	
adc_freq	0	Yes	Digitizer timebase error correction: $f_{tb}' = f_{tb} \cdot (1 + adc\_freq.v)$ The effect on the estimated frequency is opposite: $f_{est}' = f_{est} / (1 + adc\_freq.v)$
adc_sfdr	180	No	Digitizer SFDR 2D table.
adc_sfdr_f	$\emptyset$	No	
adc_sfdr_a	$\emptyset$	No	
adc_Yin_Cp	1e-15	Yes	Digitizer input admittance 1D table.
adc_Yin_Gp	1e-15	Yes	
adc_Yin_f	$\emptyset$	No	
tr_type	“”	No	Transducer type string (“rvd” or “shunt”).
tr_gain	1	Yes	Transducer gain correction 2D table (multiplicative).
tr_gain_f	$\emptyset$	No	
tr_gain_a	$\emptyset$	No	
tr_sfdr	180	No	Transducer SFDR 2D table.
tr_sfdr_f	$\emptyset$	No	
tr_sfdr_a	$\emptyset$	No	
tr_Zlo_Rp	1e3	Yes	RVD transducer low-side impedance 1D table. Note this is
tr_Zlo_Cp	1e-15	Yes	related to loading correction and it has effect only for RVD
tr_Zlo_f	$\emptyset$	No	transducer and will work only if $adc\_Yin$ is defined as well.
tr_Zbuf_Rs	0	Yes	Loading corrections: Transducer output buffer output se-
tr_Zbuf_Ls	0	Yes	ries impedance 1D table. Leave unassigned to disable buffer
tr_Zbuf_f	$\emptyset$	No	from the correction topology.
tr_Zca_Rs	1e-9	Yes	Loading corrections: Transducer high side terminal series
tr_Zca_Ls	1e-12	Yes	impedance 1D table.
tr_Zca_f	$\emptyset$	No	

Table 24: List of input quantities to the TWM-THDWFFT wrapper. Details on the correction quantities can be found in [4].

Name	Default	Unc.	Description
tr_Zcal_Rs tr_Zcal_Ls tr_Zcal_f	1e-9 1e-12 []	Yes Yes No	Loading corrections: Transducer low side terminal series impedance 1D table.
tr_Yca_Cp tr_Yca_D tr_Yca_f	1e-15 1e-12 []	Yes Yes No	Loading corrections: Transducer output terminals shunting impedance.
tr_Zcam tr_Zcam_f	1e-12 []	Yes No	Loading corrections: Transducer output terminals mutual inductance 1D table.
Zcb_Rs Zcb_Ls Zcb_f	1e-9 1e-12 []	Yes Yes No	Loading corrections: Cable series impedance 1D table.
Ycb_Rs Ycb_Ls Ycb_f	1e-15 1e-12 []	Yes Yes No	Loading corrections: Cable series impedance 1D table.

Table 25: List of output quantities of the TWM-THDWFFT wrapper. Note the uncertainty “No” means the algorithm may return some uncertainty but it should be ignored because it is either incomplete or not validated.

Name	Uncertainty	Description
H	No	Harmonics count analysed.
noise_bw	No	Bandwidth used for the noise estimation [Hz].
thd	Yes	Total Harmonic Distortion referenced to the fundamental.
thd2	Yes	Total Harmonic Distortion referenced to the RMS value.
thdn	No	Total Harmonic Distortion + Noise referenced to the fundamental.
thdn2	No	Total Harmonic Distortion + Noise referenced to the RMS value.
noise	No	RMS noise estimate.
h	Yes	Amplitudes of the harmonics.
f	No	Frequencies of the harmonics $h$ .
spec_a	No	Full spectrum from the windowed FFT.
spec_f	No	Frequencies of the spectrum components <i>spec_a</i> .
thd_raw	No	<i>thd</i> without noise spectrum leakage correction.
thd2_raw	No	<i>thd2</i> without noise spectrum leakage correction.

Table 26: List of “calcset” options supported by the TWM-THDWFFT wrapper.

Name	Description
calcset.unc	Uncertainty calculation mode. Supported: “none” or “guf” for uncertainty estimator. Note the algorithm is internally made in such a way it always calculates the uncertainty, so this option should have no effect in current version.
calcset.loc	Level of confidence [-].
calcset.verbose	Verbose level.

## 6.2 Algorithm description and uncertainty evaluation

The whole algorithm is extended and improved version of the THD analyser presented in [5]. The overview of the algorithm wrapper structure and internal functions is shown in fig. 17. The wrapper start by a call to the top level function “thd\_wfft()”, which performs entire calculation and uncertainty

estimation. Next, the wrapper may optionally plot graph showing the identified harmonics and near spectrum. Note the wrapper reduces the asymmetric uncertainty limits to symmetric as the TWM was not designed for such a case. This has no effect when the level of harmonics is at least twice the noise level. It will expand the uncertainty only for very small harmonic levels near noise level.

The “`thd_wfft()`” itself internally does just two steps: (i) Calculating spectra of input records and estimates their fundamental frequency (function “`thd_proc_waves()`”); (ii) Initiates main evaluation function “`thd_eval_thd()`”.

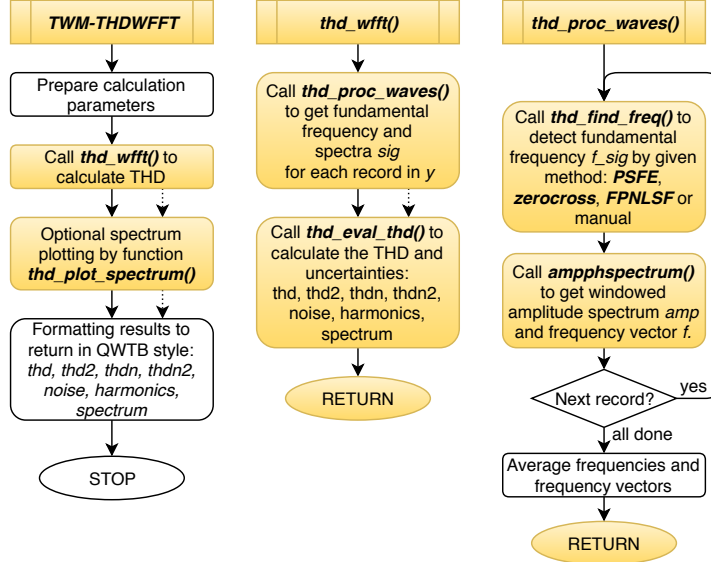


Figure 17: Flow chart of the algorithm wrapper TWM-THDWFFT. Note the rounded gold blocks are calls to other local functions which are shown in another diagram or mentioned in the text.

The function “`thd_proc_waves()`” first detects fundamental frequency of each record in  $y$ . It contains several modes of detection. The simplest is zero crossing, however it is very unreliable. Another options if FPNLSF [7], which may fail when initial estimate from zero cross detector is poor. Last and best option (default) is PSFE [3], which is capable to identify the fundamental frequency with good accuracy even with strong harmonic content. User may also override the auto detection by manual entry of the fundamental frequency. The next step is calculation of amplitude spectrum for each record  $y$  using a windowed FFT. The widest, flattest window with highest suppression of side lobes was chosen for the goal - Flattop HFT248D from [1]. This window offer side lobes suppression by 248 dB and scalloping error only 0.0104 % for range  $\pm 0.5$  DFT bin.

The internal structure of the evaluation function “`thd_eval_thd()`” is shown in fig. 18. The function does following steps:

1. Obtaining parameters of the window function Flattop HFT248D used for the processing.
2. Generation of lookup table (LUT), which will be used for the numeric solver that compensates spectrum leakage of the noise to the harmonic DFT bin (details below).
3. Decision of how many harmonics to analyse based on the user limits ( $H$  and *bandwidth*).
4. Application of all gain corrections to scale the spectra from “`thd_proc_waves()`” to actual levels.
5. Averaging of the spectra and type A uncertainty calculation.
6. Detection of harmonics. The algorithm picks the harmonics from the average spectrum one by one. It searches the highest DFT bin in preset frequency range for each estimated harmonics frequency. It also extracts the nearby noise level which is needed for compensation of the noise spectral leakage.

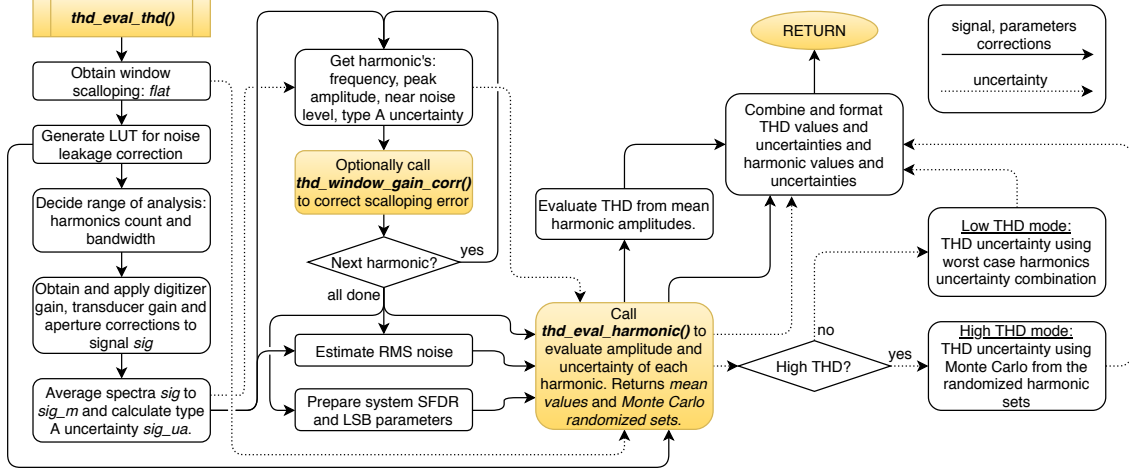


Figure 18: Flow chart of the main algorithm function “thd\_eval\_thd()” for the TWM-THDWFFT algorithm.

7. The parameters required for the uncertainty evaluation of each harmonics are obtained (system SFDR and LSB).
8. Evaluation of the harmonic values and uncertainties using function “thd\_eval\_harmonic()” (see below). This returns mean harmonic levels and calculated uncertainties and also randomized harmonic levels, because it internally uses Monte Carlo.
9. Calculation of the THD coefficients from the mean harmonic amplitudes according to various definition and calculation of their uncertainties using one of the methods (see below).

The evaluation of the THD coefficients in the step 9) is performed according to the several definitions. The most common is so called “fundamental referenced” THD:

$$thd = \frac{\sqrt{U_2^2 + U_3^2 + \dots + U_M^2}}{U_1}, \quad (18)$$

where  $U_x$  is mean harmonic voltage and  $x$  is harmonic index and  $M$  is harmonics count. The next is RMS value referenced mode, which uses total RMS of the signal in the denominator:

$$thd2 = \frac{\sqrt{U_2^2 + U_3^2 + \dots + U_M^2}}{\sqrt{U_1^2 + U_2^2 + U_3^2 + \dots + U_M^2}}. \quad (19)$$

The results should be very close for low distortion signals. Next result is combined fundamental referenced THD and noise THD+N:

$$thdn = \frac{\sqrt{U_2^2 + U_3^2 + \dots + U_M^2 + U_{noise}^2}}{U_1}, \quad (20)$$

where the  $U_{noise}$  is RMS noise in specified bandwidth (parameter *band*). Last definition is RMS referenced THD+N:

$$thdn2 = \frac{\sqrt{U_2^2 + U_3^2 + \dots + U_M^2 + U_{noise}^2}}{\sqrt{U_1^2 + U_2^2 + U_3^2 + \dots + U_M^2 + U_{noise}^2}}. \quad (21)$$

The algorithm also returns the same four coefficient without the noise leakage correction, however those are just informative.

The uncertainty evaluation for the THD coefficients uses heuristic approach. The THD coefficients are calculated from the mean values from step 8 ignoring the uncertainty and its distribution. The uncertainty calculation method depends on the “is\_high” obtained in step 8, which is set when the weighted average of the harmonic amplitudes is significantly above noise. So two cases occur:

1. *is\_high* = *true*: The distribution of the uncertainty of the harmonics is near Gaussian so the randomized amplitudes from step 8) are passed to the THD formulas above and the THD is evaluated using Monte Carlo and function “scovint()” (follows GUM guide [2]).
2. *is\_high* = *false*: The distribution of the uncertainty of the harmonics is very asymmetric, so the Monte Carlo would lead to large bias in the mean value of THD. Therefore the THD uncertainty is evaluated using the worst case combination of the harmonic uncertainties from step 8):

$$[thd_{MAX}, thd_{MIN}] = \left[ \frac{\sqrt{\sum_{m=2}^M U_{m_{MAX}}^2}}{U_{1_{MIN}}}, \frac{\sqrt{\sum_{m=2}^M U_{m_{MIN}}^2}}{U_{1_{MAX}}} \right] \quad (22)$$

where:

$$U_{m_{MAX}} = U_m + U_+(U_m), \quad (23)$$

$$U_{m_{MIN}} = U_m - U_-(U_m). \quad (24)$$

The reported asymmetric uncertainties were calculated according to:

$$[U_+(thd), U_-(thd)] = [thd_{MAX} - thd, thd - thd_{MIN}]. \quad (25)$$

The evaluation of the uncertainty of each harmonic is performed by the function “thd\_eval\_harmonic()” shown in fig. 19. This is simple heuristic function that calculates uncertainty distribution of each harmonic component depending on how close it is to the noise level. This is necessary, because the distribution for harmonics well above the noise level will be near Gaussian, whereas the possible value of the harmonic near noise level may be anywhere in the noise or slightly above. The result of this approach is very asymmetric distribution that cannot be processed using GUF method. Therefore the calculation is performed by Monte Carlo with 10000 cycles (defined as fixed option in the TWM-THDWFFT wrapper). The performance is acceptable as long as no more than 50 harmonics are analysed. The resulting randomised set of harmonic amplitudes is returned in full for further processing. However, the function also calculates the uncertainty limits for each harmonic for given level of confidence by function “scovint()” (implemented according to [2]).

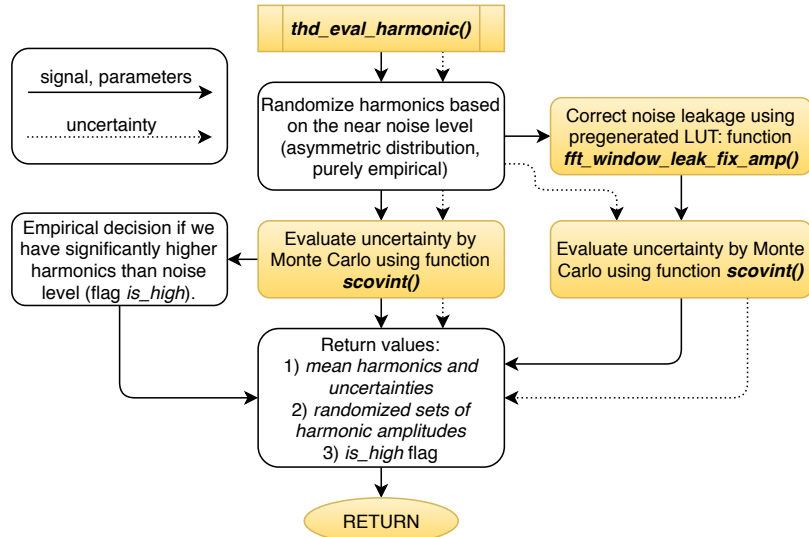


Figure 19: Flow chart of the function “thd\_eval\_harmonic()” of the TWM-THDWFFT algorithm.

The function “thd\_eval\_harmonic()” also repeats the same calculation once more with the mentioned noise leakage correction. The problem related to wide window functions such as Flattop HFT248D is the

not only the harmonic power leaks to the more DFT bins, but also the noise energy near the harmonic leaks to the harmonic DFT bin. This effect is normally not considered, when the narrower windows are used and when the harmonic is several times larger than the noise. However, this algorithm uses very wide window Flattop HFT248D and it was designed to operate near noise level. The apparent gain of the detected harmonic can be obtained by the following procedure:

1. generation of sine wave  $x(t)$  with amplitude  $U_m$ ,
2. addition of gaussian noise with level  $U_{\text{noise}}$  to the  $x(t)$ ,
3. windowing of the  $x(t)$  by selected window function (Flattop HFT248D),
4. reading the amplitude  $U_x$  from amplitude spectrum of  $X(f)$  of signal  $x(t)$ .

Alternatively the same result can be obtained by means of Monte Carlo method from equation:

$$U_x = \frac{1}{I} \sum_{i=1}^I \left| U_m + U_{\text{noise}} \sum_{k=1}^K W_k \cdot e^{-j2\pi R(i,k)} \right| \quad (26)$$

where  $K$  is number of coefficients of window function amplitude spectrum  $W_k$  and  $I$  is number of MC iterations (at least  $10^4$ ). The  $R(i, k)$  is uniformly distributed random number generator from 0 to 1. The right sum term represents a vector sum of a noise vectors with random angle and amplitude weighted by window spectrum coefficients  $W_k$ . The resulting gain vs. noise to signal ratio is shown in fig. 20.

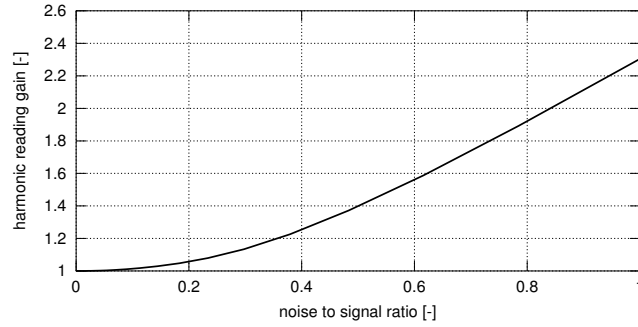


Figure 20: Error of the harmonics amplitude measurement using FFT with window Flattop HFT248D. Note the “noise” means amplitude of the noise in surrounding DFT bins, not RMS noise.

The direct inverse evaluation from the detected to actual harmonic level is not possible, so the algorithm uses iterative function based on the precalculated LUT with the gain error (the dependence in fig. 20). The correction itself is performed by the function “fft\_window\_leak\_fix\_amp()”, which takes the harmonic level, noise level detected around (assuming the noise is the same for all related DFT bins). Effect of this correction is shown in fig. 21.

### 6.3 Validation

The algorithm TWM-THDWFFT has many input quantities (45) and some of them are matrices. That is too many possible degrees of freedom. Thus, varying the quantities in some systematic way would be very complicated if the validation should cover full range of used signals and corrections. Therefore, an alternative approach was used.

QWTB test function “alg\_test.m” was created, which performs the validation using randomly generated test setups. It randomizes the signal parameters, correction quantities and uncertainties and algorithm configurations in ranges expected to occur during the real measurements. The test is run many times to cover full operating range of the algorithm. Following operations are performed for each random test setup:

1. Generate signal  $y$  with known harmonic content  $A_{\text{ref}}(h)$  and thus known THD  $thd_{\text{ref}}$ .



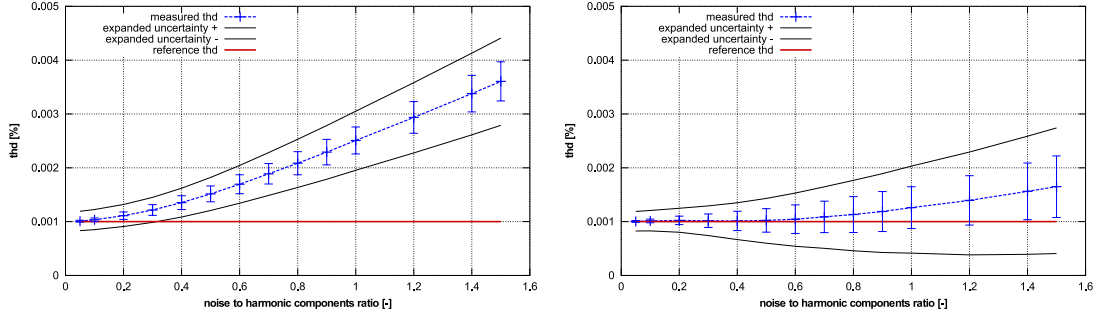


Figure 21: Deviation of THDWFFT algorithm from simulated THD level 10 ppm for various noise to higher harmonic ratios. The simulated waveform has 10 harmonic components with amplitudes  $U_m = \{0.9, 3 \cdot 10^{-6}, 3 \cdot 10^{-6}, \dots\}$  V. Left graph shows results without noise spectral leakage correction, right graph shows the same dependence with corrected values. The error bars show the standard deviation of a repeated simulations.

2. Distort the signal  $y$  by inverse corrections, i.e. simulate the transducers, and digitizer (e.g. gain errors, quantisation, SFDR ...).
3. Run the algorithm TWM-THDWFFT with enabled uncertainty evaluation to obtain the harmonic levels  $A_x(h)$ , distortion  $thd_x$  and their uncertainties  $u(A_x(h))$  and  $u(thd_x)$ .
4. Compare the reference and calculated harmonics and distortion and check if the deviations are lower than assigned uncertainties:

$$pass\_A(i, h) = |A_{ref}(h) - A_x(h)| < u(A_x(h)), \quad (27)$$

$$pass\_thd(i) = |thd_{ref} - thd_x| < u(thd_x), \quad (28)$$

where  $i$  is test run index.

5. Repeat  $N$  times from step 1, with the same test setup parameters, but with corrections randomised by their uncertainties, and with randomised noise, SFDR and jitter.
6. Check that at least 95 % of  $pass\_A(i, h)$  and  $pass\_thd(i)$  results passed (for 95 % level of confidence).

The test runs count per test setup was set to  $N = 300$ , which is far from optimal infinite set, but due to the computational requirements it could not have been much higher. Note the low count of test induces uncertainty to the obtained pass rates.

The algorithm in the uncertainty estimation mode was tested in 4 different configurations with 10000 test setups per each. I.e. the algorithm was ran 12 million times in total ( $4 \times 10000 \times 300$ ). The processing itself was performed on a supercomputer [6] so it took about 3 days at 400 parallel octave instances.

The randomization ranges of the signal are shown in table 27. The randomization ranges of the corrections are shown in table 28.

The test results were split into several groups given by the randomiser setup: (i) Scalping correction enabled/disabled; (ii) Randomisation of corrections by uncertainty enabled/disabled. When the randomisation of corrections is disabled, the test runs cover only the algorithm itself and the contributions of the correction uncertainties are ignored.

The summary of the validation test results is shown in table 29. The success rate was 100 % for all cases.

Table 27: Validation range of the signal for TWM-THDWFFT algorithm.

Parameter	Range
Sampling rate	30 to 70 kHz (no need to randomize in wider range, as all other parameters are generated relative to this rate).
Sampling time	0.3 to 5 seconds.
Fundamental frequency	Random, so there are at least 30 DFT bins between harmonics and the highest harmonic is no higher then $0.4 \cdot fs$ .
Analysed harmonics count	5 to 10.
Fundamental amplitude	0.1 to 0.9 of fullscale digitizer input.
Harmonic amplitudes	Each harmonic is randomised from 1 $\mu$ V to $A_{max}$ of fundamental, where the $A_{max}$ is randomised from 0.0001 to 0.1 of fundamental.
Phase angles	Random for all harmonics.
Averaging cycles	10.
SFDR	-140 to -80 dBc, all spurs have the same level.
Digitizer RMS noise	1 to 50 $\mu$ V.
Sampling jitter	1 to 100 ns.

Table 28: Validation range of the correction for the TWM-THDWFFT algorithm.

Parameter	Range
Transducer type	Random 'shunt' or 'rvd'.
Nominal input range	0.1 to 100 V (0.1 to 100 A)
Aperture	1 ns to 100 $\mu$ s
Digitizer gain	Randomly generated frequency transfer simulating NI 5922 FIR-like gain ripple (possibly the worst imaginable shape) and some ac-dc dependence. The transfer matrix has up to 50 frequency spots. Nominal gain value is random from 0.95 to 1.05 with uncertainty 2 $\mu$ V/V. Maximum ac-dc value at $fs/2$ is up to $\pm 1$ % with uncertainty 50 $\mu$ V/V. Gain ripple amplitude is random from 0.005 to 0.03 dB with up to 5 periods between 0 and $fs/2$ .
Digitizer SFDR	Value based on table 27.
Transducer SFDR	Value based on table 27. Note the "SFDR" from table 27 is randomly split between digitizer and transducer SFDR correction.
Digitizer bit resolution	16 to 28 bits.
Digitizer nominal range	1 V
Transducer gain	Randomly generated frequency transfer. The transfer matrix has up to 50 frequency spots. Nominal gain value is random (see above) with relative uncertainty 2 $\mu$ V/V. Maximum ac-dc value at $fs/2$ is up to $\pm 2$ % with uncertainty 50 $\mu$ V/V. Gain ripple amplitude is 0.005 dB with 4 to 10 periods between 0 and $fs/2$ .

Table 29: Validation results of the algorithm TWM-THDWFFT. The “passed test” shows percentage of passed tests under conditions defined in tables 27 and 28.

Scallop. fix.	Rand. corr.	Passed test [%]		
		<i>thd</i>	<i>h</i> (1)	<i>h</i> (2.. <i>n</i> )
no	no	100.00	100.00	100.00
	yes	100.00	100.00	100.00
yes	no	100.00	100.00	100.00
	yes	100.00	100.00	100.00

## References

- [1] Gerhard Heinzel, A. Rüdiger, and R. Schilling. Spectrum and spectral density estimation by the discrete fourier transform (dft), including a comprehensive list of window functions and some new flat-top windows. Technical report, Max-Planck-Institut für Gravitationsphysik (Albert-Einstein-Institut) Teilinstitut Hannover, Feb 2005.
- [2] JCGM. *Evaluation of measurement data - Supplement 1 to the “Guide to the expression of uncertainty in measurement” - Propagation of distributions using a Monte Carlo method*. Bureau International des Poids et Mesures.
- [3] Rado Lapuh. Estimating the fundamental component of harmonically distorted signals from noncoherently sampled data. *IEEE Transactions on Instrumentation and Measurement*, 64(6):1419–1424, June 2015.
- [4] Stanislav Mašláň. Activity A2.3.2 - Algorithms Exchange Format. <https://github.com/smaslan/TWM/tree/master/doc/A232AlgorithmExchangeFormat.docx>.
- [5] Stanislav Mašláň and Martin Šíra. Automated non-coherent sampling thd meter with spectrum analyser. In *Proceedings CPEM*, 2014.
- [6] Miroslav Valtr. ČMI HPC System Online. [https://translate.google.cz/translate?sl=cs&tl=en&js=y&prev=\\_t&hl=cs&ie=UTF-8&u=http%3A%2F%2Fprutok.cmi.cz%2Fsc%2Fdoku.php%3Fid%3Dsystem&edit-text=](https://translate.google.cz/translate?sl=cs&tl=en&js=y&prev=_t&hl=cs&ie=UTF-8&u=http%3A%2F%2Fprutok.cmi.cz%2Fsc%2Fdoku.php%3Fid%3Dsystem&edit-text=), 2014.
- [7] M. Šíra and S. Mašláň. Uncertainty analysis of non-coherent sampling phase meter with four parameter sine wave fitting by means of monte carlo. In *29th Conference on Precision Electromagnetic Measurements (CPEM 2014)*, pages 334–335, Aug 2014.

## 7 TWM-PWRTDI - Power by Time Domain Integration

TWM-PWRTDI is an algorithm for calculation of power parameters using a time domain integration of  $u(t) \cdot i(t)$  product. It is based on the use of window function to eliminate effects of non-coherent sampling as was demonstrated in [1] and [4]. Therefore, it does work even for non-coherently sampled waveforms. The algorithm itself without contribution of corrections can easily reach errors below  $1 \mu\text{W}/\text{VA}$  with proper selection of a sampling rate and windows size.

The algorithm can calculate all basic parameters: active power  $P$ , reactive power  $Q$ , apparent power  $S$ , RMS voltage  $U$ , RMS current  $I$  and power factor  $PF$ . It also returns DC components separately:  $U_{dc}$ ,  $I_{dc}$  and  $P_{dc}$ . User may choose optional AC coupling mode by setting parameter “ $ac\_coupling = 1$ ” in which case the  $U$ ,  $I$ ,  $P$ ,  $Q$ ,  $S$  and  $PF$  will be calculated without the AC component.

Note the windowed RMS method itself can calculate power in any quadrant, however it is not able to distinguish all four quadrants. The quadrant identification (proper signs for  $P$  and  $Q$ ) is obtained from a complementary windowed FFT algorithm which is running along the main RMS calculation. Note the quadrant selection may fail around  $PF = 0$  (the absolute values will be correct).

The algorithm uses following definitions for the power components: (i) The AC power components  $P$ ,  $Q$  and  $S$  are related by equation:

$$S^2 = P^2 + Q^2. \quad (29)$$

(ii) Power factor  $PF$  is calculated including DC components according to equation:

$$PF = \frac{P}{S}. \quad (30)$$

(iii) The sign of  $Q$  is calculated using harmonic components method according Budenau definition:

$$\text{sing}(Q) = \text{sign} \left\{ \sum_{h=1}^H (U(h) \cdot I(h) \cdot \sin \phi(h)) \right\}, \quad (31)$$

where  $h$  is harmonic index,  $H$  is harmonics count,  $U(h)$ ,  $I(h)$  and  $\phi(h)$  are harmonic voltage, current and phase shift. Note the absolute value of  $Q$  is still calculated from AC components following equation 29. Only the sign of  $Q$  is decided from the Budenau definition 31.

The TWM-PWRTDI algorithm wrapper is able to use single-ended or differential input sensors for voltage channel, current channel or both. The algorithm is also equipped by a fast uncertainty estimator and the Monte Carlo uncertainty calculation method for more accurate but slower uncertainty evaluation.

### 7.1 TWM wrapper parameters

The input quantities supported by the algorithm are shown in the table 30. Algorithm returns output quantities shown in the table 31. Calculation setup supported by the algorithm is shown in table 32.

Table 30: List of input quantities to the TWM-PWRTDI wrapper.  
Details on the correction quantities can be found in [5].

Name	Default	Unc.	Description
ac_coupling	0	N/A	Enables virtual AC coupling of the wattmeter. This option will cause the DC value will be ignored.
u	N/A	No	Input voltage sample data vector and complementary low-side input data vector $i_{lo}$ (for differential mode only).
i	N/A	No	Input current sample data vector and complementary low-side input data vector $i_{lo}$ (for differential mode only).
i_lo	N/A	No	
Ts	N/A	No	Sampling period or sampling rate or sample time vector.
fs	N/A	No	Note the wrapper always calculates in equidistant mode, so
t	N/A	No	$t$ is used just to calculate $Ts$ .
time_shift	0	Yes	Timeshift between voltage channel $u$ and current channel $i$ .

Table 30: List of input quantities to the TWM-PWRTDI wrapper.  
Details on the correction quantities can be found in [5].

Name	Default	Unc.	Description
u_time_shift_lo	0	Yes	Time shift between high-side channel $u$ low-side channel $u_lo$ (or $i$ and $i_lo$ for current).
i_time_shift_lo	0	Yes	
u_lsb	N/A	No	Either absolute ADC resolution $lsb$ or nominal range value $adc_nrng$ (e.g.: 5 V for 10 Vpp range) and $adc_bits$ bit resolution of ADC.
u_adc_nrng	1000	No	
u_adc_bits	40	No	
u_lo_lsb	N/A	No	
u_lo_adc_nrng	1000	No	
u_lo_adc_bits	40	No	
i_lsb	N/A	No	
i_adc_nrng	1000	No	
i_adc_bits	40	No	
i_lo_lsb	N/A	No	
i_lo_adc_nrng	1000	No	
i_lo_adc_bits	40	No	
u_adc_offset	0	Yes	Digitizer input offset voltage.
u_lo_adc_offset	0	Yes	
i_adc_offset	0	Yes	
i_lo_adc_offset	0	Yes	
u_adc_gain	1	Yes	Digitizer gain correction 2D table (multiplier).
u_adc_gain_f	□	No	
u_adc_gain_a	□	No	
u_lo_adc_gain	1	Yes	
u_lo_adc_gain_f	□	No	
u_lo_adc_gain_a	□	No	
i_adc_gain	1	Yes	
i_adc_gain_f	□	No	
i_adc_gain_a	□	No	
i_lo_adc_gain	1	Yes	
i_lo_adc_gain_f	□	No	
i_lo_adc_gain_a	□	No	
u_adc_phi	0	Yes	Digitizer phase correction 2D table (additive).
u_adc_phi_f	□	No	
u_adc_phi_a	□	No	
u_lo_adc_phi	0	Yes	
u_lo_adc_phi_f	□	No	
u_lo_adc_phi_a	□	No	
i_adc_phi	0	Yes	
i_adc_phi_f	□	No	
i_adc_phi_a	□	No	
i_lo_adc_phi	0	Yes	
i_lo_adc_phi_f	□	No	
i_lo_adc_phi_a	□	No	
adc_freq	0	Yes	Digitizer timebase error correction: $f_{tb}' = f_{tb} \cdot (1 + adc\_freq.v)$ The effect on the estimated frequency is opposite: $f_{est}' = f_{est} / (1 + adc\_freq.v)$
u_adc_jitter	0	No	Digitizer sampling period jitter [s].
u_lo_adc_jitter	0	No	
i_adc_jitter	0	No	
i_lo_adc_jitter	0	No	

Table 30: List of input quantities to the TWM-PWRTDI wrapper.  
Details on the correction quantities can be found in [5].

Name	Default	Unc.	Description
u_adc_aper u_lo_adc_aper i_adc_aper i_lo_adc_aper	0 0 0 0	No No No No	ADC aperture value [s].
u_adc_aper_corr u_lo_adc_aper i_adc_aper_corr i_lo_adc_aper	0 0 0 0	No No No No	ADC aperture error correction enable: $A' = A \cdot pi \cdot adc\_aper \cdot f\_est / \sin(pi \cdot adc\_aper \cdot f\_est)$ $phi' = phi + pi \cdot adc\_aper \cdot f\_est$
u_adc_sfdr u_adc_sfdr_f u_adc_sfdr_a u_lo_adc_sfdr u_lo_adc_sfdr_f u_lo_adc_sfdr_a i_adc_sfdr i_adc_sfdr_f i_adc_sfdr_a i_lo_adc_sfdr i_lo_adc_sfdr_f i_lo_adc_sfdr_a	180 [] [] 180 [] [] 180 [] [] 180 [] []	No No No No No No No No No No No No	Digitizer SFDR 2D table.
u_adc_Yin_Cp u_adc_Yin_Gp u_adc_Yin_f u_lo_adc_Yin_Cp u_lo_adc_Yin_Gp u_lo_adc_Yin_f i_adc_Yin_Cp i_adc_Yin_Gp i_adc_Yin_f i_lo_adc_Yin_Cp i_lo_adc_Yin_Gp i_lo_adc_Yin_f	1e-15 1e-15 [] 1e-15 1e-15 [] 1e-15 1e-15 [] 1e-15 1e-15 []	Yes Yes No Yes Yes No Yes Yes No Yes Yes No	Digitizer input admittance 1D table.
u_tr_type i_tr_type	""	No	Transducer type string ("rvd" or "shunt").
u_tr_gain u_tr_gain_f u_tr_gain_a i_tr_gain i_tr_gain_f i_tr_gain_a	1 [] [] 1 [] []	Yes No No Yes No No	Transducer gain correction 2D table (multiplicative).
u_tr_phi u_tr_phi_f u_tr_phi_a i_tr_phi i_tr_phi_f i_tr_phi_a	0 [] [] 0 [] []	Yes No No Yes No No	Transducer phase correction 2D table (additive).
u_tr_sfdr u_tr_sfdr_f u_tr_sfdr_a i_tr_sfdr i_tr_sfdr_f i_tr_sfdr_a	180 [] [] 180 [] []	No No No No No No	Transducer SFDR 2D table.

Table 30: List of input quantities to the TWM-PWRTDI wrapper.  
Details on the correction quantities can be found in [5].

Name	Default	Unc.	Description
u_tr_Zlo_Rp	1e3	Yes	RVD transducer low-side impedance 1D table. Note this is related to loading correction and it has effect only for RVD transducer and will work only if <i>adc_Yin</i> is defined as well.
u_tr_Zlo_Cp	1e-15	Yes	
u_tr_Zlo_f	<input type="checkbox"/>	No	
i_tr_Zlo_Rp	1e3	Yes	
i_tr_Zlo_Cp	1e-15	Yes	
i_tr_Zlo_f	<input type="checkbox"/>	No	
u_tr_Zbuf_Rs	0	Yes	Loading corrections: Transducer output buffer output series impedance 1D table. Leave unassigned to disable buffer from the correction topology.
u_tr_Zbuf_Ls	0	Yes	
u_tr_Zbuf_f	<input type="checkbox"/>	No	
i_tr_Zbuf_Rs	0	Yes	
i_tr_Zbuf_Ls	0	Yes	
i_tr_Zbuf_f	<input type="checkbox"/>	No	
u_tr_Zca_Rs	1e-9	Yes	Loading corrections: Transducer high side terminal series impedance 1D table.
u_tr_Zca_Ls	1e-12	Yes	
u_tr_Zca_f	<input type="checkbox"/>	No	
i_tr_Zca_Rs	1e-9	Yes	
i_tr_Zca_Ls	1e-12	Yes	
i_tr_Zca_f	<input type="checkbox"/>	No	
u_tr_Zcal_Rs	1e-9	Yes	Loading corrections: Transducer low side terminal series impedance 1D table.
u_tr_Zcal_Ls	1e-12	Yes	
u_tr_Zcal_f	<input type="checkbox"/>	No	
i_tr_Zcal_Rs	1e-9	Yes	
i_tr_Zcal_Ls	1e-12	Yes	
i_tr_Zcal_f	<input type="checkbox"/>	No	
u_tr_Yca_Cp	1e-15	Yes	Loading corrections: Transducer output terminals shunting impedance.
u_tr_Yca_D	1e-12	Yes	
u_tr_Yca_f	<input type="checkbox"/>	No	
i_tr_Yca_Cp	1e-15	Yes	
i_tr_Yca_D	1e-12	Yes	
i_tr_Yca_f	<input type="checkbox"/>	No	
u_tr_Zcam	1e-12	Yes	Loading corrections: Transducer output terminals mutual inductance 1D table.
u_tr_Zcam_f	<input type="checkbox"/>	No	
i_tr_Zcam	1e-12	Yes	
i_tr_Zcam_f	<input type="checkbox"/>	No	
u_Zcb_Rs	1e-9	Yes	Loading corrections: Cable series impedance 1D table.
u_Zcb_Ls	1e-12	Yes	
u_Zcb_f	<input type="checkbox"/>	No	
i_Zcb_Rs	1e-9	Yes	
i_Zcb_Ls	1e-12	Yes	
i_Zcb_f	<input type="checkbox"/>	No	
u_Ycb_Rs	1e-15	Yes	Loading corrections: Cable series impedance 1D table.
u_Ycb_Ls	1e-12	Yes	
u_Ycb_f	<input type="checkbox"/>	No	
i_Ycb_Rs	1e-15	Yes	
i_Ycb_Ls	1e-12	Yes	
i_Ycb_f	<input type="checkbox"/>	No	



Table 31: List of output quantities of the TWM-PWRTDI wrapper.

Name	Uncertainty	Description
U	Yes	RMS voltage [V].
I	Yes	RMS current [A].
P	Yes	Active power [W].
S	Yes	Apparent power [VA].
Q	Yes	Reactive power [VAr].
phi_ef	Yes	Effective phase angle: $\arccos(PF)$ [rad].
Udc	Yes	DC voltage component [V].
Idc	Yes	DC current component [A].
Pdc	Yes	DC power component [W].
spec_U	No	Voltage channel spectrum [V].
spec_I	No	Current channel spectrum [A].
spec_S	No	Apparant power spectrum [VA].
spec_f	No	Frequency vector of <i>spec_U</i> , <i>spec_I</i> and <i>spec_S</i> .

Table 32: List of “calcset” options supported by the TWM-PWRTDI wrapper.

Name	Description
calcset.unc	Uncertainty calculation mode. Supported: “none”, “guf” for uncertainty estimator, “mcm” for Monte Carlo.
calcset.mcm.method	Monte Carlo evaluation mode: “singlecore” - single core evaluation, “multicore” - Parallel evaluation using “parcellfun” for GNU Octave or “parfor” for Matlab “multistation” - Multicore evaluation using “multicore” package (GNU Octave only yet).
calcset.mcm.repeats	Monte Carlo iterations count. Use at least 100 to get any usable estimate.
calcset.mcm.proc_no	Number of parallel instances to use for the paralleled modes. Use zero value to not start any server processes for the “multistation” mode. This option expects user started the server processes manually in the shared folder. This option causes less overhead for the batch processing or runtime calculations.
calcset.mcm.tmpdir	Jobs sharing folder for the “multistation” mode. This should be an absolute path to the sharing folder. Keep in mind the package “multicore” will erase the content of this folder before each new calculation!
calcset.mcm.user_fun	User function to call in the “multistation” mode after startup of the serve processes. Example: “calcset.mcm.user_fun = @coklbind2”. Leave empty to not execute any function.
calcset.loc	Level of confidence [-].
calcset.verbose	Verbose level.

## 7.2 Algorithm description

The TWM-PWRTDI wrapper starts with automatic cropping of the input data to a size of multiple of two, which is required by the algorithm core. Next, the wrapper creates two virtual channels, one for voltage and one for current, because the applied corrections are identical for both so the code duplication is minimised. It also creates virtual sub-channels for the low-side signals  $u_{lo}$  and  $i_{lo}$  (differential mode). Next, the wrapper calculates windowed spectra of each input signal  $u$  and  $i$  (and  $u_{lo}$ ,  $i_{lo}$ ) and also splits the time domain signals  $u$  and  $i$  (and  $u_{lo}$ ,  $i_{lo}$ ) to AC and DC components which are treated separately.

The next step are the frequency dependent corrections of the input signals. Note the windowed RMS (WRMS) algorithm itself operates in time domain, so the frequency dependent corrections of the gain and phase must be applied in time domain to  $u$  and  $i$  (and  $u_{lo}$ ,  $i_{lo}$ ). However, the uncertainty calculator/estimator needs a spectrum, i.e. frequency domain representation of the time domain signals. Therefore, the correcting code does two things at once: (i) It calculates total combined gain and phase corrections for each virtual channel but does not apply it to time domain data  $u$  and  $i$  (and  $u_{lo}$ ,  $i_{lo}$ ) yet; (ii) It applies the same corrections to the frequency domain representation only. At the same time the spectra of the eventual differential pair  $u$  and  $u_{lo}$  (and  $i$  and  $i_{lo}$ ) are merged to a single single-ended spectrum of  $u$  and  $i$ .

In the next step, the wrapper calls the main WRMS function “proc.wrms()”, which applies the calculated corrections in time domain to  $u$ ,  $i$  (and  $u_{lo}$ ,  $i_{lo}$ ), calculates the differential time domain signal (for differential mode only) and calculates the AC RMS parameters  $U$ ,  $I$ , AC power  $P$  (see below) and the DC components  $U_{dc}$  and  $I_{dc}$ . Follows the uncertainty calculation (see below) of the RMS and active power quantities and expression of the other desired quantities and their uncertainties. For simplicity the uncertainty calculator calculates only uncertainty of the RMS voltage, RMS current a active power. The remaining uncertainties are calculated from these three. The definitions of particular parameters is shown in the table 33. Note the  $Q_{bud}$  quantity in the table is reactive power estimated from the FFT spectra of voltage and current according the Budenau definition:

$$Q_{bud} = \sum_{h=1}^H (0.5 \cdot U(h) \cdot I(h) \cdot \sin \phi(h)), \quad (32)$$

where  $h$  is harmonic component index,  $H$  is total harmonics count,  $U(h)$  and  $I(h)$  are harmonic voltage and current amplitudes and  $\phi(h)$  is voltage to current phase shift. The purpose of the  $(sign)(Q_{bud})$  term is to distinguish correct polarity of  $Q$ , because the WRMS algorithm itself cannot distinguish all four quadrants of power. One solution would be to use Hilbert transformation on either voltage or current waveform and repeat the WRMS calculation. This would allow to calculate the  $Q$  directly, however such solution seemed to complex. Therefore, instead of the Hilbert transform, the sign of  $Q$  was obtained from the Budenau’s definition. Such solution should work reliably if power factor is  $|PF| > 0.05$  and there are no excessive harmonics.

Table 33: Definitions of the TWM-PWRTDI output quantities based on the basic quantities  $U$ ,  $I$ ,  $P$ ,  $U_{dc}$  and  $I_{dc}$ . Note the input quantities marked \* are obtained from the other output quantity.

Returned quantity	AC coupled definition	DC coupled definition
DC voltage $U_{dc}$	$U_{dc}$	$U_{dc}$
DC current $I_{dc}$	$I_{dc}$	$I_{dc}$
DC power component $P_{dc}$	$U_{dc} \cdot I_{dc}$	$U_{dc} \cdot I_{dc}$
RMS voltage $U$	$U$	$\sqrt{U^2 + U_{dc}^2}$
RMS current $I$	$I$	$\sqrt{I^2 + I_{dc}^2}$
Active power $P$	$P$	$P + U_{dc} \cdot I_{dc}$
Reactive power $Q$	$\sqrt{(UI)^2 - P^2} \cdot \text{sign}(Q_{bud})$	$\sqrt{(UI)^2 - P^2} \cdot \text{sign}(Q_{bud})$
Apparent power $S$	$(UI)^2$	$\sqrt{U^2 + U_{dc}^2} \cdot \sqrt{I^2 + I_{dc}^2}$
Power factor $PF$	$P/S^*$	$P/S^*$
Effective phase angle $phi_{ef}$	$\text{atan2}(Q^*, P)$	$\text{atan2}(Q^*, P)$

### 7.2.1 Windowed RMS function “proc.wrms()”

The core of the algorithm is function “proc.wrms()”. Before the algorithm itself is described, it must be noted the “proc.wrms()” function was made in such a way it can be used for a Monte Carlo uncertainty evaluation in a parallel manner. I.e. the function is called once for each Monte Carlo iteration (see below). This affected its structure.

The function can be executed either on the input time domain signals  $u$ ,  $i$  (and  $u_{lo}$ ,  $i_{lo}$ ) which is used for evaluation of the power parameters and it can be also called repeatedly in the simulator mode, where it calculates the power of synthesized signals with prescribed parameters randomized by

input uncertainties (Monte Carlo calculation mode). The synthesizer of the waveforms is included in this function, so the following section will show its function as well.

The function starts with selection of the mode of operation. For the simulated mode, it overrides input signals  $u$ ,  $i$  (and  $u_{lo}$ ,  $i_{lo}$ ) by a synthesized ones with known spectral components and known total power, power factor, etc. It also applies various distortions, e.g. noise, quantisation errors, ...

Follows the calculation part which is common for both modes of operation. First, it applies the time domain frequency dependent correction of each virtual channel ( $u$ ,  $i$ ,  $u_{lo}$  and  $i_{lo}$ ). This is done by the “`td_fft_filter()`”. Note the function “`td_fft_filter()`” itself also estimates the phase errors it causes, which is used only in the calculation mode (they are ignored in the simulating mode). The DC corrections to the previously split DC components are also applied in this step.

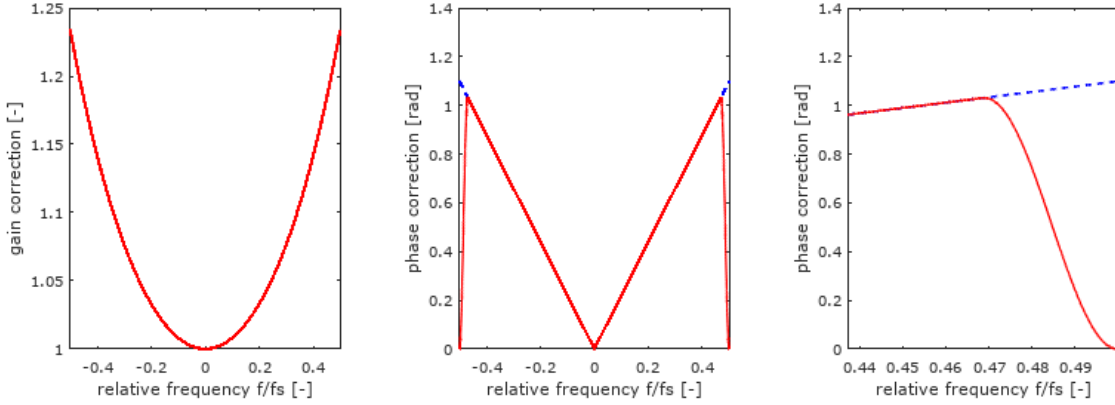


Figure 22: Example of FFT filter profile. From left right: Gain correction, Phase correction, Detail of phase correction. Blue - desired correction, red - applied correction.

The function “`td_fft_filter()`” is critical for correct functionality of the whole algorithm. The function is a frequency domain filter executed per smaller windows. The function does following steps:

1. Building a filter spectral profile from the gain/phase correction data for the positive frequencies.
2. Empirical post-processing of the filter profile to suppress the errors caused by high phase angle correction. This step applies weighting mask to the phase of the filter at its ends (at DC and Nyquist frequency). So both “ends” of the filter have zero phase. This drastically reduces inherent errors of this filtering method. See fig. 22 for an example.
3. Estimation of the filter post-processing errors on the phase.
4. Extending the filter profile to negative frequencies.
5. Performing the spectral filtering per small overlapping windows by a function “`sFreqDep_PG_Comp(y, fft_size, filter)`”:
  - (a) Obtaining Hann window function coefficients  $w$  of size  $fft\_size/2$ .
  - (b) Extend Hann by zero padding:  $w = [\text{zeros}(1, fft\_size/4), w, \text{zeros}(1, fft\_size/4)]$  to a total size of  $fft\_size$ .
  - (c) Window  $fft\_size$  input samples  $y(offset : offset + fft\_size - 1)$  by the window  $w$ .
  - (d) Performing FFT of the windowed portion of  $y$  to get spectrum  $\hat{Y}$ .
  - (e) Applying  $filter$  profile to the spectrum  $\hat{Y}$ .
  - (f) Performing inverse-FFT of the  $\hat{Y}$  to get time domain representation  $y\_frame$ .
  - (g) Extracting  $< fft\_size/4; fft\_size \cdot 3/4 >$  samples of  $y\_frame$ .
  - (h) Merging  $y\_frame$  samples with overlapping samples of output signal  $yf$  and storing result to  $yf(offset + fft\_size/2)$ .

- (i) Move *offset* to next frame by *fft\_size*/4 samples and repeat from step 5c for all possible frames.
- 6. Removing invalid portions of the filtered signal (*fft\_size*/2 samples from beginning and end of signal).

In the next step the “proc\_wrms()” evaluates the RMS parameters  $U$ ,  $I$  and  $P$  according the following definitions:

$$U = \frac{1}{W} \cdot \sqrt{\sum_{k=1}^N w(k)^2 \cdot u(k)^2}, \quad (33)$$

$$I = \frac{1}{W} \cdot \sqrt{\sum_{k=1}^N w(k)^2 \cdot i(k)^2}, \quad (34)$$

$$P = \frac{1}{W^2} \cdot \sqrt{\sum_{k=1}^N w(k)^2 \cdot u(k) \cdot i(k)}, \quad (35)$$

$$W = \sqrt{\sum_{k=1}^N w(k)^2}, \quad (36)$$

where  $k$  is a sample index,  $N$  is total samples count and  $w(k)$  is  $k$ -th sample of the window function Blackman-Harris. For clarity, the Blackman-Harris window used in the WRMS algorithm is defined by [2]:

$$w(k) = 0.35875 - 0.48829 \cdot \cos \frac{2\pi k}{N} + 0.14128 \cdot \cos \frac{4\pi k}{N} - 0.01168 \cdot \cos \frac{6\pi k}{N}. \quad (37)$$

Note the coefficients are exact (not rounded). This window was selected because the calculation errors of the RMS parameters due to the non-coherency decays fastest with growing number of signal periods (see [1]).

Last step of the function “proc\_wrms()” is performed only for the simulation mode. The function calculates the deviation of calculated power from the theoretical synthesized power (used for Monte Carlo evaluation).

### 7.3 Uncertainty calculator and estimator

The TWM-PWRTDI algorithm wrapper is equipped by two modes of uncertainty evaluation: (i) The ordinary Monte Carlo (MC) calculator; (ii) Fast estimator based on several precalculated lookup tables (LUT). The MC mode is more accurate, however it may take up to several minutes to perform even just a few hundreds of iterations. The calculation time drastically rises with the length of the record. Thus the fast estimator was created as well.

The WRMS algorithm itself can calculate a power of any voltage and current waveforms. However, calculation of uncertainty for general non-periodic waveforms would be extremely complex and slow. Therefore, the uncertainty calculation is based on the analysis of spectral components obtained from the average spectrum of the whole digitized waveform. This simplification should not have any effect, as the algorithm is primarily intended for a calibration of stationary signals.

The first step of the uncertainty evaluation for both modes is spectral analysis of the voltage and current spectra  $Uh(fh)$ ,  $Ih(fh)$  and phase shifts between the voltage and current harmonic components  $ph(fh)$ . These spectra along with their uncertainties were obtained in the corrections section (see section 7.2). The algorithm identifies the fundamental component of power by searching the dominant voltage harmonic assuming the fundamental voltage harmonic should be always present. The algorithm then searches up to 100 spectral components  $Ux(fh)$ ,  $Ix(fh)$  and  $phx(fh)$ , whose current or voltage amplitude exceeds certain threshold relative to the fundamental harmonic. These spectral components are successively removed from the spectra  $Uh(fh)$  and  $Ih(fh)$ . Whatever is left after the removal is considered and later used as a residual RMS noise estimate. The identified spectral components will be marked  $Ux(h)$ ,  $Ix(h)$  (amplitudes) and  $phx(h)$  in the following text. Their uncertainties coming from

the correction uncertainties will be marked  $u_Ux(h)$ ,  $u_Ix(h)$ ,  $u_phx(h)$ . The  $h$  is index of harmonic from one to  $H$ .

The identified spectral components  $Ux(h)$ ,  $Ix(h)$  and  $phx(h)$  are used to calculate estimate of the RMS and power parameters following the Budenau definition:

$$U_{rms} = \sqrt{\sum_{h=1}^H 0.5 \cdot Ux(h)^2}, \quad (38)$$

$$I_{rms} = \sqrt{\sum_{h=1}^H 0.5 \cdot Ix(h)^2}, \quad (39)$$

$$P = 0.5 \cdot \sum_{h=1}^H Ix(h) \cdot Ix(h) \cdot \cos(phx(h)), \quad (40)$$

$$Q = 0.5 \cdot \sum_{h=1}^H Ix(h) \cdot Ix(h) \cdot \sin(phx(h)), \quad (41)$$

$$S = 0.5 \cdot \sum_{h=1}^H Ix(h) \cdot Ix(h), \quad (42)$$

$$(43)$$

Following algorithm structure differ for Monte Carlo and Estimator.

### 7.3.1 Monte Carlo uncertainty calculator

The MC uncertainty calculator is very straightforward. It starts with preparation of the two virtual channels. One for voltage and one for current. Each channel contains a list of the identified spectral components  $Ux(h)$ ,  $Ix(h)$  and  $phx(h)$  to synthesize with assigned uncertainties coming from the corrections  $u_Ux(h)$ ,  $u_Ix(h)$ ,  $u_phx(h)$ . Each channel have also assigned RMS noise, system SFDR and LSB of the ADC. Then the WRMS processing function “`proc_wrms()`” is called in the simulator mode repeatedly for each iteration of MC. The returned randomised lists of RMS voltage, RMS current and active power are evaluated according GUM annex 1 [3] using a function “`scovint()`” to obtain absolute final uncertainties of quantities  $U$ ,  $I$  and  $P$ . The uncertainties of the other returned quantities are evaluated in the wrapper (see above) from these three uncertainties.

Note the MC evaluator itself uses function “`qwtb_mcm_exec()`”. This function is internally designed to enable parallel calculation of the MC iteration cycles. It offers three modes of parallelisation:

1. **`calcset.mcm.method = 'singlecore'`**: Single core calculation.
2. **`calcset.mcm.method = 'multicore'`**: Multicore operation using “`parcellfun()`” from “parallel” package for GNU Octave or “`parfor`” for Matlab. Note the use of Matlab’s “`parfor`” for parallelisation is just a user wish. Actual parallelisation mode is decided by Matlab. The package “`parcellfun()`” implementation does work only for Linux. Windows implementation was not functional at least up to GNU Octave version 4.2.2.
3. **`calcset.mcm.method = 'multistation'`**: Multiprocess/multistation calculation using “multicore” package for GNU Octave (Matlab is not supported yet). Note the The “multistation” method requires to define shared folder path for the job files. Otherwise it will create the shared folder in temp folder, which may not be appreciated by the SSD disks owners. The mode “multistation” also have one specific feature. It can initiate the user function after startup of the server processes. The function is defined in the “`calcset.mcm.user_fun`” variable. The example of the use for this optional input is CMI’s supercomputer “`Čokl`” [6] which requires to call a special script to assign server processes to particular CPU cores.

See table 32 for list of the additional parameters. Note at least 100 iterations is the absolute minimum for which the MC mode provides any usable uncertainty estimates. The processing time for an evaluation at 4 cores with 1000 cycles and  $N = 10000$  input samples is typically below one minute. However, the situation may change drastically when high count of harmonic components is presents in the signal.

### 7.3.2 Fast uncertainty estimator

The uncertainty estimator is significantly more complex than the Monte Carlo calculator. It consists of four separate estimation routines which contributes to the final uncertainty: (i) Uncertainty of time-domain frequency dependent filter “td\_fft\_filter()”; (ii) Uncertainty of a system SFDR; (iii) Uncertainty WRMS algorithm for a single tone signal; (iv) Uncertainty of WRMS mutual harmonic effects. These are executed in order. The estimation routine (i) is affecting steps (ii), (iii) and (iv). The obtained uncertainty components from the particular steps are combined to the total uncertainty of  $U$ ,  $I$  and  $P$ . The uncertainties of the other returned quantities are evaluated in the wrapper (see above) from these three uncertainties.

#### 7.3.2.1 Uncertainty of time-domain frequency dependent filter “td\_fft\_filter()”

The first estimator quantifies the errors introduced by the frequency dependent gain and phase filter “td\_fft\_filter()”. The uncertainty estimate is calculated using a complementary function “td\_fft\_filter\_unc()”, which is called for voltage and current channel separately. This estimator is far most problematic. The “td\_fft\_filter()” is using the time- $\leftrightarrow$ frequency- $\leftrightarrow$ time conversion (filtering in frequency domain per small sized windows). The filtering in the frequency domain can cause hardly predictable errors when high phase shift corrections are applied. This is especially problematic if there are significant spectral components near the Nyquist frequency or near DC. The function have too many degrees of freedom to create a simple but reliable estimator. Therefore, the only usable solution found to this problem was to perform a small scale Monte Carlo (MC). In particular, 10 cycles of following steps are performed:

1. Synthesize waveform with spectral components  $Ux(h)$  (resp.  $Ix(h)$ ) with random phase angles  $\phi(h)$  and with uncertain frequency  $\pm 1$  DFT bin, because accuracy of the frequency estimation from FFT spectral analysis is limited.
2. Perform the frequency dependent filtering by “td\_fft\_filter()” with calculated channel gain and phase correction data and calculate spectrum.
3. Perform the frequency dependent correction with the same correction data in frequency domain to the spectral components  $Ux(h)$  (resp.  $Ix(h)$ ) and the generated phase angles  $\phi(h)$ .
4. Compare the difference of the spectral components from 3) and 2) to estimate the filter error.

The set of error estimates is processed to find a maximum probable amplitude and phase error of each spectral component. Surprisingly this simple solution provides reliable estimates.

This gain uncertainties  $u\_fa\_U(h)$ ,  $u\_fa\_I(h)$  and phase uncertainties  $u\_fp\_U(h)$ ,  $u\_fp\_I(h)$  obtained by this estimator are used to expand the correction uncertainties  $u\_Ux(h)$ ,  $u\_Ix(h)$  and  $u\_phx(h)$  before following estimator steps:

$$u\_Ux(h) = \sqrt{u\_Ux(h)^2 + u\_fa\_U(h)^2}, \quad (44)$$

$$u\_Ix(h) = \sqrt{u\_Ix(h)^2 + u\_fa\_I(h)^2}, \quad (45)$$

$$u\_phx(h) = \sqrt{u\_phx(h)^2 + u\_fp\_U(h)^2 + u\_fp\_I(h)^2}. \quad (46)$$

#### 7.3.2.2 Uncertainty of a system SFDR

The next step is estimation of the uncertainty introduced by the system SFDR (digitizer and transducer). The effect on the  $U$ ,  $I$  and  $P$  is estimated as a worst case combination of the spurs according:

$$u\_U\_sfdr = \frac{1}{\sqrt{3}} \cdot \left( \sqrt{U^2 + 0.5 \sum_{s=1}^S U\_spur(s)^2} - U \right), \quad (47)$$

$$u\_I\_sfdr = \frac{1}{\sqrt{3}} \cdot \left( \sqrt{I^2 + 0.5 \sum_{s=1}^S I\_spur(s)^2} - I \right), \quad (48)$$

$$u\_P\_sfdr = \frac{1}{\sqrt{3}} \cdot \sqrt{0.5 \sum_{s=1}^S U\_spur(s) \cdot I\_spur(s)}, \quad (49)$$

where  $U_{spur}$  and  $I_{spur}$  are vectors of voltage and current spur amplitudes (2nd, 3rd, 4th harmonic, etc.),  $s$  is spur index and  $S$  is spurs count.

### 7.3.2.3 Uncertainty WRMS algorithm for a single tone signal

This step is estimation of the WRMS algorithm error for each identified spectral component  $Ux(h)$ ,  $Ix(h)$ . Note this estimator does not cover mutual effects between spectral components. It is just a single tone estimator for each component. The estimation is performed by the function “wrms\_unc\_st()”. This function uses precalculated LUT (see below) and empiric formulas to form an uncertainty interpolator dependent on following parameters: (i) Voltage amplitude, (ii) Current amplitude, (iii) Voltage noise, (iv) Current noise, (v) Voltage bit resolution, (vi) Current bit resolution, (vii) Periods count in the waveform, (viii) Samples per period. The usable range of each parameter for the “wrms\_unc\_st()” is shown in table 35. This interpolator returns a relative uncertainty estimate of frequency component voltage  $u_{U\_st'}(f)$ , current  $u_{I\_st'}(f)$  and active power  $u_{P\_st'}(f)$ . The component uncertainties are converted to absolute and combined to obtain RMS uncertainties:

$$u_{U\_st} = \sqrt{\frac{\sum_{f=1}^F u_{U\_st'}(f)^2 \cdot Ux(f)^2}{\sum_{f=1}^F Ux(f)^2}}, \quad (50)$$

$$u_{I\_st} = \sqrt{\frac{\sum_{f=1}^F u_{I\_st'}(f)^2 \cdot Ix(f)^2}{\sum_{f=1}^F Ix(f)^2}}, \quad (51)$$

$$u_{P\_st} = \sqrt{\sum_{f=1}^F u_{P\_st'}(f)^2}. \quad (52)$$

The LUT table itself for the interpolator of “wrms\_unc\_st()” was calculated as a worst case error of the WRMS algorithm from 50000 Monte Carlo iterations. The simulation was performed for each combination of parameters shown in table 34. I.e.  $11 \times 12 \times 15 \times 9 \times 5 = 89100$  combinations were calculated using a supercomputer (processing time roughly two days on 300 cores). Note the phase shift between voltage and current was randomised for each iteration as it had no effect on the relative active power uncertainty (when expressed in units W/VA). The bit resolution of one channel was held fixed at 32 bit as the error is defined by the worse of the voltage and current channel. Noise was also simulated for the worse of the channels only. Manual inspection of the obtained 5-dimensional space of uncertainties showed only the parameters “Periods count” and “Samples per period” are necessary in the LUT as they have hardly expressible shape given by the window function. The other parameters effects were approximated by empirical formulas. Therefore, the LUT size after compression is only 2.5 kBytes, which is perfectly acceptable.

Table 34: Simulation ranges and steps of the parameters for uncertainty estimator of “wrms\_unc\_st()” function.

Name	Description
Periods count	List: [3; 4; 5; 6; 7; 9; 11; 15; 20; 50; 100], 11 steps
Samples per period	Log. space: 7 to 100, 12 steps
U to I phase shift	random*
U to I amplitude ratio	Log. space: 0.01 to 1, 15 steps
U bit resolution	32 bits
I bit resolution	Log. space: 4 to 32 bits, 9 steps
max(U noise,I noise)	Log. space: $10^{-7}$ to $10^{-3}$ , 5 steps

Table 35: The usable range of input parameters of the single tone error estimator “wrms\_unc\_st()”. The actions on min or max value is reached are: “error” - generate error; “const” - return value of uncertainty at min. or max. of simulated range.

Name	Range	On min	On max
Voltage amplitude	0 to $\infty$	const	const
Current amplitude	0 to $\infty$	const	const
Voltage noise	0 to $\infty$	const	const
Current noise	0 to $\infty$	const	const
Voltage bit resolution	4 to $\infty$	error	const
Current bit resolution	4 to $\infty$	error	const
Periods count	3 to $\infty$	error	const
Samples per period	7 to $\infty$	const	const

#### 7.3.2.4 Uncertainty of WRMS mutual harmonic effects

This estimator calculates mutual effect of spur harmonic to analysed harmonic. The paper [1] shows example of these errors, however this effect had to be quantified extensively for means of the uncertainty estimator. Theoretically the calculation of mutual effect should be performed for each pair of components  $Ux(h)$ ,  $Ix(h)$ ,  $phx(h)$ , however that would be very slow. So an assumption was made the fundamental harmonic carries dominant portion of the active power, RMS voltage and current, so the mutual effects calculation is performed only between the fundamental component  $Ux(1)$ ,  $Ix(1)$ ,  $phx(1)$  and the rest of components  $Ux(h)$ ,  $Ix(h)$ ,  $phx(h)$ , where  $h \geq 2$ . The estimation of the mutual effect itself is done by estimator function “wrms\_unc\_spur()”. This function is an interpolator dependent on: (i) Reference harmonic voltage, (ii) Reference harmonic current, (iii) Relative spur frequency, (iv) Spur harmonic voltage, (v) Spur harmonic current, (vi) Periods of reference harmonic, (vii) Samples per period of reference harmonic. The estimator function is called once for each spur component to obtain uncertainty components  $u_{U\_sp'}(h-1)$ ,  $u_{I\_sp'}(h-1)$  and  $u_{P\_sp'}(h-1)$ . These  $(H-1)$  components are combined to a combined uncertainty due to the spur components:

$$u_{U\_sp}(h) = \sqrt{\frac{\sum_{h=1}^{H-1} u_{U\_sp'}(h)^2 \cdot Ux(h+1)^2}{\sum_{h=1}^H Ux(h)^2}}, \quad (53)$$

$$u_{I\_sp}(h) = \sqrt{\frac{\sum_{h=1}^{H-1} u_{I\_sp'}(h)^2 \cdot Ix(h+1)^2}{\sum_{h=1}^H Ix(h)^2}}, \quad (54)$$

$$u_{P\_sp}(h) = \sqrt{\sum_{h=1}^{H-1} u_{P\_sp'}(h)^2}. \quad (55)$$

The interpolator “wrms\_unc\_spurr()” itself is a combination of two precalculated LUT tables and empiric formulas. First LUT is used to estimate the uncertainty of active power. It was obtained as a worst case error of 1000 Monte Carlo iterations performed each parameter combination ( $10 \times 10 \times 7 \times 9 \times 15 = 94500$  combinations) shown in table 36. The simulation was performed without noise or quantisation errors, because these are already covered by the single tone WRMS estimator (section 7.3.2.3). The simulator performed following steps for each combination:

1. Synthesize waveforms with known apparent power  $S_{ref}$  with no spurs.
2. Calculate active power using the WRMS algorithm  $P_{dut.0}$ .
3. Synthesize waveforms with known active power with spur at voltage channel.
4. Calculate active power using the WRMS algorithm  $P_{dut.tot}$ .
5. Calculate relative error of the WRMS power:  $\delta P(i) = |P_{dut.tot} - P_{dut.0}|/S_{ref}$ .
6. Repeat 1000 times from step 1.



7. Estimate worst case uncertainty:  $\delta P = \max \delta P(i)$  for  $i = 1..1000$ .

The simulator for the first LUT generates spur only for voltage channel, because the voltage and current channels are interchangeable. Thus the same LUT is used twice for the estimation (once for voltage spur effect and once for current spur effect with swapped voltage and current parameters).

The second LUT is used to estimate the spur effect to the RMS voltage (or RMS current). It was simulated together with the first LUT. Only exception is the resulting LUT does not contain axis “U to I amplitude ratio”, as it obviously has no effect to RMS level of single channel. So the table contains only  $11 \times 10 \times 9 \times 15 = 14850$  combinations. The procedure performed for each combination is following:

1. Synthesize waveform with known RMS level  $A_{ref}$  with no spurs.
2. Calculate RMS level using the WRMS algorithm:  $A_{dut}$ .
3. Synthesize waveform with known RMS level with spur of RMS level  $S_{ref}$ .
4. Calculate RMS level using the WRMS algorithm:  $A_{dut_{tot}}$ .
5. Calculate relative error of the WRMS RMS amplitude:  $\delta A(i) = (\sqrt{|A_{dut_{tot}}^2 - S_{ref}^2|} - A_{ref}) / A_{ref}$ .
6. Repeat 1000 times from step 1.
7. Estimate worst case uncertainty:  $\delta A = \max \delta A(i)$  for  $i = 1..1000$ .

This LUT called twice to obtain spur effects for RMS voltage and RMS current.

Total size of both LUTs after compression is 265 kBytes which is still acceptable, so no further optimisations were performed. Total range of input parameters to the estimator “wrms\_unc\_spur()” is shown in table 37.

Table 36: Simulation ranges and steps of the parameters for uncertainty LUT of “wrms\_unc\_spur()” function.

Name	Description
Periods count	List: [3; 4; 5; 6; 7; 9; 12; 20; 50; 100], 10 steps
Samples per period	Log. space: 7 to 100, 10 steps
U to I phase shift	random*
U to I amplitude ratio	Log. space: 0.01 to 1, 7 steps
U or I spur amplitude	Log. space: 0.001 to 1, 9 steps
Relative spur frequency	Log. space: 0.01 to 50 DFT bins, 15 steps

Table 37: The usable range of input parameters of the single tone error estimator “wrms\_unc\_spur()”. The actions on min or max value is reached are: “error” - generate error; “const” - return value of uncertainty at min. or max. of simulated range.

Name	Range	On min	On max
Ref. component voltage	0 to $\infty$	const	const
Ref. component current	0 to $\infty$	const	const
Relative spur frequency	0.01 to $\infty$	const	const
Spur component voltage	0 to $\infty$	const	const
Spur component current	0 to $\infty$	const	const
Periods count	3 to 100	error	const
Samples per period	7 to 100	const	const

## 7.4 Validation

The algorithm TWM-PWRTDI has many input quantities (for the differential transducer connection about 120 quantities) and some of them are matrices. That is too many possible degrees of freedom.

Thus, varying the quantities in some systematic way would be very complicated if the validation should cover full range of used signals and corrections. Therefore, an alternative approach was used.

QWTB test function “alg\_test.m” was created, which performs the validation using randomly generated test setups. It randomizes the signal parameters, correction quantities and uncertainties and algorithm configurations in ranges expected to occur during the real measurements. The test is run many times to cover full operating range of the algorithm. Following operations are performed for each random test setup:

1. Generate voltage and current signals  $u$  and  $i$  with known power parameters  $P_{ref}$ .
2. Distort the signals  $u$  and  $i$  by inverse corrections, i.e. simulate the transducers, and digitizer (e.g. gain errors, phase errors, DC offsets, quantisation errors, ...).
3. Run the algorithm TWM-PWRTDI on the signals  $u$  and  $i$  with enabled uncertainty evaluation to obtain power parameters estimates  $P_x$  and their uncertainties  $u(P_{ref})$ .
4. Compare  $P_{ref}$  and  $P_x$  and decide if the errors of the algorithm for particular power parameters is smaller than the assigned uncertainties  $u(P_{ref})$ :

$$pass(i) = \text{abs}(P_{ref} - P_x) < u(P_{ref}), \quad (56)$$

where  $i$  is test run index.

5. Repeat the test  $N$  times from step 1 with the same test setup parameters, but with randomised corrections by their uncertainties, and with randomised noise, SFDR and jitter.
6. Check that at least 95 % of  $pass(i)$  results passed (for default 95 % level of confidence). The evaluation is made for each calculated power parameter separately. So it is possible to inspect which parameter fails.

The test runs count per test setup was set to  $N = 200$ , which is far from optimal “infinite” set, but due to the computational requirements it could not have been much higher. Note the low count of test induces uncertainty to the obtained pass rates.

The algorithm in the uncertainty estimation mode was tested in 4 different configurations with 10000 test setups per each. I.e. the algorithm was ran 8 million times in total ( $4 \times 10000 \times 200$ ). The processing itself was performed on a supercomputer [6] so it took only about 2 days at 400 parallel octave instances.

The test was also repeated in a smaller scale with Monte Carlo uncertainty calculation mode. 1000 test setups with 290 repetitions and 1000 Monte Carlo cycles per each repetition were performed to validate the algorithm with the Monte-Carlo uncertainty calculator. Processing time was roughly 2 days at 400 parallel octave instances.

The randomization ranges of the signal are shown in table 38. The randomization ranges of the corrections are shown in table 39.

The test results were split into several groups given by the randomiser setup: (i) Single ended/differential mode; (ii) Randomisation of corrections by uncertainty enabled/disabled; (iii) Uncertainty estimator or Monte Carlo method. When the randomisation of corrections is disabled, the test runs cover only the algorithm itself and the contributions of the correction uncertainties are ignored.

The summary of the validation test results is shown in table 40. The success rate without corrections randomisation was close to 100 %. The success rate with corrections randomisation was a bit worse, because the success rate of the test runs within the test setup is just around 95 %. Therefore the decision pass/fail is problematic. The obtained set of test results was manually investigated and no cases with far outliers were detected, e.g. the failed test setups contained occasional estimates offsets just around the uncertainty boundaries. Also no case where all test runs fails were found.

The Monte Carlo uncertainty calculation mode was a bit less successful than estimator, because its uncertainties are more accurate, so the success rate is just around 95 % even with randomisation of corrections disabled, so the detection of pass/fail is problematic.

Table 38: Validation range of the signal for TWM-PWRTDI algorithm.

<b>Parameter</b>	<b>Range</b>
Sampling rate	random 9 to 11 kHz (all other parameters are varied relative to this sampling rate, so it is not needed to randomise in wider range).
Samples count	5000 to 20000 (0.5 to 2 seconds integration time).
Fundamental frequency	random, so there are at least 10 samples per period and at least 20 full periods recorded.
Harmonics count	1 to 5 in order (no gaps).
Fundamental amplitudes	0.1 to 1 of full scale digitizer input.
Harmonic amplitudes	0.01 to 0.1 of fundamental.
Inter-harmonic frequency	anywhere between harmonics, not overlapping (at least 9 DFT bins from nearest other component). If not possible to place between harmonics, the inter-harmonic is put anywhere up to Nyquist limit.
Inter-harmonic amplitude	0.001 to 0.01 of fundamental.
Phase angles	Random for all harmonics and inter-harmonics.
DC offset	$\pm 0.05$ of fundamental.
SFDR	-120 to -80 dBc, max. 10 harmonic components, amplitude randomized for each spur in the SFDR range.
Digitizer RMS noise	1 to 10 $\mu$ V.
Sampling jitter	1 to 100 ns.

Table 39: Validation range of the correction for the TWM-PWRTDI algorithm. Note the low-side channel corrections in the differential mode are generated in the same way.

Parameter	Range
Nominal input U range	10 to 70 V
Nominal input I range	0.5 to 5 A
Aperture time	1 ns to 10 s
Digitizer gain	Randomly generated frequency transfer simulating NI 5922 FIR-like gain ripple (possibly the worst imaginable shape) and some ac-dc dependence. The transfer matrix has up to 50 frequency spots. Nominal gain value is random from 0.95 to 1.05 with uncertainty $2 \mu\text{V/V}$ . Maximum ac-dc value at $fs/2$ is up to $\pm 1 \%$ with uncertainty $50 \mu\text{V/V}$ . Gain ripple amplitude is random from 0.005 to 0.03 dB with up to 5 periods between 0 and $fs/2$ .
Digitizer phase	Randomly generated phase frequency transfer up to $\pm 1 \text{ mrad}$ with uncertainty 2 to $50 \mu\text{rad}$ .
Digitizer SFDR	Value based on table 38.
Digitizer bit resolution	16 to 28 bits.
Digitizer nominal range	1 V
Digitizer DC offset	Up to $\pm 10 \text{ mV}$ with uncertainty $0.1 \text{ mV}$ .
Low-side channel time shift	Random value so the phase shift at Nyquist frequency won't exceed $0.1 \text{ rad}$ with uncertainty 20 ns.
I-to-U channel time shift	Random value so the phase shift at Nyquist frequency won't exceed $0.1 \text{ rad}$ with uncertainty 20 ns.
Transducer gain	Randomly generated frequency transfer. The transfer matrix has up to 50 frequency spots. Nominal gain value is random (see above) with relative uncertainty $2 \mu\text{V/V}$ . Maximum ac-dc value at $fs/2$ is up to $\pm 2 \%$ with uncertainty $50 \mu\text{V/V}$ . Gain ripple amplitude is 0.005 dB with 4 to 10 periods between 0 and $fs/2$ .
Transducer phase	Randomly generated phase frequency transfer up to $\pm 1 \text{ mrad}$ with uncertainty 2 to $50 \mu\text{rad}$ .

Table 40: Validation results of the algorithm TWM-PWRTDI. The “passed test” shows percentage of passed tests under conditions defined in tables 38 and 39. Note the pass condition is when all tested quantities ( $U$ ,  $I$ ,  $P$ ,  $Q$ ,  $S$ ,  $PF$ ) passes. The “mode” signifies uncertainty evaluation mode (calculation option “calcset.unc”), where “mcm” is Monte Carlo and “guf” is estimator.

Mode	Connection	Rand. corr.	Passed test [%]
guf	single-ended	off	100.00
		on	100.00
	differential	off	100.00
		on	100.00
mcm	single-ended	off	100.00
		on	100.00
	differential	off	100.00
		on	100.00

## References

- [1] K. B. Ellingsberg. Predictable maximum rms-error for windowed rms (rmws). In *2012 Conference on Precision electromagnetic Measurements*, pages 308–309, July 2012.
- [2] Gerhard Heinzel, A. Rüdiger, and R. Schilling. Spectrum and spectral density estimation by the discrete fourier transform (dft), including a comprehensive list of window functions and some new flat-top windows. Technical report, Max-Planck-Institut für Gravitationsphysik (Albert-Einstein-Institut) Teilinstitut Hannover, Feb 2005.
- [3] JCGM. *Evaluation of measurement data - Supplement 1 to the “Guide to the expression of uncertainty in measurement” - Propagation of distributions using a Monte Carlo method*. Bureau International des Poids et Mesures.
- [4] R. Lapuh, B. Voljč, and M. Lindič. Measurement and estimation of arbitrary signal power using a window technique. In *2016 Conference on Precision Electromagnetic Measurements (CPEM 2016)*, pages 1–2, July 2016.
- [5] Stanislav Mašláň. Activity A2.3.2 - Algorithms Exchange Format. <https://github.com/smaslan/TWM/tree/master/doc/A232AlgorithmExchangeFormat.docx>.
- [6] Miroslav Valtr. ČMI HPC System Online. [https://translate.google.cz/translate?sl=cs&tl=en&js=y&prev=\\_t&hl=cs&ie=UTF-8&u=http%3A%2F%2Fprutok.cmi.cz%2Fsc%2Fdoku.php%3Fid%3Dsystem&edit-text=](https://translate.google.cz/translate?sl=cs&tl=en&js=y&prev=_t&hl=cs&ie=UTF-8&u=http%3A%2F%2Fprutok.cmi.cz%2Fsc%2Fdoku.php%3Fid%3Dsystem&edit-text=), 2014.

## 8 TWM-WRMS - RMS value by Windowed Time Domain Integration

TWM-WRMS is an algorithm for calculation RMS value and DC component of signal a time domain integration of windowed signal  $y(t)$ . The windowing function eliminates effects of non-coherent sampling as was demonstrated in [1] and [2]. Therefore, it does work even for non-coherently sampled waveforms. The algorithm itself without contribution of corrections can easily reach errors below 1  $\mu\text{V}/\text{V}$  with proper selection of a sampling rate and windows size.

The TWM-WRMS algorithm wrapper is able to use single-ended or differential input sensors. The algorithm is also equipped by a fast uncertainty estimator and the Monte Carlo uncertainty calculation method for more accurate but slower uncertainty evaluation.

### 8.1 TWM wrapper parameters

The input quantities supported by the algorithm are shown in the table 41. Algorithm returns output quantities shown in the table 42. Calculation setup supported by the algorithm is shown in table 43.

Table 41: List of input quantities to the TWM-WRMS wrapper.  
Details on the correction quantities can be found in [3].

Name	Default	Unc.	Description
ac_coupling	0	N/A	Enables virtual AC coupling for the RMS calculation. This option will cause the DC value will be ignored in the RMS calculation.
y	N/A	No	Input sample data vector and complementary low-side input data vector $y_{lo}$ (for differential mode only).
$y_{lo}$	N/A	No	
$T_s$	N/A	No	Sampling period or sampling rate or sample time vector. Note the wrapper always calculates in equidistant mode, so $t$ is used just to calculate $T_s$ .
fs	N/A	No	
t	N/A	No	
time_shift_lo	0	Yes	Time shift between high-side channel $y$ low-side channel $y_{lo}$ .
lsb	N/A	No	Either absolute ADC resolution $lsb$ or nominal range value $adc\_nrng$ (e.g.: 5 V for 10 Vpp range) and $adc\_bits$ bit resolution of ADC.
adc_nrng	1000	No	
adc_bits	40	No	
lo_lsb	N/A	No	
lo_adc_nrng	1000	No	
lo_adc_bits	40	No	
adc_offset	0	Yes	Digitizer input offset voltage.
lo_adc_offset	0	Yes	
adc_gain	1	Yes	Digitizer gain correction 2D table (multiplier).
adc_gain_f	$\emptyset$	No	
adc_gain_a	$\emptyset$	No	
lo_adc_gain	1	Yes	
lo_adc_gain_f	$\emptyset$	No	
lo_adc_gain_a	$\emptyset$	No	
adc_phi	0	Yes	Digitizer phase correction 2D table (additive).
adc_phi_f	$\emptyset$	No	
adc_phi_a	$\emptyset$	No	
lo_adc_phi	0	Yes	
lo_adc_phi_f	$\emptyset$	No	
lo_adc_phi_a	$\emptyset$	No	
adc_freq	0	Yes	Digitizer timebase error correction: $f_{tb'} = f_{tb} \cdot (1 + adc\_freq.v)$ The effect on the estimated frequency is opposite: $f_{est'} = f_{est} / (1 + adc\_freq.v)$

Table 41: List of input quantities to the TWM-WRMS wrapper.  
Details on the correction quantities can be found in [3].

Name	Default	Unc.	Description
adc_jitter	0	No	Digitizer sampling period jitter [s].
lo_adc_jitter	0	No	
adc_aper	0	No	ADC aperture value [s].
lo_adc_aper	0	No	
adc_aper_corr	0	No	ADC aperture error correction enable: $A' = A \cdot \pi \cdot \text{adc\_aper} \cdot f_{est} / \sin(\pi \cdot \text{adc\_aper} \cdot f_{est})$ $\phi_i' = \phi_i + \pi \cdot \text{adc\_aper} \cdot f_{est}$
lo_adc_aper	0	No	
adc_sfdr	180	No	Digitizer SFDR 2D table.
adc_sfdr_f	□	No	
adc_sfdr_a	□	No	
lo_adc_sfdr	180	No	
lo_adc_sfdr_f	□	No	
lo_adc_sfdr_a	□	No	
adc_Yin_Cp	1e-15	Yes	Digitizer input admittance 1D table.
adc_Yin_Gp	1e-15	Yes	
adc_Yin_f	□	No	
lo_adc_Yin_Cp	1e-15	Yes	
lo_adc_Yin_Gp	1e-15	Yes	
lo_adc_Yin_f	□	No	
tr_type	“”	No	Transducer type string (“rvd” or “shunt”).
tr_gain	1	Yes	Transducer gain correction 2D table (multiplicative).
tr_gain_f	□	No	
tr_gain_a	□	No	
tr_phi	0	Yes	Transducer phase correction 2D table (additive).
tr_phi_f	□	No	
tr_phi_a	□	No	
tr_sfdr	180	No	Transducer SFDR 2D table.
tr_sfdr_f	□	No	
tr_sfdr_a	□	No	
tr_Zlo_Rp	1e3	Yes	RVD transducer low-side impedance 1D table. Note this is related to loading correction and it has effect only for RVD transducer and will work only if <i>adc_Yin</i> is defined as well.
tr_Zlo_Cp	1e-15	Yes	
tr_Zlo_f	□	No	
tr_Zbuf_Rs	0	Yes	Loading corrections: Transducer output buffer output series impedance 1D table. Leave unassigned to disable buffer from the correction topology.
tr_Zbuf_Ls	0	Yes	
tr_Zbuf_f	□	No	
tr_Zca_Rs	1e-9	Yes	Loading corrections: Transducer high side terminal series impedance 1D table.
tr_Zca_Ls	1e-12	Yes	
tr_Zca_f	□	No	
tr_Zcal_Rs	1e-9	Yes	Loading corrections: Transducer low side terminal series impedance 1D table.
tr_Zcal_Ls	1e-12	Yes	
tr_Zcal_f	□	No	
tr_Yca_Cp	1e-15	Yes	Loading corrections: Transducer output terminals shunting impedance.
tr_Yca_D	1e-12	Yes	
tr_Yca_f	□	No	
tr_Zcam	1e-12	Yes	Loading corrections: Transducer output terminals mutual inductance 1D table.
tr_Zcam_f	□	No	
Zcb_Rs	1e-9	Yes	Loading corrections: Cable series impedance 1D table.
Zcb_Ls	1e-12	Yes	
Zcb_f	□	No	
Ycb_Rs	1e-15	Yes	Loading corrections: Cable series impedance 1D table.
Ycb_Ls	1e-12	Yes	
Ycb_f	□	No	

Table 42: List of output quantities of the TWM-WRMS wrapper.

Name	Uncertainty	Description
rms	Yes	RMS level [V] or [A].
dc	Yes	DC component [V] or [A].
spec_A	No	Amplitude spectrum [V] or [A].
spec_f	No	Frequency vector of <i>spec_A</i> .

Table 43: List of “calcset” options supported by the TWM-WRMS wrapper.

Name	Description
calcset.unc	Uncertainty calculation mode. Supported: “none”, “guf” for uncertainty estimator, “mcm” for Monte Carlo.
calcset.mcm.method	Monte Carlo evaluation mode: “singlecore” - single core evaluation, “multicore” - Parallel evaluation using “parcellfun” for GNU Octave or “parfor” for Matlab “multistation” - Multicore evaluation using “multicore” package (GNU Octave only yet).
calcset.mcm.repeats	Monte Carlo iterations count. Use at least 100 to get any usable estimate.
calcset.mcm.proc_no	Number of parallel instances to use for the paralleled modes. Use zero value to not start any server processes for the “multistation” mode. This option expects user started the server processes manually in the shared folder. This option causes less overhead for the batch processing or runtime calculations.
calcset.mcm.tmpdir	Jobs sharing folder for the “multistation” mode. This should be an absolute path to the sharing folder. Keep in mind the package “multicore” will erase the content of this folder before each new calculation!
calcset.mcm.user_fun	User function to call in the “multistation” mode after startup of the serve processes. Example: “calcset.mcm.user_fun = @coklbind2”. Leave empty to not execute any function.
calcset.loc	Level of confidence [-].
calcset.verbose	Verbose level.
calcset.fetch_luts	Optional, non-zero will prefetch uncertainty LUT tables to global variables to make the execution faster. Note this was intended ONLY for validation process where reduction of disk access is beneficial.
calcset.dbg_plots	Optional, non-zero will plot some debugging graphs.

## 8.2 Algorithm description

The TWM-WRMS algorithm is a wrapper of TWM-PWRTDI algorithm. It copies the input data and correction to both voltage and current channels of TWM-PWRTDI (see section 7), executes it and copies either voltage or current results to the TWM-WRMS results depending on the used transducer type. Internal principle of operation is thus identical as for TWM-PWRTDI. This “backwards” solution was used because it was not possible to effectively build the TWM-PWRTDI power algorithm from single channel processing using TWM-WRMS. As a result it is a bit slower, because most of the TWM-PWRTDI is not used in TWM-WRMS. Block diagram is shown in fig. 23.



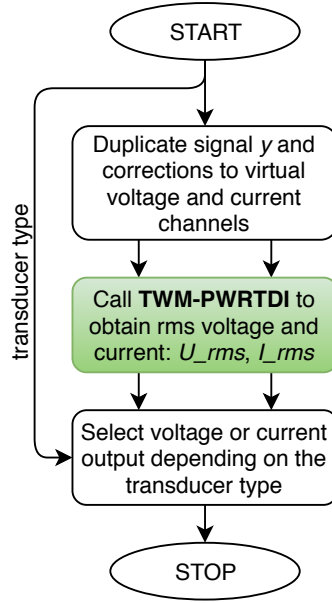


Figure 23: Internal structure of TWM-WRMS algorithm.

### 8.3 Uncertainty calculator and estimator

The TWM-WRMS algorithm wrapper is equipped by two modes of uncertainty evaluation: (i) The ordinary Monte Carlo (MC) calculator; (ii) Fast estimator based on several precalculated lookup tables (LUT). The MC mode is more accurate, however it may take up to several minutes to perform even just a few hundreds of iterations. The calculation time drastically rises with the length of the record. Thus the fast estimator was created as well.

The WRMS algorithm itself can calculate a RMS of any voltage and current waveforms. However, calculation of uncertainty for general non-periodic waveforms would be extremely complex and slow. Therefore, the uncertainty calculation is based on the analysis of spectral components obtained from the average spectrum of the whole digitized waveform. This simplification should not have any effect, as the algorithm is primarily intended for a calibration of stationary signals.

Detailed description of the uncertainty evaluation can be found in the TWM-PWRTDI algorithm.

### 8.4 Validation

Only limited validation of TWM-WRMS was performed as it internally uses TWM-PWRTDI (see section 7).

Table 44: Validation results of the algorithm TWM-WRMS. The “passed test” shows percentage of passed tests under conditions defined in tables 38 and 39. The “mode” signifies uncertainty evaluation mode (calculation option “calcset.unc”), where “mcm” is Monte Carlo and “guf” is estimator.

Mode	Connection	Rand. corr.	Passed test [%]
guf	single-ended	off	100.00
		on	100.00
	differential	off	100.00
		on	100.00
mcm	single-ended	off	100.00
		on	100.00
	differential	off	100.00
		on	100.00

## References

- [1] K. B. Ellingsberg. Predictable maximum rms-error for windowed rms (rmws). In *2012 Conference on Precision electromagnetic Measurements*, pages 308–309, July 2012.
- [2] R. Lapuh, B. Voljč, and M. Lindič. Measurement and estimation of arbitrary signal power using a window technique. In *2016 Conference on Precision Electromagnetic Measurements (CPEM 2016)*, pages 1–2, July 2016.
- [3] Stanislav Mašláň. Activity A2.3.2 - Algorithms Exchange Format. <https://github.com/smaslan/TWM/tree/master/doc/A232AlgorithmExchangeFormat.docx>.

## 9 TWM-WFFT - Windowed FFT spectrum analysis

Algorithm for single or multi-tone harmonic analysis using windowed FFT. The algorithm performs windowed FFT of the signal, applies TWM corrections and extracts FFT bin(s) with selected frequencies. It also calculates rms value estimate, however rms will be usable only for coherent sampling. The main purpose of the algorithm is interchannel phase shift and voltage ratio analysis. That will work even for non-coherent sampling, when non-rectangular window is used.

Note the harmonics spacing in the spectrum must be higher, then width of the selected window! E.g. the wide "flattop\_248D" needs at least some 25 FFT bins spacing. Also note the wider windows have higher equivalent noise bandwidth, so the noise in the analysed harmonic is amplified. See section 9.3 for more details on the effects of windows.

The TWM-WFFT algorithm wrapper is able to use single-ended or differential input sensors. The algorithm is also equipped with a fast uncertainty estimator for the harmonic components.

### 9.1 TWM wrapper parameters

The input quantities supported by the algorithm are shown in the table 45. Algorithm returns output quantities shown in the table 46. Calculation setup supported by the algorithm is shown in table 47.

Table 45: List of input quantities to the TWM-WFFT wrapper.  
Details on the correction quantities can be found in [3].

Name	Default	Unc.	Description
f_nom	N/A	N/A	Optional nominal frequency (or vector of frequencies) to extract from the spectrum. The algorithm will choose the nearest FFT bin(s). If the <i>f_nom</i> is not assigned, the algorithm will search the fundamental component by calling PSFE algorithm [1].
h_num	N/A	N/A	Optional list of relative harmonic frequencies related to the <i>f_nom</i> . E.g.: when <i>f_nom</i> = 50 Hz and <i>h_num</i> = [123], the extracted frequencies will be [50, 100, 150] Hz.
window	"rect"	N/A	Window type used before FFT. "rect" window can be used for coherent sampling without significant interharmonic components only. Another windows may be used for non-coherent sampling, however the harmonic analysis will be usable only for interchannel amplitude ratios and phase differences for the non-coherent case!
y	N/A	No	Input sample data vector and complementary low-side input data vector <i>y_lo</i> (for differential mode only).
y_lo	N/A	No	
Ts	N/A	No	Sampling period or sampling rate or sample time vector.
fs	N/A	No	Note the wrapper always calculates in equidistant mode, so <i>t</i> is used just to calculate <i>Ts</i> .
t	N/A	No	
time_stamp	0	Yes	Relative timestamp of the first sample <i>y</i> .
time_shift_lo	0	Yes	Time shift between high-side channel <i>y</i> low-side channel <i>y_lo</i> .
lsb	N/A	No	Either absolute ADC resolution <i>lsb</i> or nominal range value <i>adc_nrng</i> (e.g.: 5 V for 10 Vpp range) and <i>adc_bits</i> bit resolution of ADC.
adc_nrng	1000	No	
adc_bits	40	No	
lo_lsb	N/A	No	
lo_adc_nrng	1000	No	
lo_adc_bits	40	No	
adc_offset	0	Yes	Digitizer input offset voltage.
lo_adc_offset	0	Yes	

Table 45: List of input quantities to the TWM-WFFT wrapper.  
Details on the correction quantities can be found in [3].

Name	Default	Unc.	Description
adc_gain	1	Yes	Digitizer gain correction 2D table (multiplier).
adc_gain_f	<input type="checkbox"/>	No	
adc_gain_a	<input type="checkbox"/>	No	
lo_adc_gain	1	Yes	
lo_adc_gain_f	<input type="checkbox"/>	No	
lo_adc_gain_a	<input type="checkbox"/>	No	
adc_phi	0	Yes	Digitizer phase correction 2D table (additive).
adc_phi_f	<input type="checkbox"/>	No	
adc_phi_a	<input type="checkbox"/>	No	
lo_adc_phi	0	Yes	
lo_adc_phi_f	<input type="checkbox"/>	No	
lo_adc_phi_a	<input type="checkbox"/>	No	
adc_freq	0	Yes	Digitizer timebase error correction: $f_{tb'} = f_{tb} \cdot (1 + adc\_freq.v)$ The effect on the estimated frequency is opposite: $f_{est'} = f_{est} / (1 + adc\_freq.v)$
adc_jitter	0	No	Digitizer sampling period jitter [s].
lo_adc_jitter	0	No	
adc_aper	0	No	ADC aperture value [s].
lo_adc_aper	0	No	
adc_aper_corr	0	No	ADC aperture error correction enable: $A' = A \cdot pi \cdot adc\_aper \cdot f_{est} / \sin(pi \cdot adc\_aper \cdot f_{est})$ $phi' = phi + pi \cdot adc\_aper \cdot f_{est}$
lo_adc_aper	0	No	
adc_sfdr	180	No	Digitizer SFDR 2D table.
adc_sfdr_f	<input type="checkbox"/>	No	
adc_sfdr_a	<input type="checkbox"/>	No	
lo_adc_sfdr	180	No	
lo_adc_sfdr_f	<input type="checkbox"/>	No	
lo_adc_sfdr_a	<input type="checkbox"/>	No	
adc_Yin_Cp	1e-15	Yes	Digitizer input admittance 1D table.
adc_Yin_Gp	1e-15	Yes	
adc_Yin_f	<input type="checkbox"/>	No	
lo_adc_Yin_Cp	1e-15	Yes	
lo_adc_Yin_Gp	1e-15	Yes	
lo_adc_Yin_f	<input type="checkbox"/>	No	
tr_type	“”	No	Transducer type string (“rvd” or “shunt”).
tr_gain	1	Yes	Transducer gain correction 2D table (multiplicative).
tr_gain_f	<input type="checkbox"/>	No	
tr_gain_a	<input type="checkbox"/>	No	
tr_phi	0	Yes	Transducer phase correction 2D table (additive).
tr_phi_f	<input type="checkbox"/>	No	
tr_phi_a	<input type="checkbox"/>	No	
tr_sfdr	180	No	Transducer SFDR 2D table.
tr_sfdr_f	<input type="checkbox"/>	No	
tr_sfdr_a	<input type="checkbox"/>	No	
tr_Zlo_Rp	1e3	Yes	RVD transducer low-side impedance 1D table. Note this is related to loading correction and it has effect only for RVD transducer and will work only if <i>adc_Yin</i> is defined as well.
tr_Zlo_Cp	1e-15	Yes	
tr_Zlo_f	<input type="checkbox"/>	No	
tr_Zbuf_Rs	0	Yes	Loading corrections: Transducer output buffer output series impedance 1D table. Leave unassigned to disable buffer from the correction topology.
tr_Zbuf_Ls	0	Yes	
tr_Zbuf_f	<input type="checkbox"/>	No	

Table 45: List of input quantities to the TWM-WFFT wrapper.  
Details on the correction quantities can be found in [3].

Name	Default	Unc.	Description
tr_Zca_Rs tr_Zca_Ls tr_Zca_f	1e-9 1e-12 []	Yes Yes No	Loading corrections: Transducer high side terminal series impedance 1D table.
tr_Zcal_Rs tr_Zcal_Ls tr_Zcal_f	1e-9 1e-12 []	Yes Yes No	Loading corrections: Transducer low side terminal series impedance 1D table.
tr_Yca_Cp tr_Yca_D tr_Yca_f	1e-15 1e-12 []	Yes Yes No	Loading corrections: Transducer output terminals shunting impedance.
tr_Zcam tr_Zcam_f	1e-12 []	Yes No	Loading corrections: Transducer output terminals mutual inductance 1D table.
Zcb_Rs Zcb_Ls Zcb_f	1e-9 1e-12 []	Yes Yes No	Loading corrections: Cable series impedance 1D table.
Ycb_Rs Ycb_Ls Ycb_f	1e-15 1e-12 []	Yes Yes No	Loading corrections: Cable series impedance 1D table.

Table 46: List of output quantities of the TWM-WFFT wrapper.

Name	Uncertainty	Description
f	No	Exact frequencies of selected FFT bins.
A	Yes	Amplitude(s) of selected FFT bins.
ph	Yes	Phase angle(s) of selected FFT bins [rad]. Wrapped to $\pm\pi$ range.
dc	Yes	DC component [V] or [A].
rms	Yes	RMS level estimate [V] or [A]. Calculated from all detected harmonics (not just the selected in <i>f</i> list).
spec_A	No	Full amplitude spectrum [V] or [A].
spec_f	No	Frequency vector of <i>spec_A</i> .

Table 47: List of “calcset” options supported by the TWM-WFFT wrapper.

Name	Description
calcset.unc	Uncertainty calculation mode. Supported: “none” or “guf” for uncertainty estimator.
calcset.loc	Level of confidence [-].
calcset.verbose	Verbose level.

## 9.2 Algorithm description

The TWM-WFFT algorithm is a wrapper of SP-WFFT algorithm. For differential mode it calls SP-WFFT twice. Once for high-side and once for low-side. It applies TWM corrections (offset, digitizer gain, digitizer phase, digitizer aperture) to both differential channels (high and low side). Next it calculates the differential signal. Follows transducer gain and phase correction which is common for single-ended and differential modes. Last step is extraction of user defined harmonic components which are selected as FFT bins nearest to the selected frequencies.

### 9.3 Uncertainty calculator and estimator

The TWM-WFFT algorithm wrapper is equipped by fast uncertainty estimator. The estimator calculates uncertainty correctly only for the coherent sampling case! It uses two main components: (i) TWM corrections contribution and (ii) Noise, bit resolution, jitter and SFDR effects.

TWM corrections component (i) comprises of gain, phase corrections of the digitizer and transducer and offset correction of the digitizer. These components are calculated along with application of the corrections and will apply even for non-coherent sampling case correctly.

The other components (ii) requires further processing. The rms noise is estimated from the full spectrum with removed harmonic components. Sampling Jitter may be defined by user correction data as well as bit resolution. SFDR of the digitizer and transducer are also definable by user and their effect to extracted harmonics can be easily calculated. The uncertainty contribution coming from the noise, jitter and bit resolution were calculated following the formulas in [2], section 4.10 Noise. The components are automatically calculated for any window type. The validity of the implementation was checked by Monte Carlo simulation. However, it is not known whether these approximations are valid for non-coherent case.

The uncertainty estimator does not take into account any effects caused by the interleaving of side lobes of the particular harmonics and also effects of non-coherent sampling. I.e. harmonic spacing in the spectrum must be wide enough, so the side lobe of one harmonic does not interfere with another. All windows containing only harmonic components (Hann, Hamming, Flattops, Blackman, etc.) have final width, so for the coherent sampling they can affect the other harmonics only up to finite distance. However, in non-coherent case they have side lobes with finite amplitude in full bandwidth of the FFT. E.g. Blackman–Nuttall window have almost constant side lobes at -100 dBc, so when we have fundamental with level of 1 V and second harmonic with level of 10 mV, the second harmonic will be affected by up to  $10^{-5} \cdot 1 \text{ V}$ . That is 0.1%. This must be taken into account by user when using the algorithm for non-coherent sampling and proper window function should be selected.

Another problem related to the non-coherent sampling not covered by the estimator is scalloping loss. Whenever the actual frequency of the harmonic component does not match FFT bin frequency exactly, there will be error given by flatness of the window in range  $\pm 0.5 \text{ FFT bin}$ . E.g. even flattest window "flattop\_248D" has this flatness only roughly 0.01%, which may not be acceptable for some measurements. As it is not possible to tell algorithmically if all the frequency components are coherent, the uncertainty contribution of this effect was intendedly omitted from the calculation and user must add the effect to the uncertainty budget manually.

In general, wider window functions with more harmonic components have lower side lobes and better flatness, so they are more suitable for non-coherent measurements. However the cost for this is higher noise bandwidth, which increases type A uncertainty up to several times.

### 9.4 Validation

The algorithm TWM-WFFT has many input quantities and some of them are matrices. That is too many possible degrees of freedom. Thus, varying the quantities in some systematic way would be very complicated if the validation should cover full range of used signals and corrections. Therefore, an alternative approach was used.

QWTB test function "alg\_test.m" was created, which performs the validation using randomly generated test setups. It randomizes the signal parameters, correction quantities and uncertainties and algorithm configurations in ranges expected to occur during the real measurements. The test is run many times to cover full operating range of the algorithm. Following operations are performed for each random test setup:

1. Generate signals  $y$  with random and known harmonic content  $H_{ref}$ .
2. Distort the signal  $y$  by inverse corrections, i.e. simulate the transducers, and digitizer (e.g. gain errors, phase errors, DC offsets, quantisation errors, ...).
3. Run the algorithm TWM-WFFT on the signal  $y$  with enabled uncertainty evaluation to obtain harmonic parameter estimates  $H_x$  and their uncertainties  $u(H_x)$ .

4. Compare  $H_{\text{ref}}$  and  $H_x$  and decide if the errors of the algorithm for particular parameters is smaller than the assigned uncertainties  $u(H_x)$ :

$$\text{pass}(i) = \text{abs}(H_{\text{ref}} - H_x) < u(H_x), \quad (57)$$

where  $i$  is test run index.

5. Repeat the test  $N$  times from step 1 with the same test setup parameters, but with randomised corrections by their uncertainties, and with randomised noise, SFDR and jitter.
6. Check that at least 95 % of  $\text{pass}(i)$  results passed (for default 95 % level of confidence). The evaluation is made for each parameter separately (DC component, fundamental amplitude and phase and other harmonics' amplitudes and phases). So it is possible to inspect which parameter fails.

The test runs count per test setup was set to  $N = 500$ , which is far from optimal "infinite" set, but due to the computational requirements it could not have been much higher. Note the low count of test induces uncertainty to the obtained pass rates.

The algorithm in the uncertainty estimation mode was tested in 4 different configurations with 10000 test setups per each. I.e. the algorithm was ran 20 million times in total ( $4 \times 10000 \times 500$ ). The processing itself was performed on a supercomputer [4] so it took only about 2 days at 400 parallel octave instances.

The randomization ranges of the signal are shown in table 48. The randomization ranges of the corrections are shown in table 49.

The test results were split into several groups given by the randomiser setup: (i) Single ended/differential mode; (ii) Randomisation of corrections by uncertainty enabled/disabled. When the randomisation of corrections is disabled, the test runs cover only the algorithm itself and the contributions of the correction uncertainties are ignored. This option was chosen because corrections uncertainties may mask the algorithm uncertainty.

The summary of the validation test results is shown in table 50. In both cases the pass rates were very close to expected 95 % boundary and no cases where all test runs fails were found.

Table 48: Validation range of the signal for TWM-WFFT algorithm.

Parameter	Range
Sampling rate	random 9 to 11 kHz (all other parameters are varied relative to this sampling rate, so it is not needed to randomise in wider range).
Samples count	5000 to 20000 (0.5 to 2 seconds integration time).
Fundamental frequency	random, so there are at least 10 samples per period and at least 20 full periods recorded. It is rounded so the sampling is always coherent.
Harmonics count	1 to 5 in order (no gaps, e.g.: [1, 2, 3, 4] or [1, 2]).
Fundamental amplitudes	0.1 to 1 of full scale digitizer input.
Harmonic amplitudes	0.01 to 0.1 of fundamental.
Phase angles	Random for all harmonics.
DC offset	$\pm 0.05$ of fundamental.
SFDR	-120 to -80 dBc, max. 10 harmonic components, amplitude randomized for each spur in the SFDR range.
Digitizer RMS noise	1 to 10 $\mu\text{V}$ .
Sampling jitter	1 to 100 ns.

Table 49: Validation range of the correction for the TWM-WFFT algorithm. Note the low-side channel corrections in the differential mode are generated in the same way.

Parameter	Range
Nominal input range	0.1 to 10
Aperture time	1 ns to 10 $\mu$ s
Digitizer gain	Randomly generated frequency transfer simulating NI 5922 FIR-like gain ripple (possibly the worst imaginable shape) and some ac-dc dependence. The transfer matrix has up to 50 frequency spots. Nominal gain value is random from 0.95 to 1.05 with uncertainty 2 $\mu$ V/V. Maximum ac-dc value at $fs/2$ is up to $\pm 1\%$ with uncertainty 50 $\mu$ V/V. Gain ripple amplitude is random from 0.005 to 0.03 dB with up to 5 periods between 0 and $fs/2$ .
Digitizer phase	Randomly generated phase frequency transfer up to $\pm 1$ mrad with uncertainty 2 to 50 $\mu$ rad.
Digitizer SFDR	Value based on table 48.
Digitizer bit resolution	16 to 28 bits.
Digitizer nominal range	1 V
Digitizer DC offset	Up to $\pm 10$ mV with uncertainty 0.1 mV.
Low-side channel time shift	Random value so the phase shift at Nyquist frequency won't exceed 0.1 rad with uncertainty 20 ns.
Transducer gain	Randomly generated frequency transfer. The transfer matrix has up to 50 frequency spots. Nominal gain value is random (see above) with relative uncertainty 2 $\mu$ V/V. Maximum ac-dc value at $fs/2$ is up to $\pm 2\%$ with uncertainty 50 $\mu$ V/V. Gain ripple amplitude is 0.005 dB with 4 to 10 periods between 0 and $fs/2$ .
Transducer phase	Randomly generated phase frequency transfer up to $\pm 1$ mrad with uncertainty 2 to 50 $\mu$ rad.

Table 50: Validation results of the algorithm TWM-WFFT. The “passed test” shows percentage of passed tests under conditions defined in tables 48 and 49.

Connection	Rand. corr.	Passed test [%]				
		dc	$A(1)$	$ph(1)$	$A(2..n)$	$ph(2..n)$
Single ended	no	100.00	100.00	100.00	100.00	100.00
	yes	99.99	100.00	99.99	100.00	100.00
Differential	no	100.00	100.00	100.00	100.00	100.00
	yes	99.97	99.98	99.97	99.98	99.98

## References

- [1] Rado Lapuh. Estimating the fundamental component of harmonically distorted signals from noncoherently sampled data. *IEEE Transactions on Instrumentation and Measurement*, 64(6):1419–1424, June 2015.
- [2] Rado Lapuh. *Sampling with 3458A*. Left Right d.o.o., Sep 2018.
- [3] Stanislav Mašláň. Activity A2.3.2 - Algorithms Exchange Format. <https://github.com/smaslan/TWM/tree/master/doc/A232AlgorithmExchangeFormat.docx>.
- [4] Miroslav Valtr. ČMI HPC System Online. [https://translate.google.cz/translate?sl=cs&tl=en&js=y&prev=\\_t&hl=cs&ie=UTF-8&u=http%3A%2F%2Fprutok.cmi.cz%2Fsc%2Fdoku.php%3Fid%3Dsystem&edit-text=](https://translate.google.cz/translate?sl=cs&tl=en&js=y&prev=_t&hl=cs&ie=UTF-8&u=http%3A%2F%2Fprutok.cmi.cz%2Fsc%2Fdoku.php%3Fid%3Dsystem&edit-text=), 2014.



## 10 TWM-Flicker - Flicker algorithm

The TWM wrapper TWM-Flicker is an algorithm for evaluation of the short term flicker parameters. It calculates instantaneous flicker sensation  $P_{inst}$  and short-term flicker severity  $P_{st}$ . Sampling rate has to be higher than 7 kHz. If sampling rate is higher than 23 kHz, signal will be down sampled by algorithm. More than 600 s of signal is required as the algorithm needs at least a minute to settle the filters. Typical sampling time value is above 660 s. The algorithm requires either Signal Processing Toolbox when run in MATLAB or a signal package when run in GNU Octave. Frequency of line (carrier frequency)  $f_{line}$  can be only 50 or 60 Hz.

The algorithm was implemented according IEC 61000-4-15 [3], [4], [2] and [5].

The algorithm wrapper is equipped by a simple uncertainty estimator based on the worst observed error of the algorithm on the tabulated  $P_{st}$  values for various sampling rates.

Note the algorithm output slightly differ for Matlab and GNU Octave implementation. The cause of this difference was not yet identified. Also the observed performance in the Matlab 2017b was about five times higher then in GNU Octave 4.2.2 on the same computer.

### 10.1 TWM wrapper parameters

The input quantities supported by the algorithm are shown in the table 51. Algorithm returns output quantities shown in the table 52. Calculation setup supported by the algorithm is shown in table 53.

Table 51: List of input quantities to the TWM-Flicker wrapper.

Name	Default	Unc.	Description
f_line	N/A	N/A	Nominal frequency of the network (50 HZ or 60 Hz).
y	N/A	No	Input sample data vector.
Ts	N/A	No	Sampling period or sampling rate or sample time vector.
fs	N/A	No	Note the wrapper always calculates in equidistant mode, so
t	N/A	No	$t$ is used just to calculate $Ts$ .
lsb	N/A	No	Either absolute ADC resolution $lsb$ or nominal range value
adc_nrng	1000	No	$adc\_nrng$ (e.g.: 5 V for 10 Vpp range) and $adc\_bits$ bit res-
adc_bits	40	No	olution of ADC.
adc_offset	0	Yes	Digitizer input offset voltage.
adc_gain	1	Yes	Digitizer gain correction 2D table (multiplier).
adc_gain_f	$\square$	No	
adc_gain_a	$\square$	No	
adc_phi	0	Yes	Digitizer phase correction 2D table (additive).
adc_phi_f	$\square$	No	
adc_phi_a	$\square$	No	
	0		
adc_freq	0	Yes	Digitizer timebase error correction: $f_{tb'} = f_{tb} \cdot (1 + adc\_freq.v)$ The effect on the estimated frequency is opposite: $f_{est'} = f_{est} / (1 + adc\_freq.v)$
adc_jitter	0	No	Digitizer sampling period jitter [s].
adc_aper	0	No	ADC aperture value [s].
adc_aper_corr	0	No	ADC aperture error correction enable: $A' = A \cdot pi \cdot adc\_aper \cdot f_{est} / \sin(pi \cdot adc\_aper \cdot f_{est})$ $phi' = phi + pi \cdot adc\_aper \cdot f_{est}$
adc_Yin_Cp	1e-15	Yes	Digitizer input admittance 1D table.
adc_Yin_Gp	1e-15	Yes	
adc_Yin_f	$\square$	No	
adc_sfdr	180	No	Digitizer SFDR 2D table.
adc_sfdr_f	$\square$	No	
adc_sfdr_a	$\square$	No	

Table 51: List of input quantities to the TWM-Flicker wrapper.

Name	Default	Unc.	Description
tr_type	“”	No	Transducer type string (“rvd” or “shunt”).
tr_gain	1	Yes	Transducer gain correction 2D table (multiplicative).
tr_gain_f	<input type="checkbox"/>	No	
tr_gain_a	<input type="checkbox"/>	No	
tr_phi	0	Yes	Transducer phase correction 2D table (additive).
tr_phi_f	<input type="checkbox"/>	No	
tr_phi_a	<input type="checkbox"/>	No	
tr_sfdr	180	No	Transducer SFDR 2D table.
tr_sfdr_f	<input type="checkbox"/>	No	
tr_sfdr_a	<input type="checkbox"/>	No	
tr_Zlo_Rp	1e3	Yes	RVD transducer low-side impedance 1D table. Note this is related to loading correction and it has effect only for RVD transducer and will work only if <i>adc_Yin</i> is defined as well.
tr_Zlo_Cp	1e-15	Yes	
tr_Zlo_f	<input type="checkbox"/>	No	
tr_Zbuf_Rs	0	Yes	Loading corrections: Transducer output buffer output series impedance 1D table. Leave unassigned to disable buffer from the correction topology.
tr_Zbuf_Ls	0	Yes	
tr_Zbuf_f	<input type="checkbox"/>	No	
tr_Zca_Rs	1e-9	Yes	Loading corrections: Transducer high side terminal series impedance 1D table.
tr_Zca_Ls	1e-12	Yes	
tr_Zca_f	<input type="checkbox"/>	No	
tr_Zcal_Rs	1e-9	Yes	Loading corrections: Transducer low side terminal series impedance 1D table.
tr_Zcal_Ls	1e-12	Yes	
tr_Zcal_f	<input type="checkbox"/>	No	
tr_Yca_Cp	1e-15	Yes	Loading corrections: Transducer output terminals shunting impedance.
tr_Yca_D	1e-12	Yes	
tr_Yca_f	<input type="checkbox"/>	No	
tr_Zcam	1e-12	Yes	Loading corrections: Transducer output terminals mutual inductance 1D table.
tr_Zcam_f	<input type="checkbox"/>	No	
Zcb_Rs	1e-9	Yes	Loading corrections: Cable series impedance 1D table.
Zcb_Ls	1e-12	Yes	
Zcb_f	<input type="checkbox"/>	No	
Ycb_Rs	1e-15	Yes	Loading corrections: Cable series impedance 1D table.
Ycb_Ls	1e-12	Yes	
Ycb_f	<input type="checkbox"/>	No	

Table 52: List of output quantities of the TWM-Flicker wrapper.

Name	Uncertainty	Description
Pst	Yes	Short-term flicker severity.
Pinst	No	Instantaneous flicker sensation.

Table 53: List of “calcset” options supported by the TWM-Flicker wrapper.

Name	Description
calcset.unc	Uncertainty calculation mode. Supported: “none” or “guf”.
calcset.loc	Level of confidence [-].
calcset.verbose	Verbose level.

## 10.2 Algorithm description

The structure of the TWM-Flicker algorithm wrapper is shown in fig. 24. The wrapper first applies correction to scaled the input signal  $y$  to actual measured level. The scaling is simplistic. The user

defined frequency  $f_{line}$  with tolerance 2 Hz is assumed to be dominant component of the input signal  $y$ . Thus, the gain correction of digitizer, aperture error gain correction and transducer gain correction are obtained for the  $f_{line}$  only. Resulting combined gain correction is applied to the time domain signal  $y$ . The wrapper also applies DC gain correction despite the main QWTB wrapper “flicker\_sim” which does the flicker calculation is not using it.

After the signal is scaled, the wrapper calls the main QWTB algorithm “flicker\_sim” to evaluate the flicker parameters.

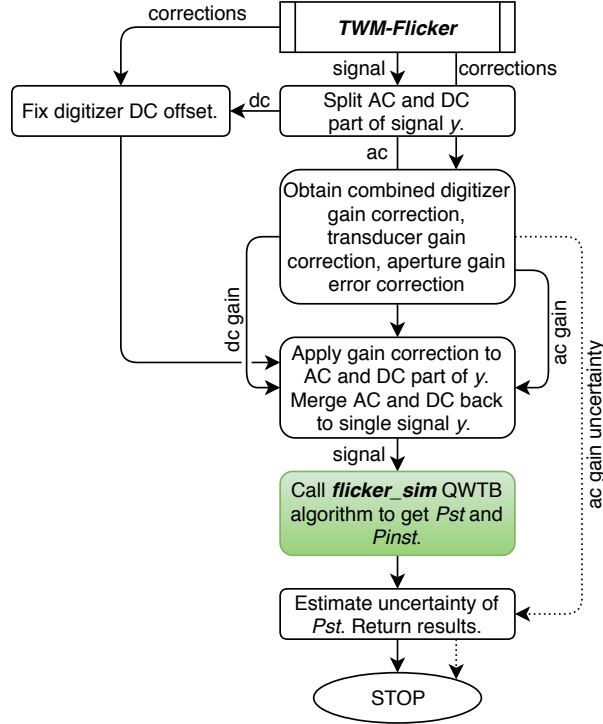


Figure 24: TWM-flicker algorithm wrapper diagram. The green blocks are calls to another QWTB wrappers.

### 10.2.1 QWTB algorithm wrapper “flicker\_sim”

The core of the flicker algorithm is QWTB wrapper “flicker\_sim”. It calculates the flicker using a function “flicker\_sim(u, fs, f\_line, ...)”. In general the algorithm calculates according to the block diagram shown in fig. 25.

The algorithm starts by checking of the input sampling rate. It will throw an error if the sampling rate is below 7 kHz. If the sampling rate is higher than 23 kHz, the algorithm will perform downsampling to a sampling rate near 17 kHz, which was empirically identified as optimal for the rest of the algorithm. Follows removal of the DC component and calculation of the RMS level of the whole signal  $u$ , which is used just for determination of the 120 V or 230 V systems.

Next step half-cycle RMS envelope calculation. The signal  $u$  is first passed via narrow passband filter (1st order Butterworth with passband 50 to 60 Hz). The filtered, theoretically noise-free signal is used for the zero-crossing detection. Next, RMS value of each half-cycle is calculated, so the  $u_{half\_rms}$  envelope is calculated. This is input for the main flicker calculation as shown in fig. 25.

Following description of the flicker algorithm blocks is direct citation of report [1]:

Block 1 is the voltage adapter that scales the input mains frequency voltage to an internal reference level. Flicker measurements can be made independently of the actual input voltage level by this way.

Block 2 is the squaring multiplier that recovers the voltage fluctuation by squaring the input voltage signal. This block is simulating the behaviour of a lamp. Block 3 contains two sections. First section is composed of a cascade of two filters, a low-pass type and a high-pass type. Low-pass filter eliminates

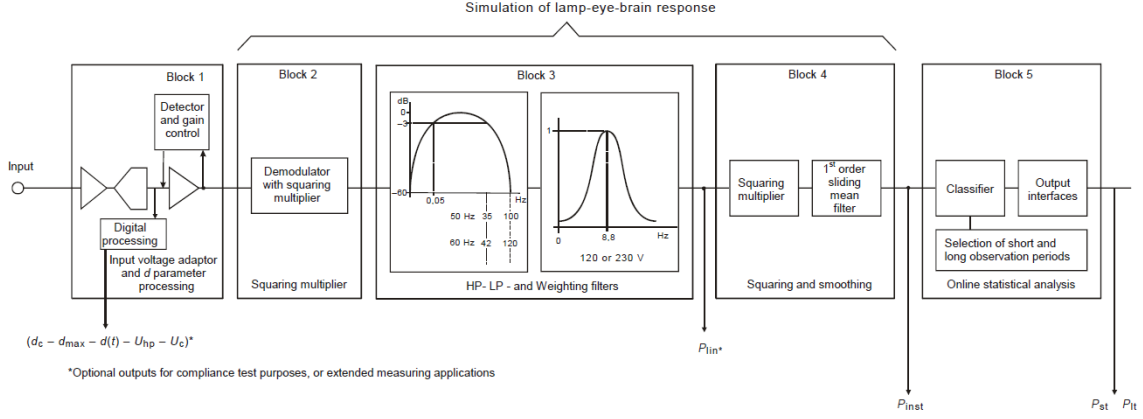


Figure 25: Flicker calculation block diagram according to IEC 61000-4-15 [3].

the double mains frequency ripple components in the signal. High-pass filter eliminates any DC voltage components in the signal. Second section is a weighting filter that simulates the frequency response of the human visual system to sinusoidal voltage fluctuations of a coiled filament gas-filled lamp (60 W/230 V or 60 W/120 V). Block 4 contains a squaring multiplier and a low-pass filter.

Combination of Block 2, Block 3 and Block 4 composes a non-linear system that simulates flicker signal applied to a lamp and human eye-brain response to this light. Output of the Block 4 is the instantaneous flicker severity  $P_{inst}$ .

Block 5 is the statistical analysis block that contains two sections. First section forms a cumulative probability function and second section forms a flicker level classifier. After the proper statistical evaluation of the  $P_{inst}$  values for 10 minutes observation, short-term flicker value  $P_{st}$  is generated by this block.

### 10.3 Uncertainty estimator

The uncertainty estimation is performed when the `calcset.unc = 'guf'`. The estimation is performed at the TWM-Flicker algorithm wrapper level as the uncertainty comes partially from the gain uncertainty and timebase error uncertainty. However, it was found the effect of the typical gain and frequency uncertainties is so low, it is not even necessary to include their effect, because the error of the algorithm itself is orders of magnitude higher. So the uncertainty of this algorithm was estimated from maximum observed deviations of the calculated  $P_{st}$  for various sampling rates at tabulated values from IEC 61000-4-15 [3]. In particular the uncertainty was set to fixed 2% of the  $P_{st}$  value for level of confidence 95%. It is quite high value, however the limits of the IEC 61000-4-15 [3] are at least three times higher, which is sufficient for a calibration purposes.

### 10.4 Validation

Validation of the algorithm was performed using a simulator function `“verify_flicker_sim()”` present on the `“flicker_sim”` QWTB wrapper folder. This function automatically performs series of the tests according different versions of IEC 61000-4-15 [3]. The test was run for various sampling rates to verify the algorithm works in full range of sampling rates. Example of the results is shown in the fig. 26.

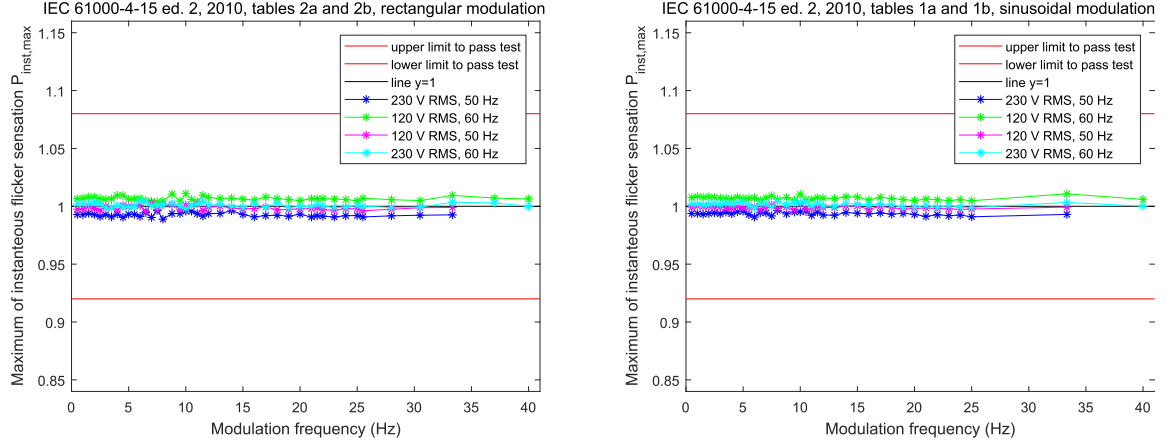


Figure 26: Example of flicker algorithm “flicker\_sim” validation against IEC 61000-4-15 [3], edition 2, for sampling rate  $fs = 50$  kHz.

## References

- [1] Report A2.3.2: Developing a Matlab script file for Flicker calculation algorithm. Empir activity completion report, TÜBİTAK Ulusal Metroloji Enstitüsü, January 2018.
- [2] Solcept AG. Solcept Open Source Flicker Measurement-Simulator. <https://www.solcept.ch/en/tools/flickersim/>.
- [3] Electromagnetic compatibility (EMC), Testing and measurement techniques, Flickermeter. Standard, August 2010.
- [4] Wilhelm Mombauer. *Messung von Spannungsschwankungen und Flickern mit dem IEC-Flickermeter*. VDE-Verlag.
- [5] NPL. NPL Reference Flickermeter Design. <http://www.npl.co.uk/electromagnetics/electrical-measurement/products-and-services/npl-reference-flickermeter-design>, 2007.

## 11 TWM-MFSF - Multi-Frequency Sine Fit

TWM-MFSF is an algorithm for estimating the frequency, amplitude, and phase of the fundamental and harmonic components in a waveform. Amplitudes and phases of harmonic components are adjusted to find minimal sum of squared differences between sampled signal and multi-harmonic model. When all sampled signal harmonics are included in the model, the algorithm is efficient and produces no bias. It can even handle aliased harmonics, if they are not aliased back exactly at frequencies where other harmonics are already present. Further, it can also handle non harmonic components, when their frequency ratio to the fundamental frequency is exactly known a-priori. It is based on the [5] and [3].

The TWM wrapper TWM-MFSF is equipped with a Monte Carlo uncertainty calculator and also a fast uncertainty estimator limited for certain types of signal and algorithm setup.

### 11.1 TWM wrapper parameters

The input quantities supported by the algorithm are shown in table 54. Algorithm returns output quantities shown in table 55. Calculation setup supported by the algorithm is shown in table 56.

Table 54: List of input quantities to the TWM-MFSF wrapper.

Name	Default	Unc.	Description
fest	0	N/A	Initial estimate of fundamental frequency [Hz]. Options:
ExpComp	N/A	N/A	List of relative frequencies of the harmonic components to fit (e.g. [1, 2, 4, 3.3] means to fit fundamental, 2nd and 4th harmonic and interharmonic $3.3 \cdot f_0$ ).
H	3	N/A	Alternative to <i>ExpComp</i> . Defines number of harmonics to fit, i.e. 3 means to fit fundamental, 2nd and 3rd harmonic.
CFT	3.5e-11	N/A	Cost Function Threshold for the MFSF minimising algorithm. Note the uncertainty estimator was calculated for the default value only!
comp_timestamp	0	N/A	Enable compensation of phase shift by time stamp value: $\phi_i' = \phi_i - 2 \cdot \pi \cdot f_{fit} \cdot time\_stamp$ .
y	N/A	No	Input sample data vector.
Ts	N/A	No	Sampling period or sampling rate or sample time vector.
fs	N/A	No	Note the wrapper always calculates in equidistant mode, so $t$ is used just to calculate $Ts$ .
t	N/A	No	
lsb	N/A	No	Either absolute ADC resolution <i>lsb</i> or nominal range value
adc_nrng	1000	No	<i>adc_nrng</i> (e.g.: 5 V for 10 Vpp range) and <i>adc_bits</i> bit res-
adc_bits	40	No	olution of ADC.
adc_offset	0	Yes	Digitizer input offset voltage.
adc_gain	1	Yes	Digitizer gain correction 2D table (multiplier).
adc_gain_f	$\emptyset$	No	
adc_gain_a	$\emptyset$	No	
adc_phi	0	Yes	Digitizer phase correction 2D table (additive).
adc_phi_f	$\emptyset$	No	
adc_phi_a	$\emptyset$	No	
adc_freq	0	Yes	Digitizer timebase error correction: $f_{tb'} = f_{tb} \cdot (1 + adc\_freq.v)$ The effect on the estimated frequency is opposite: $f_{est'} = f_{est} / (1 + adc\_freq.v)$
adc_jitter	0	No	Digitizer sampling period jitter [s].
adc_aper	0	No	ADC aperture value [s].

Table 54: List of input quantities to the TWM-MFSF wrapper.

Name	Default	Unc.	Description
adc_aper_corr	0	No	ADC aperture error correction enable: $A' = A \cdot \pi \cdot \text{adc\_aper} \cdot f_{est} / \sin(\pi \cdot \text{adc\_aper} \cdot f_{est})$ $\phi_i' = \phi_i + \pi \cdot \text{adc\_aper} \cdot f_{est}$
adc_Yin_Cp	1e-15	Yes	Digitizer input admittance 1D table.
adc_Yin_Gp	1e-15	Yes	
adc_Yin_f	$\emptyset$	No	
adc_sfdr	180	No	Digitizer SFDR 2D table.
adc_sfdr_f	$\emptyset$	No	
adc_sfdr_a	$\emptyset$	No	
tr_type	“”	No	Transducer type string (“rvd” or “shunt”).
tr_gain	1	Yes	Transducer gain correction 2D table (multiplicative).
tr_gain_f	$\emptyset$	No	
tr_gain_a	$\emptyset$	No	
tr_phi	0	Yes	Transducer phase correction 2D table (additive).
tr_phi_f	$\emptyset$	No	
tr_phi_a	$\emptyset$	No	
tr_sfdr	180	No	Transducer SFDR 2D table.
tr_sfdr_f	$\emptyset$	No	
tr_sfdr_a	$\emptyset$	No	
tr_Zlo_Rp	1e3	Yes	RVD transducer low-side impedance 1D table. Note this is related to loading correction and it has effect only for RVD transducer and will work only if <i>adc_Yin</i> is defined as well.
tr_Zlo_Cp	1e-15	Yes	
tr_Zlo_f	$\emptyset$	No	
tr_Zbuf_Rs	0	Yes	Loading corrections: Transducer output buffer output series impedance 1D table. Leave unassigned to disable buffer from the correction topology.
tr_Zbuf_Ls	0	Yes	
tr_Zbuf_f	$\emptyset$	No	
tr_Zca_Rs	1e-9	Yes	Loading corrections: Transducer high side terminal series impedance 1D table.
tr_Zca_Ls	1e-12	Yes	
tr_Zca_f	$\emptyset$	No	
tr_Zcal_Rs	1e-9	Yes	Loading corrections: Transducer low side terminal series impedance 1D table.
tr_Zcal_Ls	1e-12	Yes	
tr_Zcal_f	$\emptyset$	No	
tr_Yca_Cp	1e-15	Yes	Loading corrections: Transducer output terminals shunting impedance.
tr_Yca_D	1e-12	Yes	
tr_Yca_f	$\emptyset$	No	
tr_Zcam	1e-12	Yes	Loading corrections: Transducer output terminals mutual inductance 1D table.
tr_Zcam_f	$\emptyset$	No	
Zcb_Rs	1e-9	Yes	Loading corrections: Cable series impedance 1D table.
Zcb_Ls	1e-12	Yes	
Zcb_f	$\emptyset$	No	
Ycb_Rs	1e-15	Yes	Loading corrections: Cable series impedance 1D table.
Ycb_Ls	1e-12	Yes	
Ycb_f	$\emptyset$	No	

Table 55: List of output quantities of the TWM-MFSF wrapper. The quantities marked \* may have partial or none assigned uncertainty depending on the selected uncertainty calculation mode. They will be available only for Monte Carlo uncertainty method.

Name	Uncertainty	Description
f	Yes	Vector of frequencies of all fitted components [Hz].
A	Yes	Vector of amplitudes of all fitted components.
ph	Yes*	Vector of phases of all fitted components [rad].
thd	Yes	Total harmonic distortion of the fitted components [%]. Note it is a fundamental referenced value.

Table 56: List of “calcset” options supported by the TWM-MFSF wrapper.

Name	Description
calcset.unc	Uncertainty calculation mode. Supported: “none”, “guf” for uncertainty estimator, “mcm” for Monte Carlo.
calcset.mcm.method	Monte Carlo evaluation mode: “singlecore” - single core evaluation, “multicore” - Parallel evaluation using “parcellfun” for GNU Octave or “parfor” for Matlab “multistation” - Multicore evaluation using “multicore” package (GNU Octave only yet).
calcset.mcm.repeats	Monte Carlo iterations count. Use at least 100 to get any usable estimate.
calcset.mcm.proc_no	Number of parallel instances to use for the paralleled modes. Use zero value to not start any server processes for the “multistation” mode. This option expects user started the server processes manually in the job sharing folder. This option causes less overhead for the batch processing or runtime calculations.
calcset.mcm.tmpdir	Jobs sharing folder for the “multistation” mode. This should be an absolute path to the sharing folder. Keep in mind the package “multicore” will erase the content of this folder before each new calculation!
calcset.mcm.user_fun	User function to call in the “multistation” mode after startup of the server processes. Example: “calcset.mcm.user_fun = @coklbind2”. Leave empty to not execute any function.
calcset.loc	Level of confidence [-].
calcset.verbose	Verbose level.
calcset.dbg_plots	Non-zero value shows debugging plots of the MFSF uncertainty calculator.

## 11.2 Algorithm description

Internal structure of the TWM-MFSF wrapper is shown in the fig. 27. The wrapper supports only single-ended input, so the signal conditioning is simple. The wrapper starts by a call of the QWTB algorithm “MFSF” to calculate the estimates of the harmonics. This call is performed with uncertainty option disabled, because at this point the required parameters for its calculation are not know.

Follows correction of the timebase frequency error. Next, the DC offset of the digitizer is corrected. In the next step, the wrapper compensates the aperture error, digitizer gain and phase errors and transducer gain and phase errors. At the same time the uncertainties of the corrections are calculated.

Next, the uncertainty calculator/estimator takes place. First, the required parameters for the calculation are prepared: jitter, system SFDR and digitizer resolution. Then, the wrapper calls the QWTB



“MFSF” algorithm for the second time, but this time with enabled uncertainty calculation. Returned uncertainties are scaled by the correction factors so they match the scaled estimates. Next, the algorithm uncertainties are combined with the correction uncertainties and the required quantities are expressed and returned.

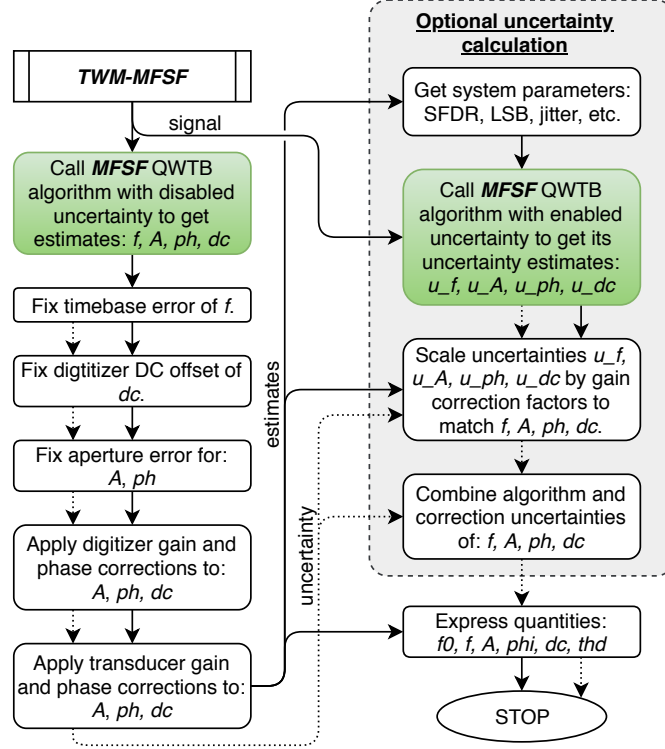


Figure 27: Structure of TWM-MFSF algorithm wrapper. Note the green blocks are calls to another QWTB wrappers.

### 11.2.1 QWTB algorithm MFSF

The structure of the QWTB wrapper “MFSF”, which contains the fitting function “MFSF()” itself is shown in fig. 28. The wrapper starts with optional override of the internal initial estimator of fundamental component frequency by function “ipdft\_spect()”. Follows the call of the “MFSF()” function itself. The function returns fitted harmonic coefficients  $f$ ,  $A$ ,  $ph$  and offset  $O$ . It also calculated Total Harmonic Distortion (THD) following the “fundamental referenced” definition:

$$THD = \sqrt{\frac{\sum_{h=2}^H A(h)^2}{A(1)^2}}, \quad (58)$$

where  $h$  is harmonic index and  $H$  is harmonics count.

The Multi-Frequency Sine-Fit algorithm itself (function “MFSF()”) is used to estimate the harmonic components that are present in non-coherently sampled periodic signal. The main input parameter is the sampled record  $y(n \cdot T_s)$  having the length  $N$ , the sampling period  $T_s$  and the index signal harmonics to be estimated  $k = [1, h]$ . Optionally, the method for initial guess estimation and the cost function threshold can be defined (the default value for the threshold is  $3.5 \cdot 10^{-11}$ ). The outputs of the algorithm are: (i) frequency of the fundamental signal  $f_1$ , (ii) amplitudes  $A_1$  to  $A_h$  and (iii) the phases  $\phi_1$  to  $\phi_h$  of the analysed fundamental signal and harmonics, (iv) offset of the sampled signal  $A_0$ , (v) total harmonic distortion THD, (vi) total number of iterations and (vii) variance amplitude estimate.

The frequency of the fundamental signal  $f_1$ , and complex amplitudes  $A_{comp,k}$  are estimated first by nonlinear-least-square algorithm which iteratively minimize the  $K_{NLS}$  function (equation 59) using

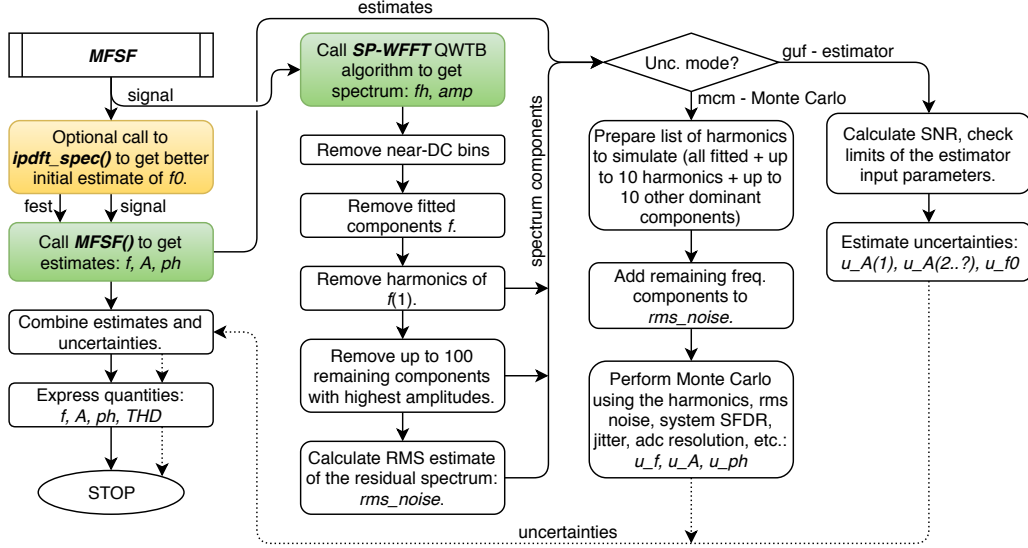


Figure 28: Structure of MFSF algorithm wrapper. Note the green blocks are calls to another QWTB wrappers, the gold cells are calls to another functions described in the text.

Gauss-Newton procedure [4]. The first approximate frequency of the record  $y$  is estimated using either peak amplitude DFT bin frequency or interpolated DFT frequency estimate.

$$K_{\text{NLS}}(A_{\text{comp},0}, A_{\text{comp},1}, \dots, A_{\text{comp},h}, f_1) = \sum_{n=1}^N \left( y(n \cdot T_s) - \sum_{k=-h}^h A_k \cdot \exp^{j \cdot k \cdot n \cdot 2 \cdot \pi \cdot f_1 \cdot T_s} \right)^2, \quad (59)$$

$$A_{-k} = A_k^*. \quad (60)$$

After the complex harmonic amplitudes  $A_{\text{comp},k}$  are defined the amplitudes  $A_k$  and the phases  $\phi_k$  of the fundamental signal and harmonic components as well as the offset  $A_0$  and the THD of the record are calculated using following equations:

$$A_k = \sqrt{A_{\text{comp,real},k}^2 + A_{\text{comp,imag},k}^2}, k \in [1, h], \quad (61)$$

$$\phi_k = \arctan \frac{A_{\text{comp,imag},k}}{A_{\text{comp,real},k}}, k \in [1, h], \quad (62)$$

$$A_0 = A_{\text{comp},0}, \quad (63)$$

$$THD = \frac{\sum_{k=2}^h A_k^2}{A_1^2}. \quad (64)$$

### 11.2.2 Uncertainty calculation

The TWM-MFSF supports two modes of uncertainty calculation. First option is the Monte Carlo mode, which is slower, but more accurate and it can handle any number of fitted components. Second option is fast estimator, which is less accurate, but considerably faster.

Note the uncertainty calculation is split between the “TWM-MFSF” wrapper and “MFSF” wrapper as shown in fig. 27. The uncertainty of the algorithm is calculated in the “MFSF” wrapper, whereas the uncertainty of the corrections is included in the TWM wrapper “TWM-MFSF”.

First part of the uncertainty calculation is in the “MFSF” wrapper and it is common for both modes of calculation. The spectrum analysis of the input signal is performed by the “SP-WFFT” algorithm with the windowing function “Flattp HFT116D” [1], which has low scalloping and good spectral resolution. The spectrum is heuristically analysed:

1. The fitted components are removed from the spectrum. These are not relevant for the uncertainty

evaluation, as they are already known from the “MFSF()” function itself, but they must be removed from the spectrum before searching the additional frequency components.

2. All harmonics of the fundamental frequency “ $f_0$ ” exceeding the threshold relative to the fundamental component are identified and removed in a full bandwidth.
3. Up to 100 residual components (harmonic or inter-harmonic) exceeding the threshold relative to the fundamental component are identified and removed in a full bandwidth.
4. The residual signal is taken as RMS noise.

Following steps differ for the Monte Carlo mode and estimator.

#### 11.2.2.1 Monte Carlo

The Monte Carlo would be extremely slow if all harmonics and inter-harmonics are taken into account, because in fact it takes longer to synthesize the waveform with all the frequency components than to apply MFSF algorithm. So, before Monte Carlo itself, a selection of the dominant components is performed. All fitted components are simulated, up to 10 harmonics of “ $f_0$ ” are simulated and 10 of the remaining harmonic and inter-harmonics with highest amplitudes are simulated. The rest of the components identified from the spectrum is added to the RMS noise and simulated together as a noise.

The Monte Carlo (MC) simulation itself is performed by the function “proc\_MFSF()”, which is called once for each MC iteration cycle. The function does following steps:

1. Randomize fundamental frequency  $f_0$  in a small range  $\pm 0.001$  Hz/Hz to prevent accidental lock in some local minimum of uncertainty.
2. Generate time vector with the jitter effect.
3. Generate list of fitted harmonics and randomise their amplitudes by  $\pm 1$  % to reflect fitted amplitude uncertainty. Generate random phase angles of the harmonics, because it is not easy to state what was accuracy of the fit. This should produce the worst case errors.
4. Randomise the fitted harmonics by system SFDR.
5. Generate additional harmonics of the  $f_0$ , based on the identified list from the spectrum. Randomize their amplitudes by  $\pm 1$  % and generate random phase.
6. Generate inter-harmonics based on the spectral analysis. Randomise frequency by  $\pm 1$  DFT bin to reflect resolution of FFT spectrum, amplitude by 1 % and generate random phase.
7. Synthesize waveform with all the harmonics and inter-harmonics.
8. Add RMS noise.
9. Add random offset with very pessimistic uncertainty, because MFSF may not estimate the DC correctly, when not all harmonics are in the fitted list.
10. Perform quantisation of the waveform.
11. Call “MFSF()” to get estimates of  $f$ ,  $A$ ,  $ph$  and  $O$ .
12. Compare the estimates to the actually generated parameters.

The results from the iterations are processed according to the GUM Annex 1 [2] using function “scovint()” to get uncertainties of the estimated components.

Note the MC evaluator itself uses function “qwtb\_mcm\_exec()”. This function is internally designed to enable parallel calculation of the MC iteration cycles. It offers three modes of parallelisation:

1. **calcset.mcm.method = ‘singlecore’**: Single core calculation.

2. **calcset.mcm.method = ‘multicore’**: Multicore operation using “parcellfun()” from “parallel” package for GNU Octave or “parfor” for Matlab. Note the use of Matlab’s “parfor” for parallelisation is just a user wish. Actual parallelisation mode is decided by Matlab. The package “parcellfun()” implementation does work only for Linux. Windows implementation was not functional at least up to GNU Octave version 4.2.2.
3. **calcset.mcm.method = ‘multistation’**: Multiprocess/multistation calculation using “multi-core” package for GNU Octave (Matlab is not supported yet). Note the The “multistation” method requires to define shared folder path for the job files. Otherwise it will create the shared folder in temp folder, which may not be appreciated by the SSD disks owners. The mode “multistation” also have one specific feature. It can initiate the user function after startup of the server processes. The function is defined in the “calcset.mcm.user\_fun” variable. The example of the use for this optional input is CMI’s supercomputer “Čokl” [6] which requires to call a special script to assign server processes to particular CPU cores.

See table 56 for list of the additional parameters. Note at least 100 iterations is the absolute minimum for which the MC mode provides any usable uncertainty estimates. The processing time for an evaluation at 4 cores with 1000 cycles and  $N = 10000$  input samples, 3 fitted harmonics and 10 additional spur harmonics is typically below 20 seconds. However, the situation may change drastically when more harmonics is fitted or high count of spur harmonic components is presents in the signal.

### 11.2.2.2 Fast estimator

The MFSF algorithm estimates several output parameters therefore the uncertainty was analysed for the frequency and the amplitude of the fundamental signal  $f_1$  and  $A_1$ , and for the amplitudes of the other harmonic components  $A_2$  to  $A_h$ . The phases, the offset  $A_0$  and the THD are additional informative parameters calculated by the MFSF algorithm, therefore the uncertainty analysis for those parameters was not performed.

Three uncertainty contributions were considered in this study (see Table 57): resolution, jitter and noise. Additionally, several other parameters related to the sampled signal or sampling (i.e. condition) are expected to affect the uncertainty therefore enormous number of Monte Carlo simulation would be needed for accurate uncertainty analysis.

Table 57: A list of parameters that were varied during the Monte-Carlo simulations.

Uncertainty contribution	Variation range	Reference value
RMS jitter	1 ns - 10 ns	<b>1 ns</b> (0 ns)
resolution	10 pV - 100 mV	<b>10 <math>\mu</math>V</b> (0 V)
noise, SNR <sup>*1</sup>	$10^2$ - $10^6$	<b>1000</b> (infinite)
<b>Condition parameters</b>		
amplitude of the fundamental signal, $A_1$	0.1 V – 1000 V	1 V
frequency of the fundamental signal, $f_1$	10 Hz – 200 Hz	100 Hz
SFDR <sup>*2</sup>	0 – 0.5	0.1
sampling frequency, $f_s$	5 kHz – 200 kHz	10 kHz
number of samples, $N$	500 Sa – 100 kSa	10 kSa

<sup>\*1</sup> SNR in this study is defined as an amplitude of the fundamental signal vs. the RMS noise ratio.

<sup>\*2</sup> SFDR is spurious-free dynamic range which is defined as the harmonic amplitude to fundamental signal amplitude ratio.

Herein, different and slightly simplified approach was used. We run 18 different Monte Carlo simulation sets. For each set only one uncertainty contribution was considered using the bold reference value given in Table 57. The other two uncertainty contributions were neglected by using the reference values given in the brackets. Additionally, only one condition parameter has been varied at the time using the variation range as defined in Table 57 while we used the reference values for the other condition parameters. We also verified the linearity of uncertainty contribution by varying its value over a certain variation range while neglecting the other uncertainty contributions (by using the reference values given

in brackets) and keeping all condition parameters at reference values. For each combination of uncertainty contribution, condition and variation range we performed 25000 simulation where one additional harmonic component has been randomly chosen between 2nd and 10th components. Additionally, the initial phases of the fundamental signal and harmonic component have been randomly varied between  $+\pi$  and  $-\pi$ . For each simulation a Gaussian distribution has been obtained. The uncertainty contribution (Gaussian distribution,  $k = 1$ ) for each estimated parameter (i.e.  $f_1$ ,  $A_1$ ,  $A_k$ ) due to the resolution, noise and jitter are defined by equations 68 to 76. The uncertainty contributions for each estimated parameter are finally combined, and recalculated for Gaussian distribution,  $k = 2$ :

$$u_{f_1} = 2 \cdot \sqrt{u_{f_1,\text{res}}^2 + u_{f_1,\text{noise}}^2 + u_{f_1,\text{jitter}}^2}, \quad (65)$$

$$u_{A_1} = 2 \cdot \sqrt{u_{A_1,\text{res}}^2 + u_{A_1,\text{noise}}^2 + u_{A_1,\text{jitter}}^2}, \quad (66)$$

$$u_{A_h} = 2 \cdot \sqrt{u_{A_h,\text{res}}^2 + u_{A_h,\text{noise}}^2 + u_{A_h,\text{jitter}}^2}. \quad (67)$$

$$u_{f,\text{res}} = 0.52 \text{ mHz} \cdot \left( \frac{f_s}{10 \text{ kHz}} \right)^{1.6} \cdot \left( \frac{N}{10 \text{ kSa}} \right)^{-2} \cdot \left( \frac{res}{A_1} \right), \quad (68)$$

$$u_{A_1,\text{res}} = 0.5 \cdot \left( \frac{f_1}{f_s} \right)^{0.5} \cdot res, \quad (69)$$

$$u_{A_h,\text{res}} = 1.3 \cdot \left( \frac{f_1}{f_s} \right)^{0.5} \cdot res, \quad (70)$$

$$u_{f,\text{noise}} = 5.5 \text{ } \mu\text{Hz} \cdot \left( \frac{f_s}{10 \text{ kHz}} \right) \cdot \left( \frac{N}{10 \text{ kSa}} \right)^{-1.5} \cdot \left( \frac{SNR}{1000} \right)^{-1}, \quad (71)$$

$$u_{A_1,\text{noise}} = 10 \text{ } \mu\text{Hz} \cdot \left( \frac{N}{10 \text{ kSa}} \right)^{-0.5} \cdot \left( \frac{A_1}{1 \text{ V}} \right)^1 \cdot \left( \frac{SNR}{1000} \right)^{-1}, \quad (72)$$

$$u_{A_h,\text{noise}} = 25 \text{ } \mu\text{Hz} \cdot \left( \frac{N}{10 \text{ kSa}} \right)^{-0.5} \cdot \left( \frac{A_1}{1 \text{ V}} \right)^1 \cdot \left( \frac{SNR}{1000} \right)^{-1}, \quad (73)$$

$$u_{f,\text{jitter}} = 1 \text{ } \mu\text{Hz} \cdot \left( \frac{f_s}{10 \text{ kHz}} \right)^{1.2} \cdot \left( \frac{N}{10 \text{ kSa}} \right)^{-1.7} \cdot \left( \frac{f_1}{100 \text{ Hz}} \right)^{0.55} \cdot \left( \frac{jitter}{1 \text{ ns}} \right)^{1.2}, \quad (74)$$

$$u_{A_1,\text{jitter}} = 2.1 \text{ } \mu\text{V} \cdot \left( \frac{A_1}{1 \text{ V}} \right)^1 \cdot \left( \frac{f_1}{100 \text{ Hz}} \right)^1 \cdot \left( \frac{jitter}{1 \text{ ns}} \right)^1, \quad (75)$$

$$u_{A_h,\text{jitter}} = 5 \text{ } \mu\text{Hz} \cdot \left( \frac{N}{10 \text{ kHz}} \right)^{-0.5} \cdot \left( \frac{A_1}{1 \text{ V}} \right)^1 \cdot \left( \frac{f_1}{100 \text{ Hz}} \right)^1 \cdot \left( \frac{jitter}{1 \text{ ns}} \right)^1. \quad (76)$$

### 11.3 Validation

The algorithm TWM-MFSF has many input quantities and some of them are matrices. That is too many possible degrees of freedom. Thus, varying the quantities in some systematic way would be very complicated if the validation should cover full range of used signals and corrections. Therefore, an alternative approach was used.

QWTB test function “alg\_test.m” was created, which performs the validation using randomly generated test setups. It randomizes the signal parameters, correction quantities and uncertainties and algorithm configurations in ranges expected to occur during the real measurements. The test is run many times to cover full operating range of the algorithm. Following operations are performed:

1. Generate signal with known frequency, amplitude, phase of the fundamental fundamental and harmonics component and with a know DC offset.
2. Distort the signal by inverse corrections, i.e. simulate the transducers, and digitizer (e.g. gain errors, quantisation, SFDR ...).

3. Run the algorithm TWM-MFSF with enabled uncertainty evaluation to obtain the estimated values and corresponding uncertainties of the frequency (fundamental signal), amplitude (fundamental signal and harmonics), phase (fundamental signal and harmonics), DC and THD estimation.
4. Compare the reference and calculated values and check if the deviations are lower than assigned uncertainties.
5. Repeat  $N$  times from step 1, with different setup parameters, different corrections randomised by their uncertainties, and with randomised noise, SFDR and jitter.
6. Check that at least 95 % of results passed (for 95 % level of confidence).

Following validation applies only to the fast uncertainty estimator. The Monte-Carlo uncertainty calculator was not validated.

The total number of Monte-Carlo simulations was 200000. The parameters of the input signal, the digitizer and transducer settings were randomly varied. The sampling frequency was between 5 kHz and 200 kHz and the number of samples between 500 Sa and 100 kSa. The frequency of fundamental signal was between 10 Hz and 200 Hz. The frequency of the harmonics and interharmonics were always above frequency of the fundamental signal but below the Nyquist frequency. The number of harmonics that were added to the fundamental signal and that needs to be estimated by the algorithm was 3. The number of interharmonics was 1. The amplitude of the fundamental signal was between 0.1 V and 1000 V and the amplitude of the harmonics and interharmonic between 0.00001 and 0.05 and between 0.00001 and 0.02 of the amplitude of the fundamental signal, respectively (the amplitudes have been varied individually for each harmonics and interharmonic). The DC offset was between -10 and +10 of the amplitude of the fundamental signal. The phases of the fundamental signal as well as of the harmonics and interharmonic were individually and randomly varied between +3.14 rad and -3.14 rad. The ADC noise was between  $1e-11$  and  $1e-3$  of the amplitude of the fundamental signal while the jitter was between  $1e-9$ s and  $1e-7$ s. Additionally, the spur has been added to the signal (spurious free dynamic range was  $100e-6$ , number of spurs 10). ADC aperture was between  $1e-5$ s and  $4e-5$ s, ADC gain between 1 and 1.5, ADC phase between +1.57 rad and -1.57 rad, frequency correction of the digitizer timebase between  $-5e-3$  and  $5e-3$ , ADC offset between 0.005 V and 0.005 V and number of bits between 22 and 24. Relative time-stamp of the first sample was varied between -10 s and 10 s. The transducer gain was between 0.5 and 20 and the transducer phase was between +1.57 rad and -1.57 rad. The resistive voltage divider low-side impedance value (i.e. resistance and capacitance) were between  $100\ \Omega$  and  $500\ \Omega$  and  $0.1\ \text{pF}$  and  $10\ \text{pF}$ , respectively (only resistive voltage divider was used in the simulations). The randomisation of corrections was also enabled which means that not only the uncertainty of the algorithm but also the contributions of the correction uncertainties were included in the Monte-Carlo simulations.

The success rate of the TWM-MFSF algorithm for the fundamental frequency estimation was 99.91 %, 99.63 % for the amplitude of the fundamental signal, 99.40 % for the amplitude of the harmonics, 99.77 % for the phase of the fundamental signal, 77.62 % for the phase of the harmonics, 68.24 % for the DC and 59.59 % for the THD.

Note the preliminary tests for the Monte Carlo method show much higher success rates at least for the harmonics, however the processing time is much higher.

## References

- [1] Gerhard Heinzel, A. Rüdiger, and R. Schilling. Spectrum and spectral density estimation by the discrete fourier transform (dft), including a comprehensive list of window functions and some new flat-top windows. Technical report, Max-Planck-Institut für Gravitationsphysik (Albert-Einstein-Institut) Teilinstitut Hannover, Feb 2005.
- [2] JCGM. *Evaluation of measurement data - Supplement 1 to the "Guide to the expression of uncertainty in measurement" - Propagation of distributions using a Monte Carlo method*. Bureau International des Poids et Mesures.
- [3] Rado Lapuh. *Sampling with 3458A*. Left Right d.o.o., Sep 2018.

- [4] R. Pintelon and J. Schoukens. An improved sine-wave fitting procedure for characterizing data acquisition channels. *IEEE Transactions on Instrumentation and Measurement*, 45(2):588–593, April 1996.
- [5] J. Schoukens, R. Pintelon, and G. Vandersteen. A sinewave fitting procedure for characterizing data acquisition channels in the presence of time base distortion and time jitter. *IEEE Transactions on Instrumentation and Measurement*, 46(4):1005–1010, Aug 1997.
- [6] Miroslav Valtr. ČMI HPC System Online. [https://translate.google.cz/translate?sl=cs&tl=en&js=y&prev=\\_t&hl=cs&ie=UTF-8&u=http%3A%2F%2Fprutok.cmi.cz%2Fsc%2Fdoku.php%3Fid%3Dsystem&edit-text=](https://translate.google.cz/translate?sl=cs&tl=en&js=y&prev=_t&hl=cs&ie=UTF-8&u=http%3A%2F%2Fprutok.cmi.cz%2Fsc%2Fdoku.php%3Fid%3Dsystem&edit-text=), 2014.

## 12 TWM-PWRFFT - Power by FFT

Algorithm for calculation of power parameters from FFT spectra of voltage and current channels. It calculates the power in full bandwidth. It designed for coherent sampling.

The algorithm can calculate all basic parameters: active power  $P$ , reactive power  $Q$ , apparent power  $S$ , RMS voltage  $U$ , RMS current  $I$  and power factor  $PF$ . It also returns DC components separately:  $U_{dc}$ ,  $I_{dc}$  and  $P_{dc}$ . User may choose optional AC coupling mode by setting parameter “ $ac\_coupling = 1$ ” in which case the  $U$ ,  $I$ ,  $P$ ,  $Q$ ,  $S$  and  $PF$  will be calculated without the AC component.

The algorithm uses following definitions for the power components: (i) The AC power components  $P$ ,  $Q$  and  $S$  are related by equation:

$$S^2 = P^2 + Q^2. \quad (77)$$

(ii) Power factor  $PF$  is calculated including DC components according to equation:

$$PF = \frac{P}{S}. \quad (78)$$

(iii) The sign of  $Q$  is calculated using harmonic components method according Budenau definition:

$$\text{sing}(Q) = \text{sign} \left\{ \sum_{h=1}^H (U(h) \cdot I(h) \cdot \sin \phi(h)) \right\}, \quad (79)$$

where  $h$  is harmonic index,  $H$  is harmonics count,  $U(h)$ ,  $I(h)$  and  $\phi(h)$  are harmonic voltage, current and phase shift. Note the absolute value of  $Q$  is still calculated from AC components following equation 77. Only the sign of  $Q$  is decided from the Budenau definition 79.

The TWM-PWRFFT algorithm wrapper is able to use single-ended or differential input sensors for voltage channel, current channel or both. The algorithm is also equipped by a fast uncertainty estimator.

### 12.1 TWM wrapper parameters

The input quantities supported by the algorithm are shown in the table 58. Algorithm returns output quantities shown in the table 59. Calculation setup supported by the algorithm is shown in table 60.

Table 58: List of input quantities to the TWM-PWRFFT wrapper.  
Details on the correction quantities can be found in [1].

Name	Default	Unc.	Description
ac_coupling	0	N/A	Enables virtual AC coupling of the wattmeter. This option will cause the DC value will be ignored.
u	N/A	No	Input voltage sample data vector and complementary low-side input data vector $u_{lo}$ (for differential mode only).
i	N/A	No	Input current sample data vector and complementary low-side input data vector $i_{lo}$ (for differential mode only).
Ts	N/A	No	Sampling period or sampling rate or sample time vector.
fs	N/A	No	Note the wrapper always calculates in equidistant mode, so $t$ is used just to calculate $Ts$ .
t	N/A	No	
time_shift	0	Yes	Timeshift between voltage channel $u$ and current channel $i$ .
u_time_shift_lo	0	Yes	Time shift between high-side channel $u$ low-side channel $u_{lo}$ (or $i$ and $i_{lo}$ for current).
i_time_shift_lo	0	Yes	



Table 58: List of input quantities to the TWM-PWRFFT wrapper.  
Details on the correction quantities can be found in [1].

Name	Default	Unc.	Description
u_lsb	N/A	No	Either absolute ADC resolution <i>lsb</i> or nominal range value <i>adc_nrng</i> (e.g.: 5 V for 10 Vpp range) and <i>adc_bits</i> bit resolution of ADC.
u_adc_nrng	1000	No	
u_adc_bits	40	No	
u_lo_lsb	N/A	No	
u_lo_adc_nrng	1000	No	
u_lo_adc_bits	40	No	
i_lsb	N/A	No	
i_adc_nrng	1000	No	
i_adc_bits	40	No	
i_lo_lsb	N/A	No	
i_lo_adc_nrng	1000	No	
i_lo_adc_bits	40	No	
u_adc_offset	0	Yes	Digitizer input offset voltage.
u_lo_adc_offset	0	Yes	
i_adc_offset	0	Yes	
i_lo_adc_offset	0	Yes	
u_adc_gain	1	Yes	Digitizer gain correction 2D table (multiplier).
u_adc_gain_f	□	No	
u_adc_gain_a	□	No	
u_lo_adc_gain	1	Yes	
u_lo_adc_gain_f	□	No	
u_lo_adc_gain_a	□	No	
i_adc_gain	1	Yes	
i_adc_gain_f	□	No	
i_adc_gain_a	□	No	
i_lo_adc_gain	1	Yes	
i_lo_adc_gain_f	□	No	
i_lo_adc_gain_a	□	No	
u_adc_phi	0	Yes	Digitizer phase correction 2D table (additive).
u_adc_phi_f	□	No	
u_adc_phi_a	□	No	
u_lo_adc_phi	0	Yes	
u_lo_adc_phi_f	□	No	
u_lo_adc_phi_a	□	No	
i_adc_phi	0	Yes	
i_adc_phi_f	□	No	
i_adc_phi_a	□	No	
i_lo_adc_phi	0	Yes	
i_lo_adc_phi_f	□	No	
i_lo_adc_phi_a	□	No	
adc_freq	0	Yes	Digitizer timebase error correction: $f_{tb'} = f_{tb} \cdot (1 + adc\_freq.v)$ The effect on the estimated frequency is opposite: $f_{est'} = f_{est} / (1 + adc\_freq.v)$
u_adc_jitter	0	No	Digitizer sampling period jitter [s].
u_lo_adc_jitter	0	No	
i_adc_jitter	0	No	
i_lo_adc_jitter	0	No	
u_adc_aper	0	No	ADC aperture value [s].
u_lo_adc_aper	0	No	
i_adc_aper	0	No	
i_lo_adc_aper	0	No	

Table 58: List of input quantities to the TWM-PWRFFT wrapper.  
Details on the correction quantities can be found in [1].

Name	Default	Unc.	Description
u_adc_aper_corr	0	No	ADC aperture error correction enable: $A' = A \cdot \pi \cdot \text{adc\_aper} \cdot f_{est} / \sin(\pi \cdot \text{adc\_aper} \cdot f_{est})$ $\phi_i' = \phi_i + \pi \cdot \text{adc\_aper} \cdot f_{est}$
u_lo_adc_aper	0	No	
i_adc_aper_corr	0	No	
i_lo_adc_aper	0	No	
u_adc_sfdr	180	No	Digitizer SFDR 2D table.
u_adc_sfdr_f	□	No	
u_adc_sfdr_a	□	No	
u_lo_adc_sfdr	180	No	
u_lo_adc_sfdr_f	□	No	
u_lo_adc_sfdr_a	□	No	
i_adc_sfdr	180	No	
i_adc_sfdr_f	□	No	
i_adc_sfdr_a	□	No	
i_lo_adc_sfdr	180	No	
i_lo_adc_sfdr_f	□	No	
i_lo_adc_sfdr_a	□	No	
u_adc_Yin_Cp	1e-15	Yes	Digitizer input admittance 1D table.
u_adc_Yin_Gp	1e-15	Yes	
u_adc_Yin_f	□	No	
u_lo_adc_Yin_Cp	1e-15	Yes	
u_lo_adc_Yin_Gp	1e-15	Yes	
u_lo_adc_Yin_f	□	No	
i_adc_Yin_Cp	1e-15	Yes	
i_adc_Yin_Gp	1e-15	Yes	
i_adc_Yin_f	□	No	
i_lo_adc_Yin_Cp	1e-15	Yes	
i_lo_adc_Yin_Gp	1e-15	Yes	
i_lo_adc_Yin_f	□	No	
u_tr_type	“”	No	Transducer type string (“rvd” or “shunt”).
i_tr_type			
u_tr_gain	1	Yes	Transducer gain correction 2D table (multiplicative).
u_tr_gain_f	□	No	
u_tr_gain_a	□	No	
i_tr_gain	1	Yes	
i_tr_gain_f	□	No	
i_tr_gain_a	□	No	
u_tr_phi	0	Yes	Transducer phase correction 2D table (additive).
u_tr_phi_f	□	No	
u_tr_phi_a	□	No	
i_tr_phi	0	Yes	
i_tr_phi_f	□	No	
i_tr_phi_a	□	No	
u_tr_sfdr	180	No	Transducer SFDR 2D table.
u_tr_sfdr_f	□	No	
u_tr_sfdr_a	□	No	
i_tr_sfdr	180	No	
i_tr_sfdr_f	□	No	
i_tr_sfdr_a	□	No	

Table 58: List of input quantities to the TWM-PWRFFT wrapper.  
Details on the correction quantities can be found in [1].

Name	Default	Unc.	Description
u_tr_Zlo_Rp	1e3	Yes	RVD transducer low-side impedance 1D table. Note this is related to loading correction and it has effect only for RVD transducer and will work only if <i>adc_Yin</i> is defined as well.
u_tr_Zlo_Cp	1e-15	Yes	
u_tr_Zlo_f	□	No	
i_tr_Zlo_Rp	1e3	Yes	
i_tr_Zlo_Cp	1e-15	Yes	
i_tr_Zlo_f	□	No	
u_tr_Zca_Rs	1e-9	Yes	Loading corrections: Transducer high side terminal series impedance 1D table.
u_tr_Zca_Ls	1e-12	Yes	
u_tr_Zca_f	□	No	
i_tr_Zca_Rs	1e-9	Yes	
i_tr_Zca_Ls	1e-12	Yes	
i_tr_Zca_f	□	No	
u_tr_Zcal_Rs	1e-9	Yes	Loading corrections: Transducer low side terminal series impedance 1D table.
u_tr_Zcal_Ls	1e-12	Yes	
u_tr_Zcal_f	□	No	
i_tr_Zcal_Rs	1e-9	Yes	
i_tr_Zcal_Ls	1e-12	Yes	
i_tr_Zcal_f	□	No	
u_tr_Yca_Cp	1e-15	Yes	Loading corrections: Transducer output terminals shunting impedance.
u_tr_Yca_D	1e-12	Yes	
u_tr_Yca_f	□	No	
i_tr_Yca_Cp	1e-15	Yes	
i_tr_Yca_D	1e-12	Yes	
i_tr_Yca_f	□	No	
u_tr_Zcam	1e-12	Yes	Loading corrections: Transducer output terminals mutual inductance 1D table.
u_tr_Zcam_f	□	No	
i_tr_Zcam	1e-12	Yes	
i_tr_Zcam_f	□	No	
u_Zcb_Rs	1e-9	Yes	Loading corrections: Cable series impedance 1D table.
u_Zcb_Ls	1e-12	Yes	
u_Zcb_f	□	No	
i_Zcb_Rs	1e-9	Yes	
i_Zcb_Ls	1e-12	Yes	
i_Zcb_f	□	No	
u_Ycb_Rs	1e-15	Yes	Loading corrections: Cable series impedance 1D table.
u_Ycb_Ls	1e-12	Yes	
u_Ycb_f	□	No	
i_Ycb_Rs	1e-15	Yes	
i_Ycb_Ls	1e-12	Yes	
i_Ycb_f	□	No	

Table 59: List of output quantities of the TWM-PWRFFT wrapper.

Name	Uncertainty	Description
U	Yes	RMS voltage [V].
I	Yes	RMS current [A].
P	Yes	Active power [W].
S	Yes	Apparent power [VA].
Q	Yes	Reactive power [VAr].
phi_ef	Yes	Effective phase angle: $\arccos(PF)$ [rad].
Udc	Yes	DC voltage component [V].
Idc	Yes	DC current component [A].
Pdc	Yes	DC power component [W].
spec_U	No	Voltage channel spectrum [V].
spec_I	No	Current channel spectrum [A].
spec_S	No	Apparant power spectrum [VA].
spec_f	No	Frequency vector of <i>spec_U</i> , <i>spec_I</i> and <i>spec_S</i> .

Table 60: List of “calcset” options supported by the TWM-PWRFFT wrapper.

Name	Description
calcset.unc	Uncertainty calculation mode. Supported: “none”, “guf” for uncertainty estimator
calcset.loc	Level of confidence [-].
calcset.verbose	Verbose level.

## 12.2 Algorithm description

The TWM-PWRFFT algorithm internally uses TWM-WFFT (section 9) algorithm to calculate spectra of voltage and current channels. The amplitude spectra  $U_H(f)$  and  $I_H(f)$  and the phase difference  $\phi_H(f)$  between them are processed to obtain the power parameters:

$$U = \sqrt{\sum_{f=1}^F 0.5 \cdot U_H(f)^2}, \quad (80)$$

$$I = \sqrt{\sum_{f=1}^F 0.5 \cdot I_H(f)^2}, \quad (81)$$

$$P = \sum_{f=1}^F 0.5 \cdot U_H(f) \cdot I_H(f) \cdot \cos(\phi_H(f)), \quad (82)$$

$$Q_{bud} = \sum_{f=1}^F 0.5 \cdot U_H(f) \cdot I_H(f) \cdot \sin(\phi_H(f)), \quad (83)$$

$$Q = \sqrt{S^2 - P^2} \cdot \text{sign}(Q_{bud}), \quad (84)$$

where  $f$  is frequency component and  $F$  is total spectrum components count. For DC coupling mode, the DC components are included:

$$U = \sqrt{U_H(0)^2 + U^2}, \quad (85)$$

$$I = \sqrt{I_H(0)^2 + I^2}, \quad (86)$$

$$P = U_H(0) \cdot I_H(0) + P. \quad (87)$$

The  $S$  and  $PF$  are then calculated using following formulas:

$$S = U \cdot I, \quad (88)$$

$$PF = \frac{P}{S}. \quad (89)$$

### 12.2.1 Uncertainty calculation

Uncertainty is calculated from the spectrum component uncertainties returned by the TWM-WFFT algorithm.

$$u(U) = \sqrt{\frac{1}{(2 \cdot U)^2} \sum_{f=1}^F u(U_H(f))^2 \cdot U_H(f)^2}, \quad (90)$$

$$u(I) = \sqrt{\frac{1}{(2 \cdot I)^2} \sum_{f=1}^F u(I_H(f))^2 \cdot I_H(f)^2}, \quad (91)$$

$$u(P) = \sqrt{0.5 \sum_{f=1}^F \left\{ \begin{aligned} &I_H(f)^2 \cdot \cos(\phi_H(f))^2 \cdot u(U_H(f))^2 \\ &+ U_H(f)^2 \cdot \cos(\phi_H(f))^2 \cdot u(U_H(f))^2 \\ &+ U_H(f)^2 \cdot I_H(f)^2 \cdot \sin(\phi_H(f))^2 \cdot u(\phi_H(f))^2 \end{aligned} \right\}}, \quad (92)$$

$$u(S) = \sqrt{I^2 \cdot u(U)^2 + U^2 \cdot u(I)^2}, \quad (93)$$

$$u(Q) = \sqrt{\frac{S^2 \cdot u(S)^2 + P^2 \cdot u(P)^2}{S^2 - P^2}}. \quad (94)$$

For DC coupling mode, the uncertainties are expanded (empiric formulas):

$$u(P_{DC}) = \sqrt{1.5 \cdot I_{DC}^2 \cdot u(U_{DC})^2 + 1.5 \cdot U_{DC}^2 \cdot u(I_{DC})^2 + u(P)^2}, \quad (95)$$

$$u(U_{DC}) = \sqrt{u(U_{DC})^2 + 1.5 \cdot u(U)^2}, \quad (96)$$

$$u(I_{DC}) = \sqrt{u(I_{DC})^2 + 1.5 \cdot u(I)^2}, \quad (97)$$

$$u(U) = \sqrt{\frac{U_{DC}^2 \cdot u(U_{DC})^2 + U^2 \cdot u(U)^2}{U_{DC}^2 + U^2}}, \quad (98)$$

$$u(I) = \sqrt{\frac{I_{DC}^2 \cdot u(I_{DC})^2 + I^2 \cdot u(I)^2}{I_{DC}^2 + I^2}}, \quad (99)$$

$$u(S) = \sqrt{I^2 \cdot u(U)^2 + U^2 \cdot u(I)^2}. \quad (100)$$

Power factor  $PF$  uncertainty is calculated empirically using Monte Carlo:

```
for k = 1:2000
    Px = P + (1 - 2*rand)*u(P)*3^0.5;
    Sx = S + (1 - 2*rand)*u(S)*3^0.5;
    v_PF[k] = Px/Sx;
end
u(PF) = max(abs(v_PF - PF))/3^0.5;
```

### 12.2.2 Validation

The algorithm TWM-PWRFFT has many input quantities (for the differential transducer connection about 120 quantities) and some of them are matrices. That is too many possible degrees of freedom. Thus, varying the quantities in some systematic way would be very complicated if the validation should cover full range of used signals and corrections. Therefore, an alternative approach was used.

QWTB test function “alg\_test.m” was created, which performs the validation using randomly generated test setups. It randomizes the signal parameters, correction quantities and uncertainties and algorithm configurations in ranges expected to occur during the real measurements. The test is run many times to cover full operating range of the algorithm. Following operations are performed for each random test setup:

1. Generate voltage and current signals  $u$  and  $i$  with known power parameters  $P_{ref}$ .

2. Distort the signals  $u$  and  $i$  by inverse corrections, i.e. simulate the transducers, and digitizer (e.g. gain errors, phase errors, DC offsets, quantisation errors, ...).
3. Run the algorithm TWM-PWRFFT on the signals  $u$  and  $i$  with enabled uncertainty evaluation to obtain power parameters estimates  $P_x$  and their uncertainties  $u(P_{\text{ref}})$ .
4. Compare  $P_{\text{ref}}$  and  $P_x$  and decide if the errors of the algorithm for particular power parameters is smaller than the assigned uncertainties  $u(P_{\text{ref}})$ :

$$\text{pass}(i) = \text{abs}(P_{\text{ref}} - P_x) < u(P_{\text{ref}}), \quad (101)$$

where  $i$  is test run index.

5. Repeat the test  $N$  times from step 1 with the same test setup parameters, but with randomised corrections by their uncertainties, and with randomised noise, SFDR and jitter.
6. Check that at least 95 % of  $\text{pass}(i)$  results passed (for default 95 % level of confidence). The evaluation is made for each calculated power parameter separately. So it is possible to inspect which parameter fails.

The test runs count per test setup was set to  $N = 500$ , which is far from optimal “infinite” set, but due to the computational requirements it could not have been much higher. Note the low count of test induces uncertainty to the obtained pass rates.

The algorithm in the uncertainty estimation mode was tested in 4 different configurations with 10000 test setups per each. I.e. the algorithm was ran 20 million times in total ( $4 \times 10000 \times 500$ ). The processing itself was performed on a supercomputer [2] so it took only about 5 days at 200 parallel octave instances.

The randomization ranges of the signal are shown in table 61. The randomization ranges of the corrections are shown in table 62.

The test results were split into several groups given by the randomiser setup: (i) Single ended/differential mode; (ii) Randomisation of corrections by uncertainty enabled/disabled. When the randomisation of corrections is disabled, the test runs cover only the algorithm itself and the contributions of the correction uncertainties are ignored.

The summary of the validation test results is shown in table 63. The success rate without corrections randomisation was close to 100 %. The success rate with corrections randomisation was a bit worse, because the success rate of the test runs within the test setup is just around 95 %. Therefore the decision pass/fail is problematic. The obtained set of test results was manually investigated and no cases with far outliers were detected, e.g. the failed test setups contained occasional estimates offsets just around the uncertainty boundaries. Also no case where all test runs fails were found.

Table 61: Validation range of the signal for TWM-PWRFFT algorithm.

Parameter	Range
Sampling rate	random 9 to 11 kHz (all other parameters are varied relative to this sampling rate, so it is not needed to randomise in wider range).
Samples count	5000 to 20000 (0.5 to 2 seconds integration time).
Fundamental frequency	random, so there are at least 10 samples per period and at least 20 full periods recorded but always coherent.
Harmonics count	1 to 5 in order (no gaps).
Fundamental amplitudes	0.1 to 1 of full scale digitizer input.
Harmonic amplitudes	0.01 to 0.1 of fundamental.
Phase angles	Random for all harmonics and inter-harmonics.
DC offset	$\pm 0.05$ of fundamental.
SFDR	-120 to -80 dBc, max. 10 harmonic components, amplitude randomized for each spur in the SFDR range.
Digitizer RMS noise	1 to 10 $\mu\text{V}$ .
Sampling jitter	1 to 100 ns.

Table 62: Validation range of the correction for the TWM-PWRFFT algorithm. Note the low-side channel corrections in the differential mode are generated in the same way.

Parameter	Range
Nominal input U range	10 to 70 V
Nominal input I range	0.5 to 5 A
Aperture time	1 ns to 10 s
Digitizer gain	Randomly generated frequency transfer simulating NI 5922 FIR-like gain ripple (possibly the worst imaginable shape) and some ac-dc dependence. The transfer matrix has up to 50 frequency spots. Nominal gain value is random from 0.95 to 1.05 with uncertainty 2 $\mu\text{V}/\text{V}$ . Maximum ac-dc value at $fs/2$ is up to $\pm 1\%$ with uncertainty 50 $\mu\text{V}/\text{V}$ . Gain ripple amplitude is random from 0.005 to 0.03 dB with up to 5 periods between 0 and $fs/2$ .
Digitizer phase	Randomly generated phase frequency transfer up to $\pm 1$ mrad with uncertainty 2 to 50 $\mu\text{rad}$ .
Digitizer SFDR	Value based on table 61.
Digitizer bit resolution	16 to 28 bits.
Digitizer nominal range	1 V
Digitizer DC offset	Up to $\pm 10$ mV with uncertainty 0.1 mV.
Low-side channel time shift	Random value so the phase shift at Nyquist frequency won't exceed 0.1 rad with uncertainty 20 ns.
I-to-U channel time shift	Random value so the phase shift at Nyquist frequency won't exceed 0.1 rad with uncertainty 20 ns.
Transducer gain	Randomly generated frequency transfer. The transfer matrix has up to 50 frequency spots. Nominal gain value is random (see above) with relative uncertainty 2 $\mu\text{V}/\text{V}$ . Maximum ac-dc value at $fs/2$ is up to $\pm 2\%$ with uncertainty 50 $\mu\text{V}/\text{V}$ . Gain ripple amplitude is 0.005 dB with 4 to 10 periods between 0 and $fs/2$ .
Transducer phase	Randomly generated phase frequency transfer up to $\pm 1$ mrad with uncertainty 2 to 50 $\mu\text{rad}$ .

Table 63: Validation results of the algorithm TWM-PWRFFT. The “passed test” shows percentage of passed tests under conditions defined in tables 61 and 62. Note the pass condition is when all tested quantities ( $U$ ,  $I$ ,  $P$ ,  $Q$ ,  $S$ ,  $PF$ ) passes.

Connection	Rand. corr.	Passed test [%]
single-ended	off	100.00
	on	100.00
differential	off	100.00
	on	99.95

## References

- [1] Stanislav Mašláň. Activity A2.3.2 - Algorithms Exchange Format. <https://github.com/smaslan/TWM/tree/master/doc/A232AlgorithmExchangeFormat.docx>.
- [2] Miroslav Valtr. ČMI HPC System Online. [https://translate.google.cz/translate?sl=cs&tl=en&js=y&prev=\\_t&hl=cs&ie=UTF-8&u=http%3A%2F%2Fprutok.cmi.cz%2Fsc%2Fdoku.php%3Fid%3Dsystem&edit-text=](https://translate.google.cz/translate?sl=cs&tl=en&js=y&prev=_t&hl=cs&ie=UTF-8&u=http%3A%2F%2Fprutok.cmi.cz%2Fsc%2Fdoku.php%3Fid%3Dsystem&edit-text=), 2014.

## 13 TWM-LowZ - Low Impedance Measurement Algorithm

The algorithm uses harmonic analysis to calculate complex voltage ratio, resp. impedance of UUT standard based on reference shunt value. It was developed in scope of project EMPIR LiBforSecUse [1]. The UUT standard can be connected single ended (4-terminal mode), differentially (4 terminal-pair mode 4TP) or in dual 4-terminal way (2x4T) which is different method for 4TP impedance measurement.

### 13.1 TWM wrapper parameters

The input quantities supported by the algorithm are shown in the table 64. Algorithm returns output quantities shown in the table 65. Calculation setup supported by the algorithm is shown in table 66.

Table 64: List of input quantities to the TWM-LowZ wrapper.  
Details on the correction quantities can be found in [3].

Name	Default	Unc.	Description
f_est		N/A	Fundamental frequency to analyse or nothing to estimate using PSFE.
mode	“WFFT”	N/A	Mode of harmonic analysis. Default value is “WFFT” for TWM-WFFT algorithm. It partially supports also “PSFE” and “FPNLSF”.
window	“rect”	N/A	Windowing mode for WFFT mode. Default is “rect”. Other values supported by WFFT algorithms are allowed.
equ		N/A	Equivalent circuit name to express the calculated complex impedance. E.g.: LsRs, CsRs, Zphir, etc.
invert	0	N/A	Set to non-zero when one of the standard has inverted polarity of sensing terminals.
mode_4TP	“4TP”	N/A	4TP mode connection. “4TP” for standard 4TP connection or “2x4T” for dual 4T connection.
u	N/A	No	Input vector of sample data from UUT standard and complementary low-side input data vector <i>u_lo</i> (for differential mode only).
u_lo	N/A	No	
i	N/A	No	Input vector of sample data of current channel (reference shunt).
i_lo	N/A	No	
Ts	N/A	No	Sampling period or sampling rate or sample time vector. Note the wrapper always calculates in equidistant mode, so <i>t</i> is used just to calculate <i>Ts</i> .
fs	N/A	No	
t	N/A	No	
time_shift	0	Yes	Timeshift between voltage channel <i>u</i> and current channel <i>i</i> .
u_time_shift_lo	0	Yes	Time shift between high-side channel <i>u</i> low-side channel <i>u_lo</i> (or <i>i</i> and <i>i_lo</i> for current).
i_time_shift_lo	0	Yes	
u_lsb	N/A	No	Either absolute ADC resolution <i>lsb</i> or nominal range value <i>adc_nrng</i> (e.g.: 5 V for 10 Vpp range) and <i>adc_bits</i> bit resolution of ADC.
u_adc_nrng	1000	No	
u_adc_bits	40	No	
u_lo_lsb	N/A	No	
u_lo_adc_nrng	1000	No	
u_lo_adc_bits	40	No	
i_lsb	N/A	No	
i_adc_nrng	1000	No	
i_adc_bits	40	No	
u_adc_offset	0	Yes	Digitizer input offset voltage.
u_lo_adc_offset	0	Yes	
i_adc_offset	0	Yes	



Table 64: List of input quantities to the TWM-LowZ wrapper.  
Details on the correction quantities can be found in [3].

Name	Default	Unc.	Description
u_adc_gain	1	Yes	Digitizer gain correction 2D table (multiplier).
u_adc_gain_f	□	No	
u_adc_gain_a	□	No	
u_lo_adc_gain	1	Yes	
u_lo_adc_gain_f	□	No	
u_lo_adc_gain_a	□	No	
i_adc_gain	1	Yes	
i_adc_gain_f	□	No	
i_adc_gain_a	□	No	
u_adc_phi	0	Yes	Digitizer phase correction 2D table (additive).
u_adc_phi_f	□	No	
u_adc_phi_a	□	No	
u_lo_adc_phi	0	Yes	
u_lo_adc_phi_f	□	No	
u_lo_adc_phi_a	□	No	
i_adc_phi	0	Yes	
i_adc_phi_f	□	No	
i_adc_phi_a	□	No	
adc_freq	0	Yes	Digitizer timebase error correction: $f_{tb}' = f_{tb} \cdot (1 + adc\_freq.v)$ The effect on the estimated frequency is opposite: $f_{est}' = f_{est} / (1 + adc\_freq.v)$
u_adc_jitter	0	No	Digitizer sampling period jitter [s].
u_lo_adc_jitter	0	No	
i_adc_jitter	0	No	
u_adc_aper	0	No	ADC aperture value [s].
u_lo_adc_aper	0	No	
i_adc_aper	0	No	
u_adc_aper_corr	0	No	ADC aperture error correction enable: $A' = A \cdot pi \cdot adc\_aper \cdot f_{est} / \sin(pi \cdot adc\_aper \cdot f_{est})$ $phi' = phi + pi \cdot adc\_aper \cdot f_{est}$
u_lo_adc_aper	0	No	
i_adc_aper_corr	0	No	
u_adc_sfdr	180	No	Digitizer SFDR 2D table.
u_adc_sfdr_f	□	No	
u_adc_sfdr_a	□	No	
u_lo_adc_sfdr	180	No	
u_lo_adc_sfdr_f	□	No	
u_lo_adc_sfdr_a	□	No	
i_adc_sfdr	180	No	
i_adc_sfdr_f	□	No	
i_adc_sfdr_a	□	No	
u_adc_Yin_Cp	1e-15	Yes	Digitizer input admittance 1D table.
u_adc_Yin_Gp	1e-15	Yes	
u_adc_Yin_f	□	No	
u_lo_adc_Yin_Cp	1e-15	Yes	
u_lo_adc_Yin_Gp	1e-15	Yes	
u_lo_adc_Yin_f	□	No	
i_adc_Yin_Cp	1e-15	Yes	
i_adc_Yin_Gp	1e-15	Yes	
i_adc_Yin_f	□	No	
u_tr_type	“”	No	Transducer type string (“rvd” or “shunt”).
i_tr_type			

Table 64: List of input quantities to the TWM-LowZ wrapper.  
Details on the correction quantities can be found in [3].

Name	Default	Unc.	Description
u_tr_gain	1	Yes	Transducer gain correction 2D table (multiplicative).
u_tr_gain_f	<input type="checkbox"/>	No	
u_tr_gain_a	<input type="checkbox"/>	No	
i_tr_gain	1	Yes	
i_tr_gain_f	<input type="checkbox"/>	No	
i_tr_gain_a	<input type="checkbox"/>	No	
u_tr_phi	0	Yes	Transducer phase correction 2D table (additive).
u_tr_phi_f	<input type="checkbox"/>	No	
u_tr_phi_a	<input type="checkbox"/>	No	
i_tr_phi	0	Yes	
i_tr_phi_f	<input type="checkbox"/>	No	
i_tr_phi_a	<input type="checkbox"/>	No	
u_tr_sfdr	180	No	Transducer SFDR 2D table.
u_tr_sfdr_f	<input type="checkbox"/>	No	
u_tr_sfdr_a	<input type="checkbox"/>	No	
i_tr_sfdr	180	No	
i_tr_sfdr_f	<input type="checkbox"/>	No	
i_tr_sfdr_a	<input type="checkbox"/>	No	
u_tr_Zlo_Rp	1e3	Yes	RVD transducer low-side impedance 1D table. Note this is related to loading correction and it has effect only for RVD transducer and will work only if <i>adc_Yin</i> is defined as well.
u_tr_Zlo_Cp	1e-15	Yes	
u_tr_Zlo_f	<input type="checkbox"/>	No	
i_tr_Zlo_Rp	1e3	Yes	
i_tr_Zlo_Cp	1e-15	Yes	
i_tr_Zlo_f	<input type="checkbox"/>	No	
u_tr_Zca_Rs	1e-9	Yes	Loading corrections: Transducer high side terminal series impedance 1D table.
u_tr_Zca_Ls	1e-12	Yes	
u_tr_Zca_f	<input type="checkbox"/>	No	
i_tr_Zca_Rs	1e-9	Yes	
i_tr_Zca_Ls	1e-12	Yes	
i_tr_Zca_f	<input type="checkbox"/>	No	
u_tr_Zcal_Rs	1e-9	Yes	Loading corrections: Transducer low side terminal series impedance 1D table.
u_tr_Zcal_Ls	1e-12	Yes	
u_tr_Zcal_f	<input type="checkbox"/>	No	
i_tr_Zcal_Rs	1e-9	Yes	
i_tr_Zcal_Ls	1e-12	Yes	
i_tr_Zcal_f	<input type="checkbox"/>	No	
u_tr_Yca_Cp	1e-15	Yes	Loading corrections: Transducer output terminals shunting impedance.
u_tr_Yca_D	1e-12	Yes	
u_tr_Yca_f	<input type="checkbox"/>	No	
i_tr_Yca_Cp	1e-15	Yes	
i_tr_Yca_D	1e-12	Yes	
i_tr_Yca_f	<input type="checkbox"/>	No	
u_tr_Zcam	1e-12	Yes	Loading corrections: Transducer output terminals mutual inductance 1D table.
u_tr_Zcam_f	<input type="checkbox"/>	No	
i_tr_Zcam	1e-12	Yes	
i_tr_Zcam_f	<input type="checkbox"/>	No	
u_Zcb_Rs	1e-9	Yes	Loading corrections: Cable series impedance 1D table.
u_Zcb_Ls	1e-12	Yes	
u_Zcb_f	<input type="checkbox"/>	No	
i_Zcb_Rs	1e-9	Yes	
i_Zcb_Ls	1e-12	Yes	
i_Zcb_f	<input type="checkbox"/>	No	

Table 64: List of input quantities to the TWM-LowZ wrapper.  
Details on the correction quantities can be found in [3].

Name	Default	Unc.	Description
u_Ycb_Rs	1e-15	Yes	Loading corrections: Cable series impedance 1D table.
u_Ycb_Ls	1e-12	Yes	
u_Ycb_f	[]	No	
i_Ycb_Rs	1e-15	Yes	
i_Ycb_Ls	1e-12	Yes	
i_Ycb_f	[]	No	

Table 65: List of output quantities of the TWM-LowZ wrapper.

Name	Uncertainty	Description
f	No	Fundamental frequency [Hz].
Iref	No	RMS current of reference shunt [A].
Idc	No	DC current level of reference shunt [A].
Udut	No	RMS voltage drop at UUT impedance [V].
Udc	No	DC voltage drop at UUT impedance [V].
Udc_lo	No	DC voltage drop at UUT low terminal in 4TP mode [V].
Udc_hi	No	DC voltage drop at UUT high terminal in 4TP mode [V].
Udc_ref	No	DC voltage drop at reference standard [V].
Z_mode	Yes	Modulus of UUT impedance [ $\Omega$ ].
Z_phi	Yes	Phase angle of UUT impedance [rad].
Z_sh_mode	Yes	Modulus of UUT shield impedance in 2x4T mode [ $\Omega$ ].
Z_sh_phi	Yes	Phase angle of UUT shield impedance in 2x4T mode [rad].
mjr	Yes	Major UUT impedance component based on “equ” parameter.
mnr	Yes	Minor UUT impedance component based on “equ” parameter.
mjr_sh	Yes	Major UUT shield impedance component based on “equ” parameter for 2x4T mode.
mnr_sh	Yes	Minor UUT shield impedance component based on “equ” parameter for 2x4T mode.
mjr_name	No	Major UUT impedance component name string based on “equ”.
mnr_name	No	Minor UUT impedance component name string based on “equ”.
spec_U	No	UUT impedance voltage spectrum [V].
spec_I	No	Ref shunt current spectrum [A].
spec_f	No	Frequency vector of <i>spec_U</i> , <i>spec_I</i> .

Table 66: List of “calcset” options supported by the TWM-LowZ wrapper.

Name	Description
calcset.unc	Uncertainty calculation mode. Supported: “none”, “guf” for uncertainty estimator
calcset.loc	Level of confidence [-].
calcset.verbose	Verbose level.

## 13.2 Algorithm description

The TWM-LowZ algorithm internally uses TWM-WFFT (section 9), TWM-PSFE (section 1) or TWM-FPNLSF (section 3) algorithm to calculate voltage drops at reference shunt connected to current channel and UUT impedance connected to voltage channel. The algorithm expects use of a current shunt as a reference impedance. The value of reference impedance is given by current transducer correction file. The UUT (voltage) channel uses unity transfer correction.

The algorithm supports three main connections. First and simplest is simple series connection of two impedances following example shown in Fig. 29. Polarity of UUT impedance can be eventually inverted and guard of the high-side digitizer can be connected via buffer to reduce current leakage from the impedances joint. Note the algorithm does not take into account the leaking current, so there will be certain error growing with frequency and impedance value and it is not part of calculated uncertainty.

Another possible connection is for 4TP UUT standard shown in Fig. 30. In this case the UUT impedance is connected to two digitizer channels in differential connection. This method directly uses the nested algorithms such as TWM-WFFT to calculate UUT impedance drop. This connection has potential problem with common mode voltage at high-side impedance. Any errors in linearity of the upper two digitizers will cause large errors of measured UUT impedance especially if it is very low impedance compared to ref. impedance.

The problem of common mode voltage is partly solved by a third possible connection shown in Fig. 31. This mode was named 2x4T as in principle it is two simultaneous 4-terminal measurements summed together. One digitizer measures voltage drop between live terminals of the UUT and another one between shields of UUT. According to definition of 4TP impedance, the two impedances are summed together. There will be however still effect of limited common mode rejection of the digitizers. However, the effect can be neglected by active guarding of the digitizers.

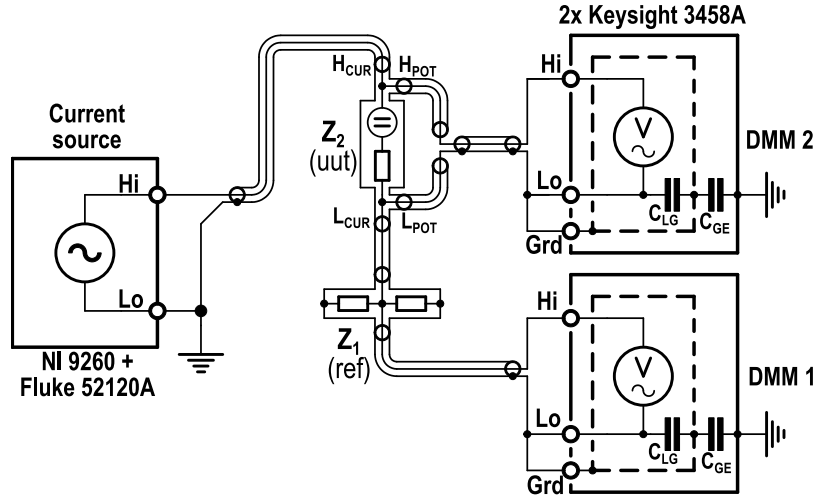


Figure 29: Connection of bridge circuit for measurement of impedance in 4T connection using TWM-LowZ algorithm.

The calculated impedance of UUT is returned directly in modulus-phase angle format and also converted to desired two component equivalent circuit. Further details can be found in documentation of Open-Z-Bridge tool [2] which uses TWM with this algorithm.

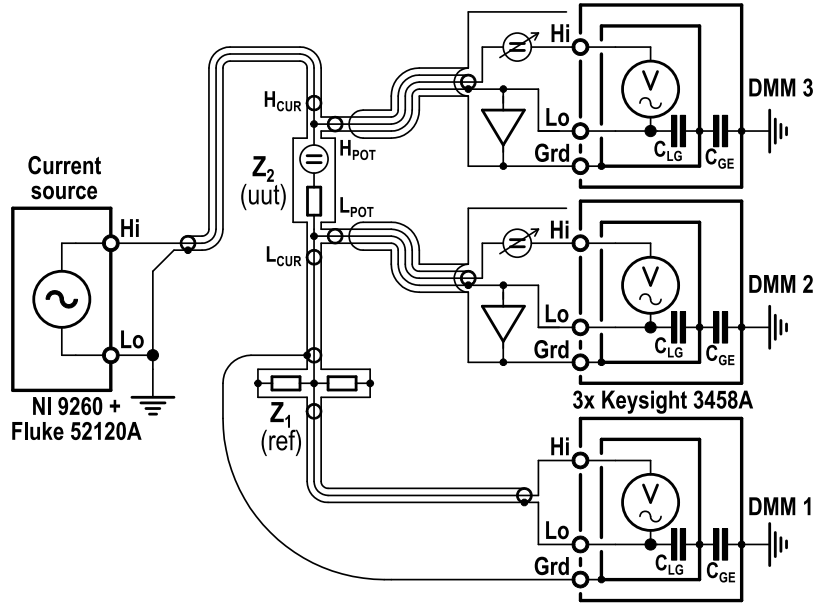


Figure 30: Connection of bridge circuit for measurement of impedance in 4TP connection using TWM-LowZ algorithm.

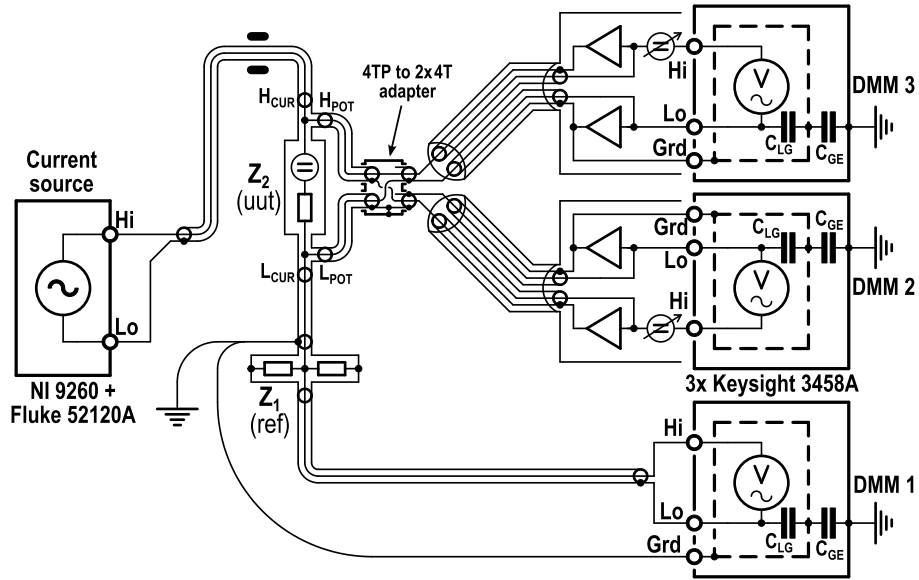


Figure 31: Connection of bridge circuit for measurement of impedance in 2x4T connection using TWM-LowZ algorithm.

### 13.2.1 Uncertainty calculation

Uncertainty calculation of the algorithm comes directly from the nested algorithms. The only fully tested algorithm was TWM-WFFT (calculation mode “WFFT”). Note the uncertainty does not account for additional effects of leakage currents as mentioned above.

### 13.2.2 Validation

The algorithm was validated ad hoc using numeric simulator in all supported modes, however detailed uncertainty calculation validation as for other algorithms was not performed. It relies on correct uncertainty calculation of the nested algorithms (TWM-WFFT).

## References

- [1] EURAMET. LiBforSecUse - EMPIR project: Traceability Routes for Electrical Power Quality Measurement. <https://www.ptb.de/empir2018/libforsecuse/project/overview/>. April 2022, [online].
- [2] Stanislav Mašláň. Open-Z-Bridge - Open source low-impedance bridge SW using TWM tool. <https://github.com/smaslan/open-z-bridge>.
- [3] Stanislav Mašláň. Activity A2.3.2 - Algorithms Exchange Format. <https://github.com/smaslan/TWM/tree/master/doc/A232AlgorithmExchangeFormat.docx>.